SUPPORTING INFORMATION

Modulating the reactivity of phosphanylidenephosphoranes towards water with Lewis acids

F. Dankert,[a] M. Fischer,[a] and C. Hering-Junghans[a]*

[a] Dr. Fabian Dankert, Dr. Malte Fischer, Dr. Christian Hering-Junghans

Leibniz-Institut für Katalyse e.V. (LIKAT)
Albert-Einstein Straße 29a, 18059 Rostock, Germany
E-mail: christian.hering-junghans@catalysis.de
Website: https://www.catalysis.de/forschung/katalyse-mit-erneuerbaren-rohstoffen/bioinspirierte-katalyse

This file includes:

1 Experimental

General Information. If not stated otherwise, all manipulations were carried out under oxygen- and moisture-free conditions under an inert atmosphere of argon using meticulous Schlenk techniques. All reactants (except demin. H_2O and HCl in Et_2O) were stored and handled in a mBraun glovebox. Solvents and reactants were either obtained from commercial sources, local trade or synthesized as depicted in Table S1. Activation of molecular sieves was achieved through heating with a heatgun at >600°C and applying vacuum for several hours.

Table S1: Origin and purification of solvents and reactants.

Substance	Origin	Purification
Mes*$PPMe_3$	Synthesized according to literature procedures.[1]	-
^{Mes}TerPPMe_3	Synthesized according to literature procedures.[1]	-
^{Dip}TerPPMe_3	Synthesized according to literature procedures.[1]	-
BAr^F	Synthesized according to literature procedures.[2]	
H_2O (demineralized)	Local trade	-
$GaCl_3$	Alfa Aesar, ultra dry, 99.999%	Packed under Ar and used as received, transferred to glovebox
GaI_3	Alfa Aesar, ultra dry, 99.999%	Packed under Ar and used as received, transferred to glovebox
2M HCl in Et_2O	SIGMA ALDRICH	Packed under Ar and used as received.
Benzene	local trade	Dried over Na/benzophenone, stored over activated, 3Å molecular sieves
Toluene	local trade	Purified with a solvent Purification system, partially condensed to 3Å molecular sieves and transferred to glovebox
MeCN	SIGMA ALDRICH, HPLC grade ≥99.9%	Purified with a solvent Purification system, distilled from P_2O_5 and stored over 3Å molecular sieves

Table S1 continued.

Substance	Origin	Purification
DCM	Local trade	Purified with a solvent Purification system, distilled from CaH_2 and stored over 3Å molecular sieves
C_6D_6	euro-isotope	Dried over Na/benzophenone, freshly distilled prior to use
CD_2Cl_2	euro-isotope	Dried over CaH_2, freshly distilled prior to use
n-hexane	local trade	Stored over activated, 3Å molecular sieves
n-pentane	SIGMA ALDRICH, >99%	Cannulated to activated, 3Å molecular sieves

NMR spectra were recorded on Bruker spectrometers (AVANCE 400 or Fourier 300) and were referenced internally to the deuterated solvent (^{13}C: C_6D_6 δ_{ref} = 128.06 ppm; CD_2Cl_2 δ_{ref} = 54.000) or to protic impurities in the deuterated solvent (^1H: C_6D_5H δ_{ref} = 7.16 ppm; $CDHCl_2$ δ_{ref} = 5.32). All measurements were carried out at ambient temperature unless denoted otherwise. NMR signals were assigned using experimental data (e.g. chemical shifts, coupling constants (=*J*), integrals) where applicable.

IR spectra of crystalline samples or purified powders were recorded on a Bruker Alpha II FT-IR spectrometer equipped with an ATR unit at ambient temperature under an argon atmosphere. Relative intensities are reported according to the abbreviations: very weak (=vw), weak (=w), medium (=m), strong (=s), very strong (=vs), broad (=br).

Elemental analyses were tried to obtain with a Leco Tru Spec elemental analyzer device.

Mass spectra were obtained using a Thermo Electron MAT 95-XP (EI) and an Agilent 1200/6210 Time-of-Flight LC-MS (ESI) device.

2 Structure elucidation and refinement

X-ray Structure Determination: X-ray quality crystals were selected in Fomblin YR-1800 perfluoroether (Alfa Aesar) at ambient temperature. The samples were cooled to 150(2) K during measurement if not stated otherwise. The data were collected on a STOE IPDS II diffractometer or a Bruker Apex II Duo diffractometer using MoK_α (λ = 0.71073 Å) or CuK_α radiation (λ = 1.54178 Å), respectively. The structures were solved by intrinsic phasing (SHELXT)[3] and refined by full matrix least squares procedures (SHELXL)[4] within the Olex2 platform.[5] Semi-empirical absorption corrections (multiscan and additional spherical absorption correction) were applied to the diffraction data recorded with the STOE device using the LANA application within the STOE X-AREA platform.[6] Semi-empirical absorption corrections (multiscan and additional spherical absorption correction) were applied to the diffraction data collected with the Bruker device using the SADABS application within the APEX II platform.[7] All non-hydrogen atoms were refined anisotropically, hydrogen atoms were included in the refinement at calculated positions using a riding model. P-H protons were in all cases refined as independent isotropic atoms according to reasonable electron density indicating the respective P-H position. All special refinement details (if required) for disordered or twinned structures as well as molecular structure representations are summarized down below. A summary on standard crystallographic parameters is also provided.

Special Refinement Details:

2:Mes*: The obtained colorless needles were found to be twinned. A suitable .hklf5 file was written using the twinning tool within Olex2. BASF (Batch scale or also twin scale factor) converged to 0.920(2) for the main and 0.080(2) for the minor component. Hence the internal R value R_{int} is given as n/a (see table S2).

3:Mes^{Ter}: The compound is found to crystallize in the non-centrosymmetric, orthorhombic space group *Aea*2. The absolute structure parameter converged to a value of 0.066(10). A subsequent TWIN LAW was employed (inversion twinning, -1, 0, 0, 0, -1, 0, 0, 0, -1) and BASF 0.066(10).

4:Mes*: The compound is found to crystallize in the non-centrosymmetric, orthorhombic space group *Pmn*2_1. The absolute structure parameter converged to a value of 0.174(18). A subsequent TWIN LAW was employed (inversion twinning, -1, 0, 0, 0, -1, 0, 0, 0, -1) and BASF 0.174(18). The *t*Bu group in para-position is disordered around the center of inversion. Split positions have occupancies of 0.5. Note that half of the tBu group is symmetry generated using 1-X, +Y, +Z. Note that comparably high residual electron density around heavy atoms is generally due to absorption effects.

4:^{Mes}Ter: The whole O-GaI3 appears to be slightly disordered. However, no suitable disorder model could be refined for the GaI_3 fragment. We therefore decided to just split the oxygen atom into two positions using an equal anisotropic displacement parameter (EADP) due to close proximity (O1 and O1A). Occupancies were set to 0.5. The unresolved disorder causes higher electron density around this fragment.

6:Mes*: The *t*Bu group in para position appeared to be rotationally disordered. To fix the disorder SADI as well as EADP commands were applied. According to the free

variable (FVAR), the components converged to occupancies of approximately 0.79 and 0.21.

6:^{Dip}Ter: The compound crystallizes as its dichloromethane solvate. Two dichloromethane molecules show a reasonable refinement when given occupancy 1. A third DCM molecule is found, however, occupancy 1 is unreasonable. We tried to estimate its occupancy using a free occupancy, but refinement was unstable in this case. We therefore set the occupancy to 0.7 and reached reasonable anisotropic displacement of this solvent molecule. To fix disorder around two of the refined DCM positions, DFIX and EADP commands were applied. For the final refinement we subsequently employed the SQUEEZE implementation within OLEX2 to model a solvent mask for a further disordered co-crystalline DCM molecule.

7:Mes*: Note that comparably high residual electron density around heavy atoms is generally due to absorption effects.

8:Mes*:

The *t*Bu group in para position appeared to be rotationally disordered. To fix the disorder SADI, DANG as well as EADP commands were applied. According to FVAR2, the components converged to occupancies of approximately 0.73 and 0.27. Each halogen position revealed electron density with about 220 pm and >250 pm from the central Ga position indicating simultaneous Cl/I-bonding. Therefore, we refined a mixed substituted GaX_3 moiety following the general formula $GaCl_xI_{3-x}$. Three free variables we applied to each halogen position which converged to total occupancy of $Cl_{2.1}$ and $I_{0.9}$ following the formula $GaCl_xI_{3-x}$. Due to their close proximity, the Cl and I positions were each refined to have the same EADP. The three different FVARs converged approximately as follows: FVAR3: Cl: 0.34, I: 0.66; FVAR4: Cl: 0.85, I: 0.15 and FVAR5: Cl: 0.95, I: 0.05.

9:^{Mes}Ter: The compound crystallized with two independent molecules. It is notable that we have refined the structure as a superstructure. An initial refinement with the following cell of **a =** 12.9253(16) **b =** 14.2118(17) **c =** 19.491(3), **α** = 76.41(1) **β =** 75.29(1) **γ =** 69.769(9) failed due to severe disorder of one independent molecule within the asymmetric unit. However, comparably weak superstructure reflections were considered next and a new cell of **a =**12.9253 **b =** 21.2504 **c =** 24.9838, **α** = 109.535 **β =** 97.03 **γ =** 90.092 was applied. A subsequent refinement then turned out to be successful. However, the central aryl rings as well as parts of the flanking aryl rings still seem to be disordered. No suitable disorder model could be refined for both independent molecules, though. Hence, we employed a series of SIMU, RIGU and ISOR restraints.

11:Mes*: Note that comparably high residual electron density around heavy atoms is generally due to absorption effects

12:^{Dip}Ter: The PMe_3 unit as well as the H atom at P showed disorder through tilting of the P-P bond. Two split positions were successfully refined with occupancies of approximately 0.85 and 0.15 according to FVAR2. The $GaCl_4^-$ anion is also disordered through tilting and two split positions were refined. The occupancies are estimated to be 0.58 and 0.42 according to FVAR3. For one C atom of the minor occupied PMe_3 unit an EADP command was applied. To fix the disorder around $GaCl_4^-$, several DFIX, DANG and SADI restraints had to be used.

Molecular Structure Representations: All molecular structure representations in the ESI as well as the main article have been prepared with the Diamond software package.[8] A mixed representation of ellipsoid plots as well as wires/sticks was chosen for clarity. All ellipsoids are represented at the 50% probability level unless stated otherwise.

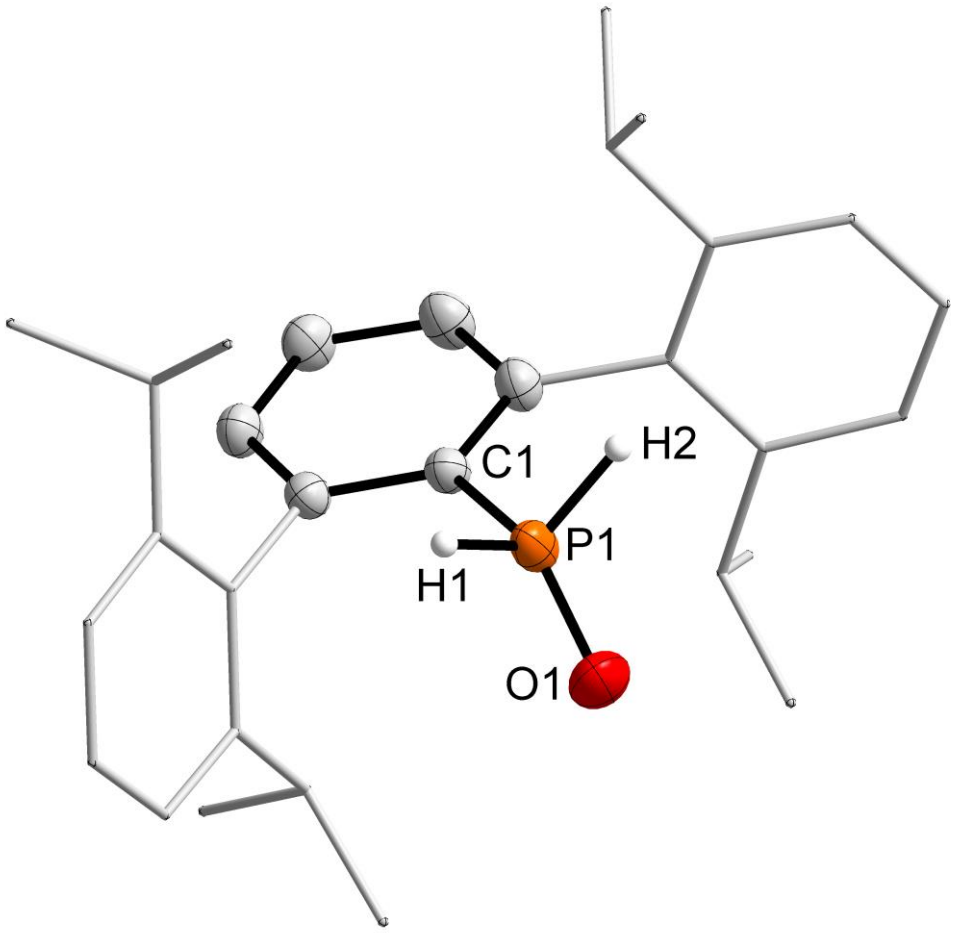

Figure S1: Molecular structure of **1:^{Dip}Ter** in the crystal. Selected bond lengths [pm] and angles [°]: C1-P1 179.70(12), O1-P1 147.19(11), C1-P1-O1 118.69(5).

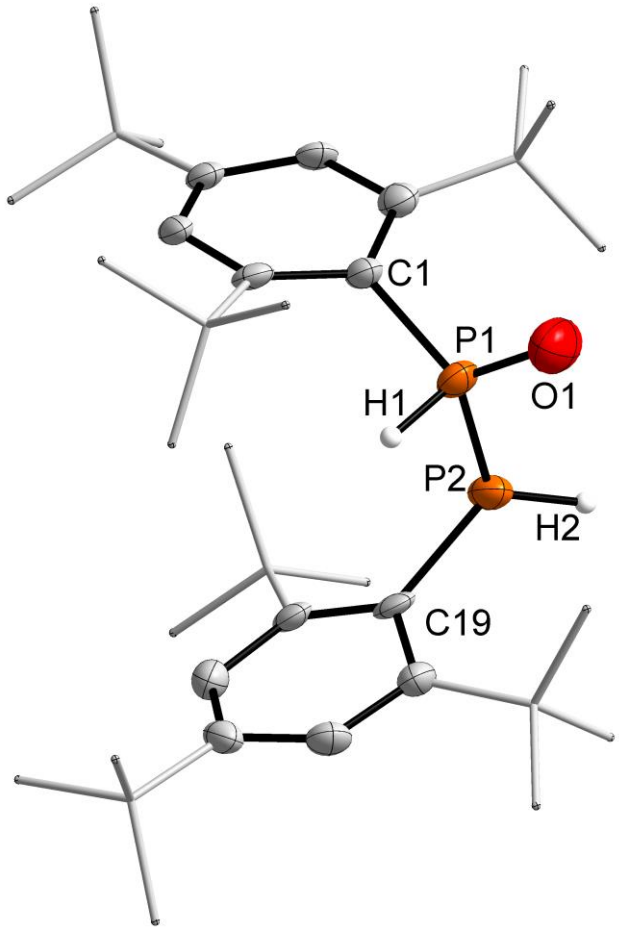

Figure S2: Molecular structure of **2:Mes*** in the crystal. Selected bond lengths [pm] and angles [°]: C1-P1 183.32(44), O1-P1 147.50(45), P1-P2 225.71(20), C19-P2 184.08(53), C1-P1-P2 105.88(16), C19-P2-P1 101.21(16).

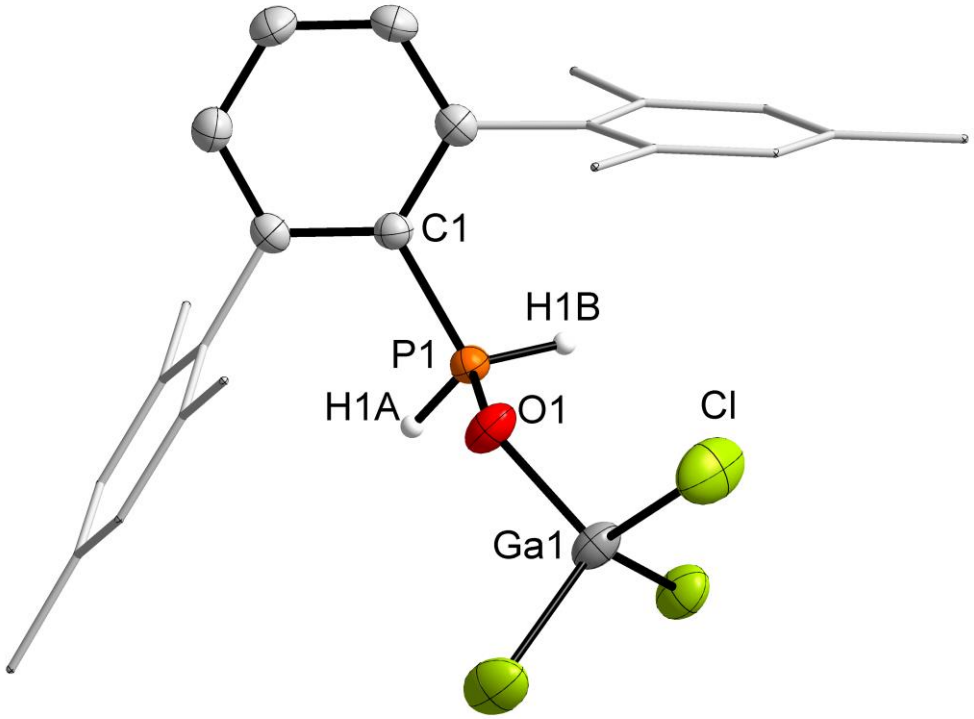

Figure S3: Molecular structure of **3:^{Mes}Ter** in the crystal. Selected bond lengths [pm] and angles [°]: C1-P1 177.45(26), O1-P1 152.48(24), O1-Ga1 187.08(21), C1-P1-O1 110.98(11).

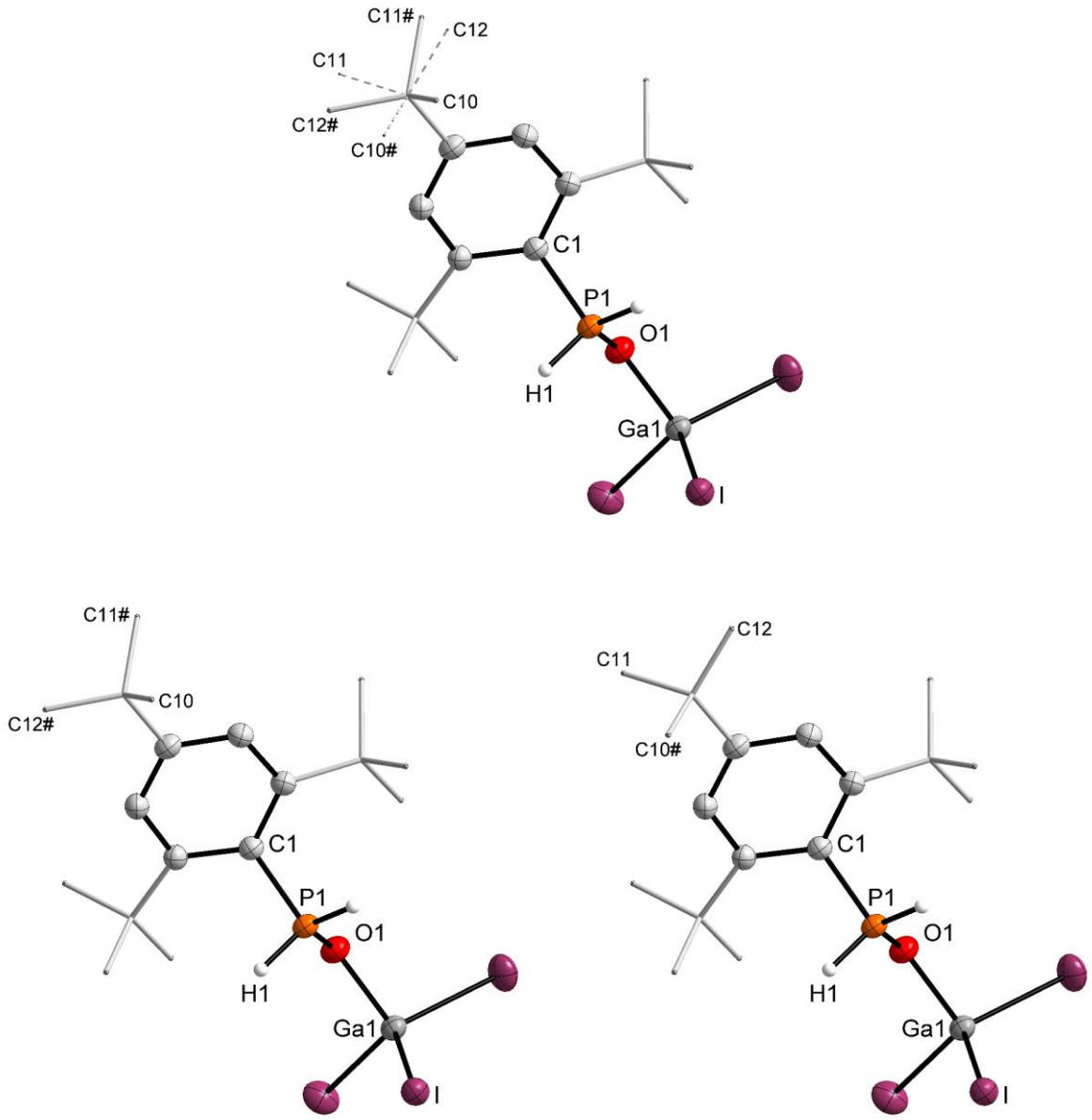

Figure S4: Molecular structure of **4:Mes*** in the crystal including disordered parts. Atoms depicted with # and half of the molecule in general are symmetry generated using 1-x, y, z. Selected bond lengths [pm] and angles [°]: C1-P1 177.99(49), O1-P1 153.02(38), O1-Ga1 188.34(36), C1-P1-O1 119.48(20), P1-O1-Ga1 130.98(23).

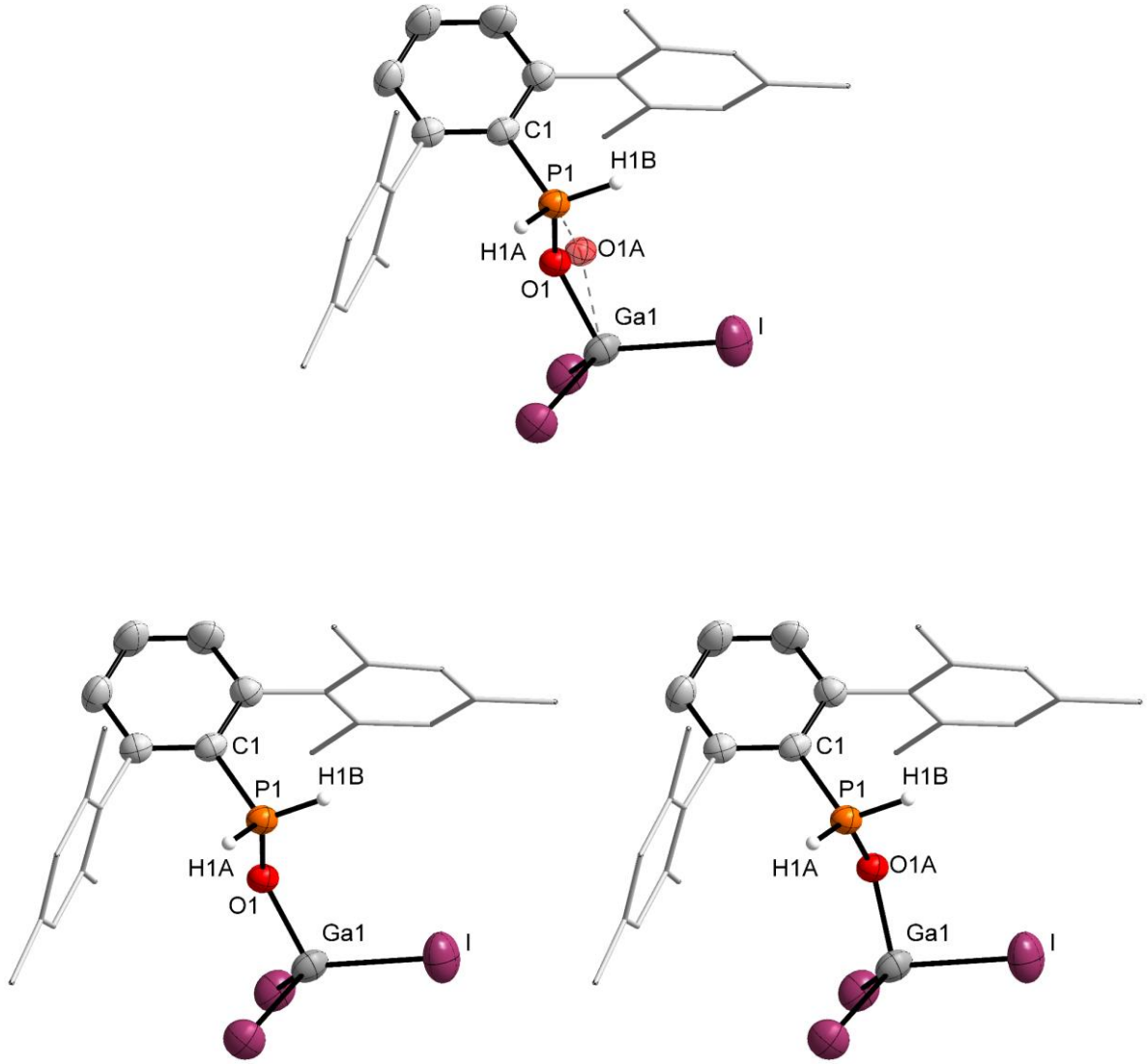

Figure S5: Molecular structure of **4:^{Mes}Ter** in the crystal including disordered parts. Selected bond lengths [pm] and angles [°]: C1-P1 178.38(45), O1-P1 152.62(93), O1-Ga1 187.54(86), C1-P1-O1 107.51(39), P1-O1-Ga1 136.05(57).

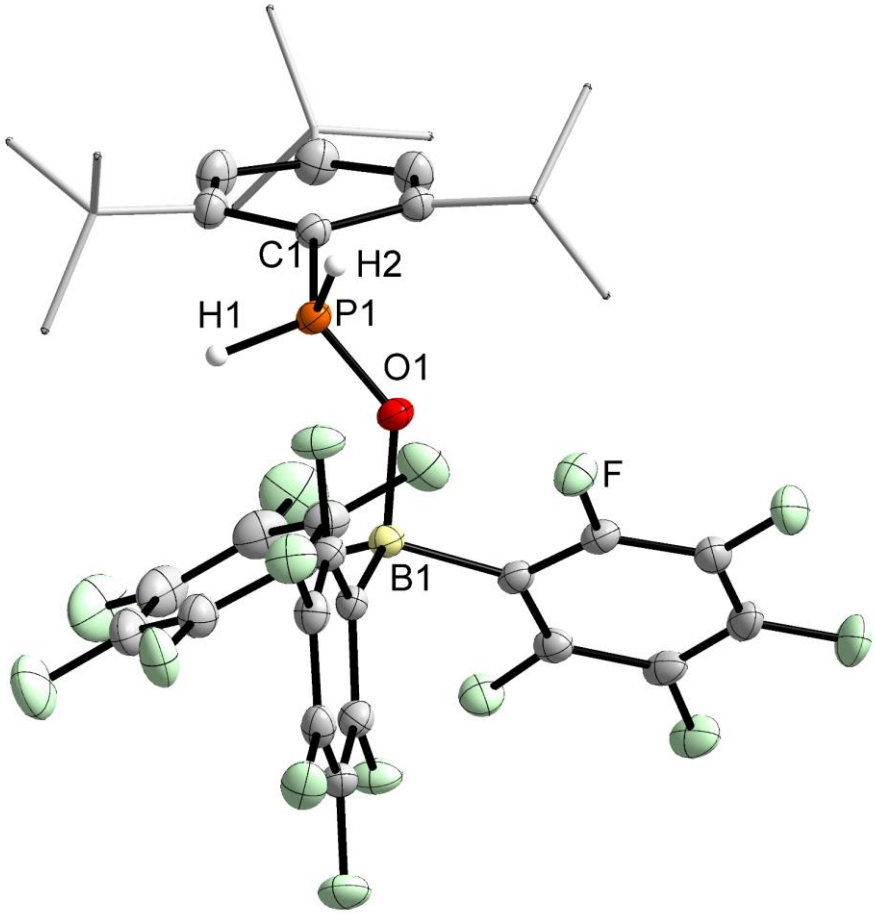

Figure S6: Molecular structure of **5:Mes*** in the crystal. Selected bond lengths [pm] and angles [°]: C1-P1 178.60(14), O1-P1 152.73(13), O1-B1 153.71(22), C1-P1-O1 .111.62(6), P1-O1-B1 136.04(10).

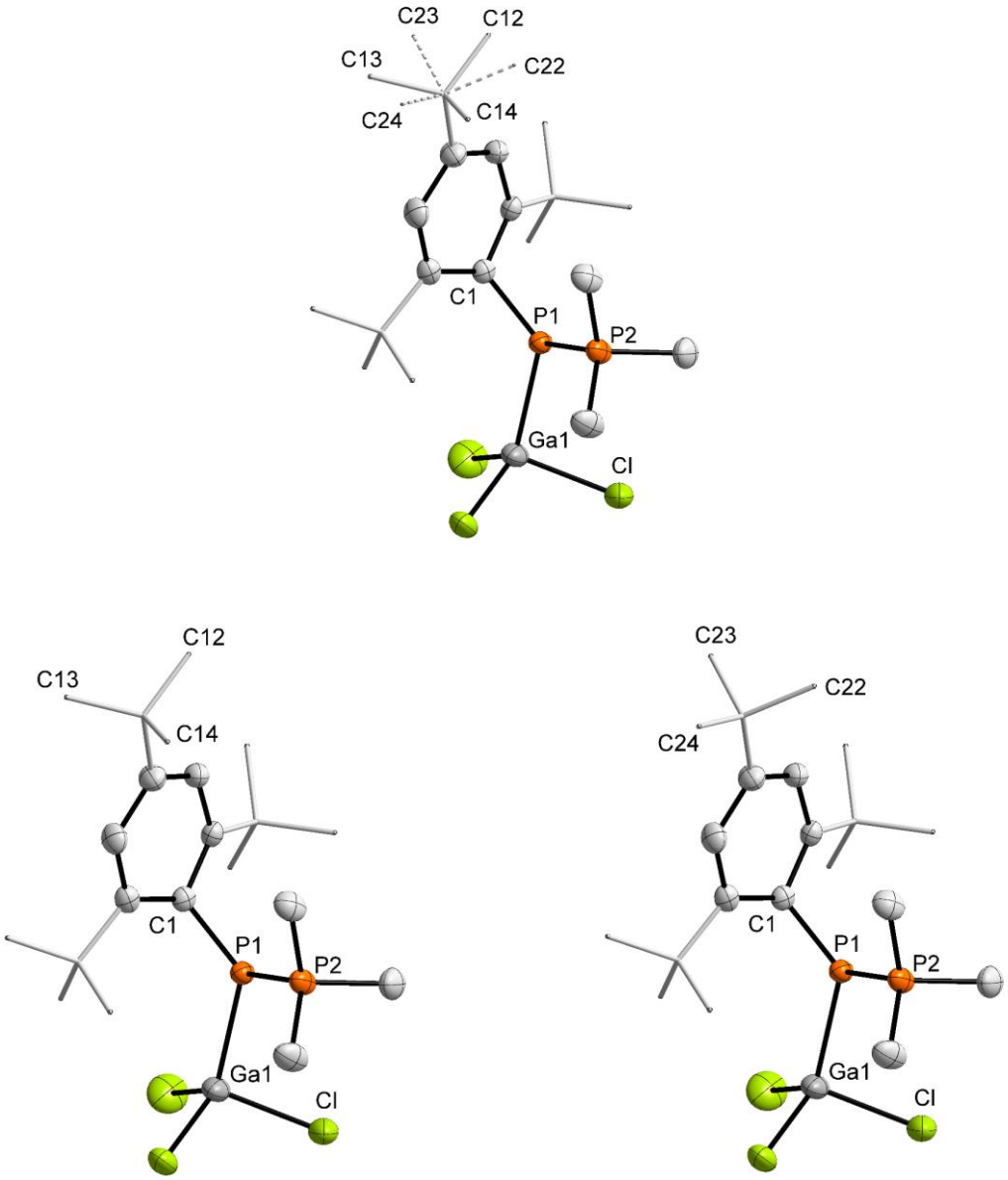

Figure S7: Molecular structure of **6:Mes*** in the crystal including disordered parts. Selected bond lengths [pm] and angles [°]: C1-P1 186.41(22), P1-P2 217.47(9), P1-Ga1 234.75(7), C1-P1-P2 100.77(7), C1-P1-Ga1 130.13(7), Ga1-P1-P2 102.59(3).

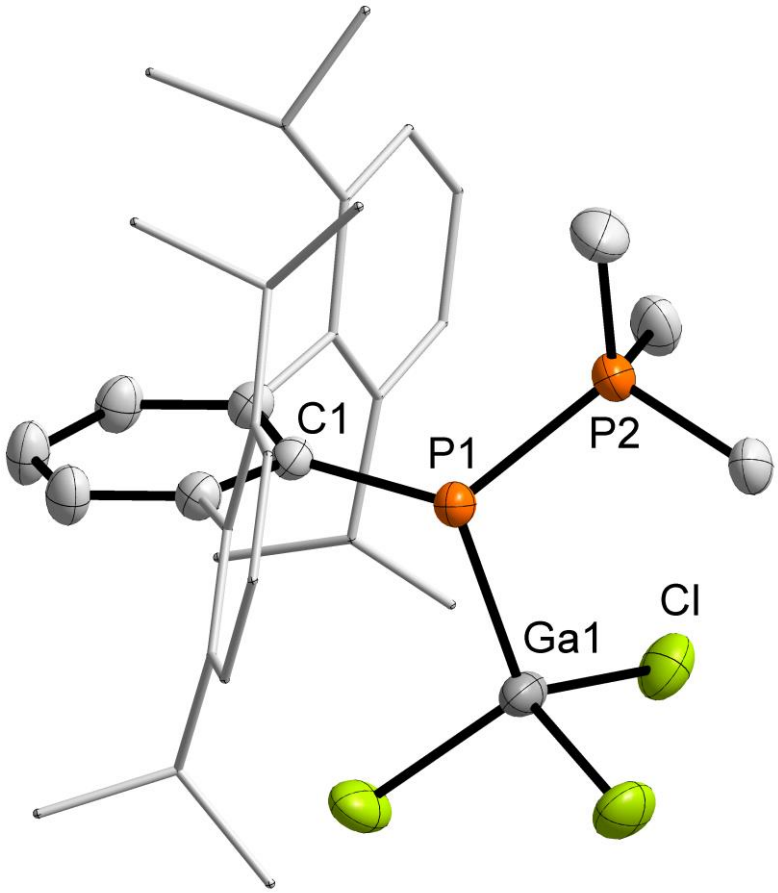

Figure S8: Molecular structure of **6:^{Dip}Ter** in the crystal. Selected bond lengths [pm] and angles [°]: **:** C1-P1 184.45(22), P1-P2 215.81(8), P1-Ga1 235.86(7), C1-P1-Ga1 109.54(7), C1-P1-P2 117.40(7), Ga1-P1-P2 99.87(3).

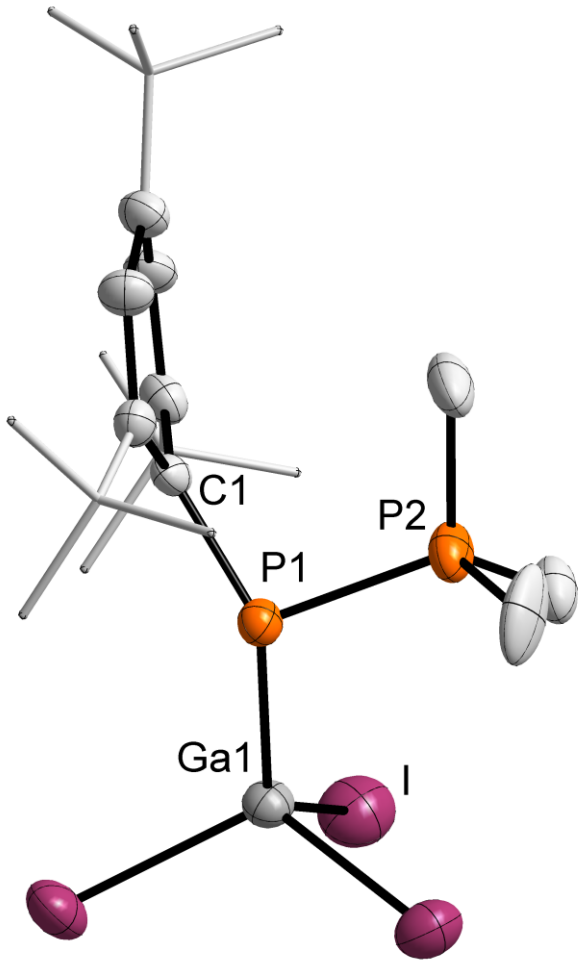

Figure S9: Molecular structure of **7:Mes*** in the crystal. Selected bond lengths [pm] and angles [°]: C1-P1 185.94(81), P1-P2 217.94(29), P1-Ga1 236.43(22), C1-P1-P2 100.93(27), C1-P1-Ga1 130.39(26), Ga1-P1-P2 104.75(9).

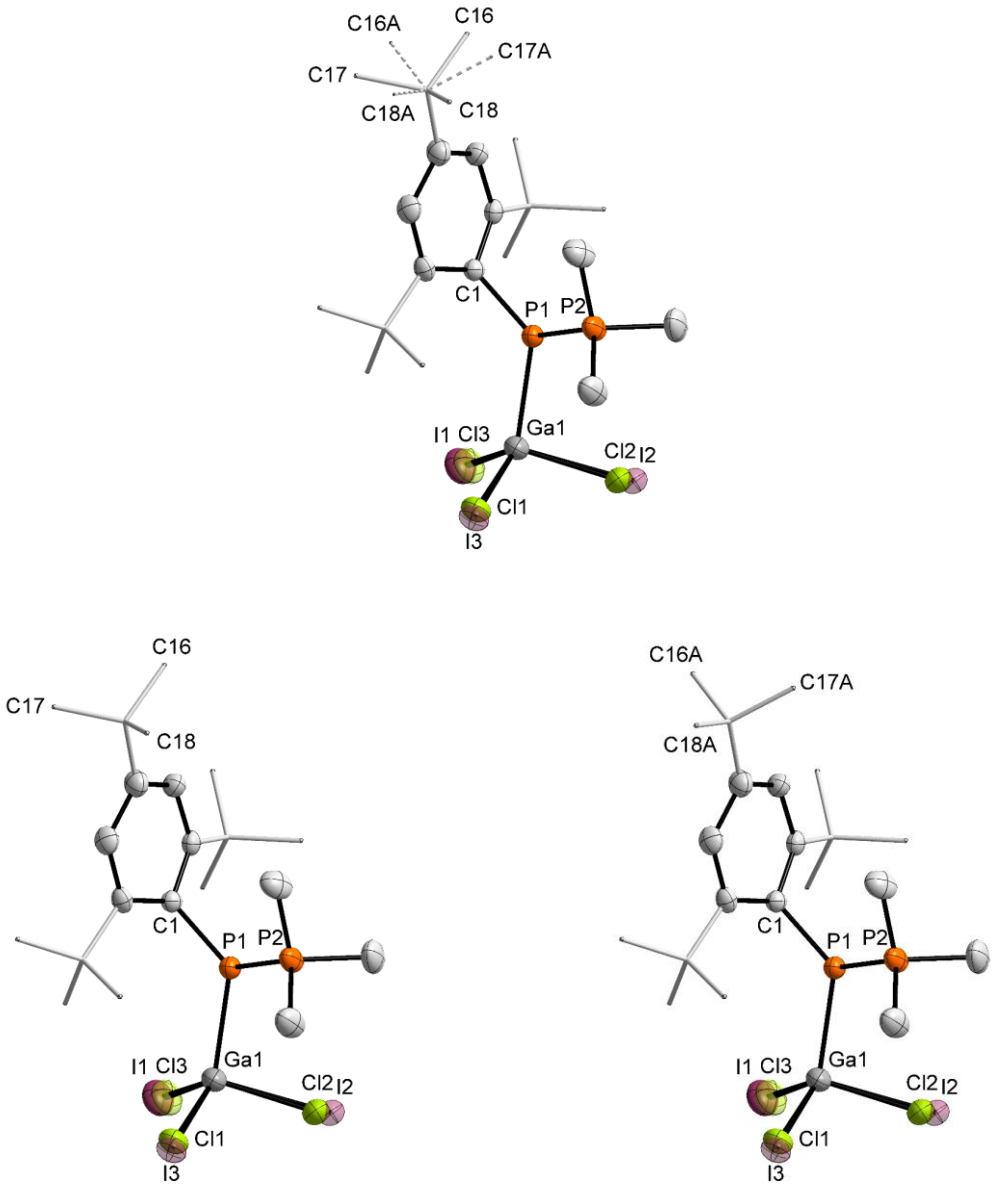

Figure S10: Molecular structure of **8:Mes*** in the crystal including disordered parts. Transparent ellipsoids indicate minor occupied atom positions (see special refinement details). Selected bond lengths [pm] and angles [°]: C1-P1 186.45(43), P1-P2 217.98(16), P1-Ga1 235.09(12), C1-P1-P2 100.51(13), C1-P1-Ga1 130.60(14), Ga1-P1-P1 103.32(6).

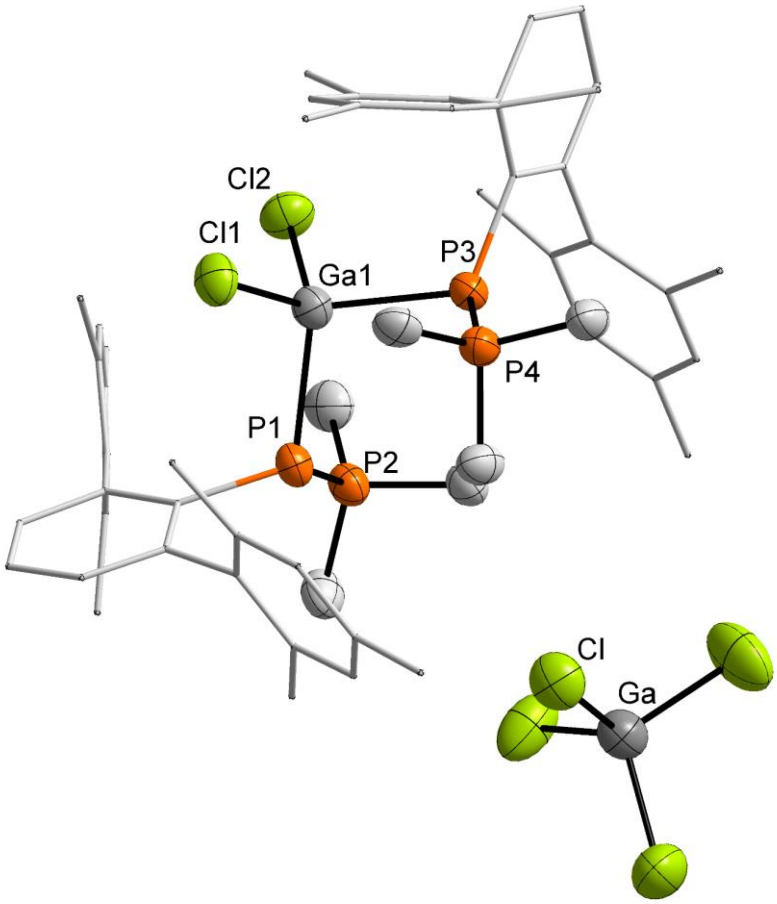

Figure S11: Molecular structure of one of two crystallographic independent discrete ion pairs of **9:^{Mes}Ter** in the crystal. Selected bond lengths [pm] and angles [°]: P1-P2 216.28(24), P1-Ga1 239.52(18), Ga1-P3 239.76(16), P3-P4 216.43(23), P1-Ga1-P3 103.76(6), Ga1-P1-P2 103.35(7), Ga1-P3-P4 102.74(8).

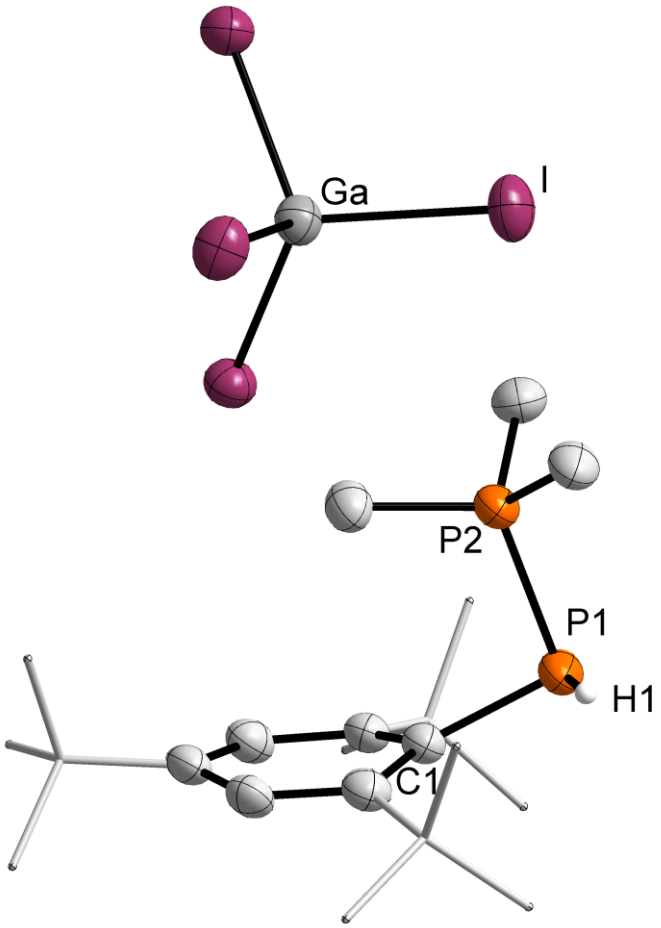

Figure S12: Molecular structure of the discrete ion pair **10:Mes*** in the crystal. Selected bond lengths [pm] and angles [°]: C1-P1 184.35(50), P1-P2 222.35(20), C1-P1-P2 97.41(17).

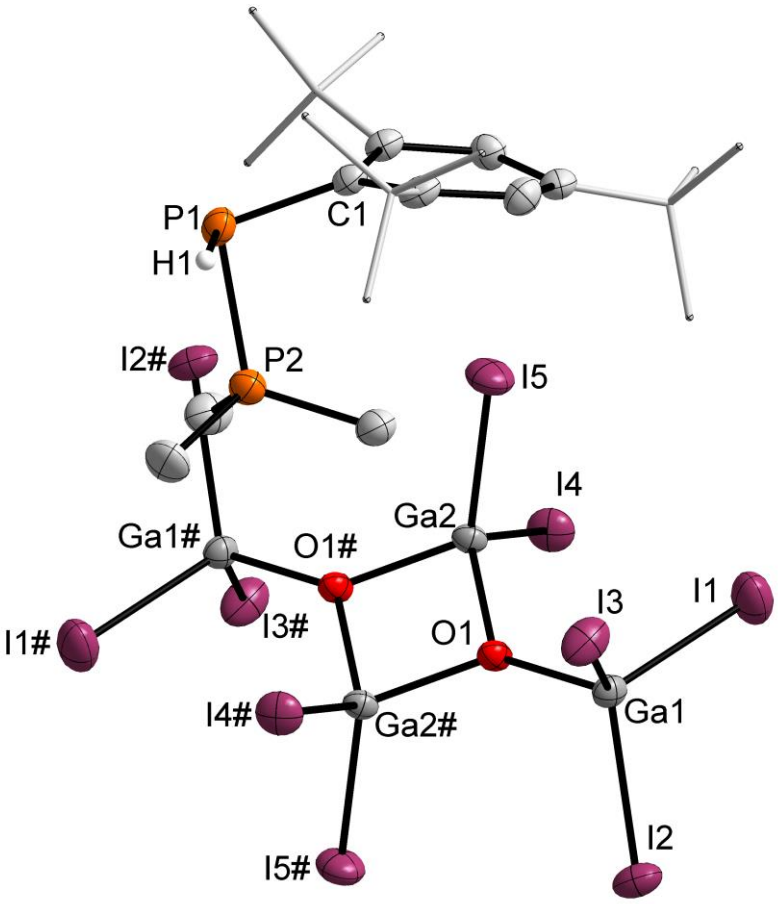

Figure S13: Molecular structure of the discrete ion pair **11:Mes*** in the crystal. Atoms depicted with # and half of the molecule in general are symmetry generated using 2-x, 1-y, 1-z. A symmetry generated $[Mes^*P(H)PMe_3]^+$ ion is not displayed. Selected bond lengths [pm] and angles [°]: C1-P1 184.07(43), P1-P2 221.29(19), Ga1-I1 248.74(8), Ga1-I2 253.31(7), Ga1-I3 252.86(6), Ga1-O1 187.29(27), Ga2-O1 188.62(33), Ga2-I4 250.59(6), Ga2-I5 249.61(7), O1···O1# 251.25(36), Ga2···Ga2# 281.05(9), C1-P1-P2 98.81(16), Ga1-O1-Ga2 129.33(15), O1-Ga2-O1# 83.59(12), Ga2-O1-Ga2# 96.40(13).

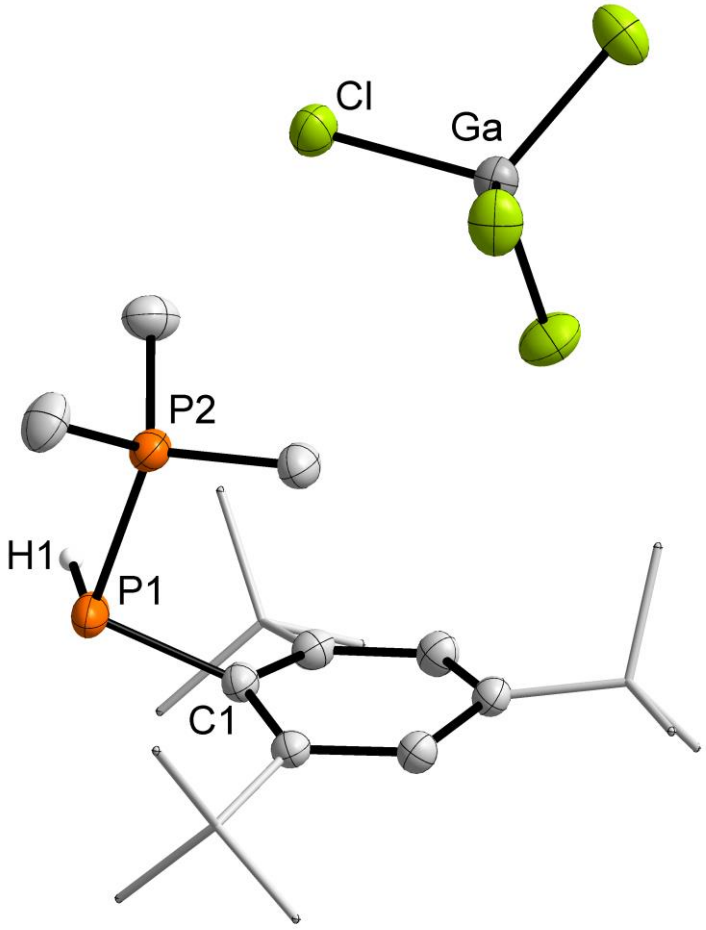

Figure S14: Molecular structure of the discrete ion pair **12:Mes*** in the crystal. Selected bond lengths [pm] and angles [°]: C1-P1 183.43(14), P1-P2 221.84(7), C1-P1-P1 97.14(5).

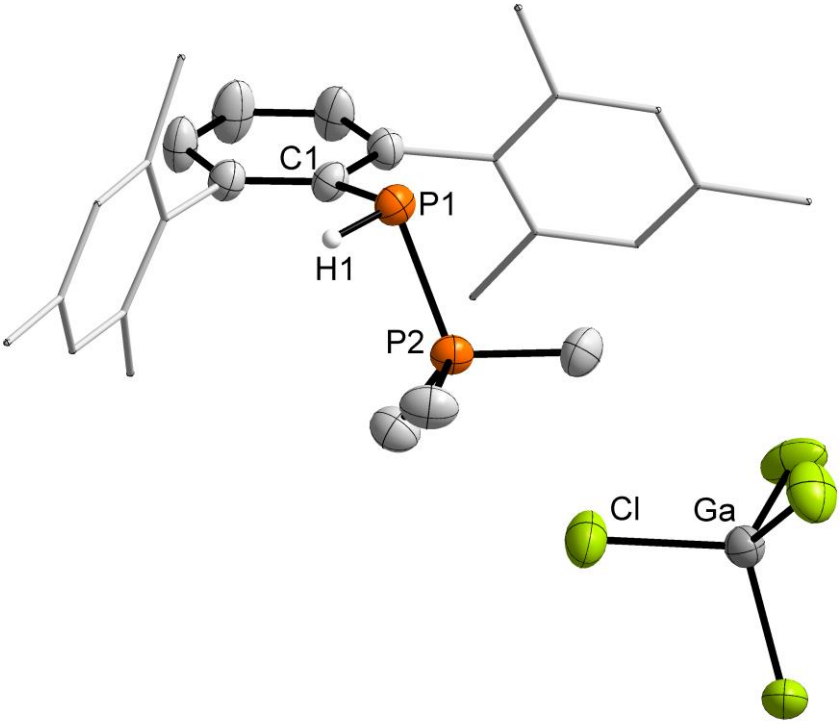

Figure S15: Molecular structure of the discrete ion pair **12:^{Mes}Ter** in the crystal. Selected bond lengths [pm] and angles [°]: C1-P1 184.07(42), P1-P2 218.68(15), C1-P1-P2 107.04(14).

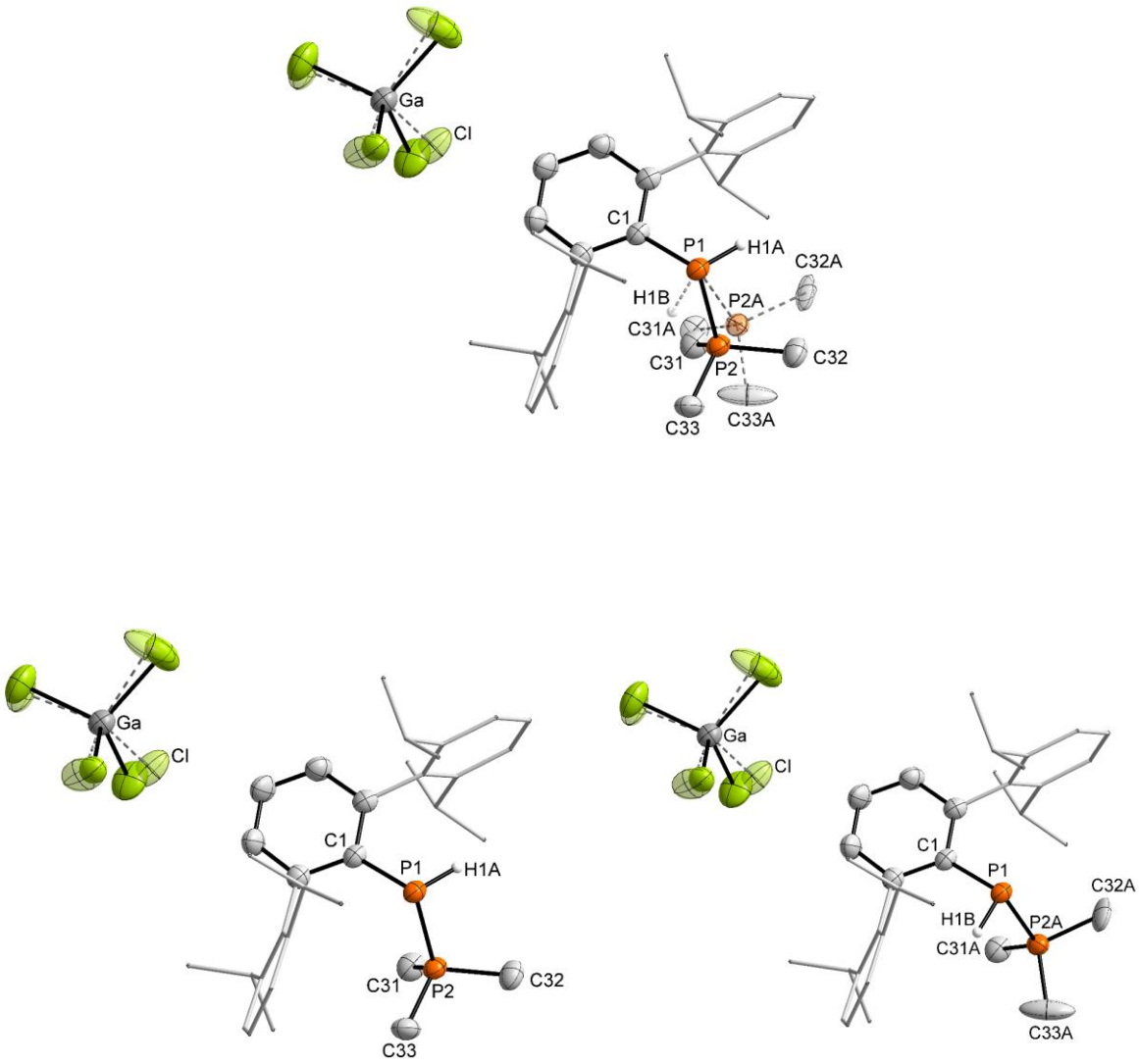

Figure S16: Molecular structure of the discrete ion pair **12:^{Dip}Ter** in the crystal including disordered parts. Selected bond lengths [pm] and angles [°]: C1-P1 184.49(29), P1-P2 216.92(18), C1-P1-P2 106.71(9).

Summary of X-ray Crystallographic Refinement:

Table S2: Crystallographic details #1. * = twin refinement was employed (see special refinement details).

Compound	**1:^{Dip}Ter***	**2:Mes***
Empirical formula	$C_{30}H_{39}OP$	$C_{36}H_{60}OP_2$
Formula weight	446.58	570.78
Temperature/K	150(2)	150(2)
Crystal system	monoclinic	monoclinic
Space group	$P2_1/n$	$P2_1/n$
a/Å	12.2456(2)	11.2606(7)
b/Å	16.9887(3)	10.4141(8)
c/Å	13.3272(2)	30.070(2)
α/°	90	90
β/°	100.3830(8)	99.501(5)
γ/°	90	90
Volume/Å^3	2727.15(8)	3477.9(4)
Z	4	4
ρ_{calc}g/cm^3	1.088	1.090
μ/mm^{-1}	0.119	1.304
F(000)	968.0	1256.0
Crystal size/mm^3	0.43 × 0.23 × 0.17	0.19 × 0.04 × 0.03
Radiation	MoKα (λ = 0.71073)	CuKα (λ = 1.54178)
2Θ range for data collection/°	3.924 to 57.998	5.96 to 120.142
Index ranges	-16 ≤ h ≤ 12, -22 ≤ k ≤ 23, -18 ≤ l ≤ 18	-12 ≤ h ≤ 12, 0 ≤ k ≤ 11, 0 ≤ l ≤ 33
Reflections collected	33442	5098*
Independent reflections	7254 [R_{int} = 0.0251, R_{sigma} = 0.0233]	5098 [R_{int} = n/a*, R_{sigma} = 0.1200]
Data/restraints/parameters	7254/0/305	5098/0/371
Goodness-of-fit on F^2	1.057	1.036
Final R indexes [I>=2σ (I)]	R_1 = 0.0461, wR_2 = 0.1221	R_1 = 0.0848, wR_2 = 0.2077
Final R indexes [all data]	R_1 = 0.0581, wR_2 = 0.1318	R_1 = 0.1141, wR_2 = 0.2235
Largest diff. peak/hole / e Å^{-3}	0.43/-0.26	0.52/-0.33
Absolute structure parameter	-	-
CCDC #	2166339	2166340

Table S3: Crystallographic details #2.

Compound	**3:^{Mes}Ter**	**4:Mes***	**4:^{Mes}Ter**
Empirical formula	$C_{24}H_{27}Cl_3GaOP$	$C_{18}H_{31}GaI_3OP$	$C_{24}H_{27}GaI_3OP$
Formula weight	538.49	744.82	812.84
Temperature/K	150(2)	150(2)	150(2)
Crystal system	orthorhombic	orthorhombic	triclinic
Space group	*Aea*2	*Pmn*2$_1$	*P*-1
a/Å	19.5931(10)	14.8750(8)	10.8322(12)
b/Å	19.2681(9)	7.1776(5)	11.4626(12)
c/Å	13.4080(7)	11.9265(6)	13.0010(14)
α/°	90	90	107.115(8)
β/°	90	90	104.929(8)
γ/°	90	90	99.870(9)
Volume/Å^3	5061.8(4)	1273.35(13)	1436.3(3)
Z	8	2	2
ρ_{calc}g/cm^3	1.413	1.943	1.880
μ/mm^{-1}	1.481	4.784	4.251
F(000)	2208.0	704.0	768.0
Crystal size/mm^3	0.29 × 0.27 × 0.23	0.31 × 0.23 × 0.22	0.31 × 0.28 × 0.19
Radiation	MoKα (λ = 0.71073)	MoKα (λ = 0.71073)	MoKα (λ = 0.71073)
2Θ range for data collection/°	4.158 to 54.996	4.378 to 56.98	3.468 to 50.992
Index ranges	-25 ≤ h ≤ 25, -24 ≤ k ≤ 24, -17 ≤ l ≤ 17	-19 ≤ h ≤ 19, -9 ≤ k ≤ 9, -16 ≤ l ≤ 15	-12 ≤ h ≤ 13, -13 ≤ k ≤ 13, -15 ≤ l ≤ 14
Reflections collected	36150	17392	14121
Independent reflections	5634 [R_{int} = 0.0262, R_{sigma} = 0.0211]	3232 [R_{int} = 0.0239, R_{sigma} = 0.0134]	5355 [R_{int} = 0.0124, R_{sigma} = 0.0162]
Data/restraints/parameters	5634/1/286	3232/1/144	5355/3/282
Goodness-of-fit on F^2	0.997	1.130	1.110
Final R indexes [I>=2σ (I)]	R_1 = 0.0250, wR_2 = 0.0590	R_1 = 0.0175, wR_2 = 0.0445	R_1 = 0.0450, wR_2 = 0.1294
Final R indexes [all data]	R_1 = 0.0293, wR_2 = 0.0597	R_1 = 0.0177, wR_2 = 0.0446	R_1 = 0.0550, wR_2 = 0.1334
Largest diff. peak/hole / e Å^{-3}	0.46/-0.15	1.07/-0.31	3.38/-1.59
Absolute structure parameter	0.066(10)	0.174(18)	-
CCDC #	2166341	2166342	2166343

Table S4: Crystallographic details #3.

Compound	**5:Mes***	**6:Mes***	**6:^{Dip}Ter**·2.7DCM
Empirical formula	$C_{36}H_{31}BF_{15}PO$	$C_{21}H_{38}Cl_3GaP_2$	$C_{35.7}H_{51.4}Cl_{8.4}GaP_2$
Formula weight	806.39	528.52	910.01
Temperature/K	150(2)	150(2)	150(2)
Crystal system	triclinic	monoclinic	monoclinic
Space group	*P*-1	$P2_1/n$	$P2_1/n$
a/Å	10.1182(9)	8.8319(9)	11.0543(14)
b/Å	10.1216(9)	29.260(2)	25.215(2)
c/Å	19.4301(18)	10.3380(11)	16.013(3)
α/°	88.8323(25)	90	90
β/°	82.0559(25)	94.085(8)	96.350(12)
γ/°	63.1869(22)	90	90
Volume/Å^3	1756.9(3)	2664.8(5)	4436.1(10)
Z	2	4	4
ρ_{calc}g/cm^3	1.524	1.317	1.363
μ/mm^{-1}	0.188	1.459	1.222
F(000)	820.0	1104.0	1878.0
Crystal size/mm^3	0.35 × 0.19 × 0.03	0.06 × 0.18 × 0.24	0.31 × 0.21 × 0.16
Radiation	MoKα (λ = 0.71073)	MoKα (λ = 0.71073)	MoKα (λ = 0.71073)
2Θ range for data collection/°	4.238 to 60	4.188 to 53.996	3.026 to 52.996
Index ranges	-14 ≤ h ≤ 14, -14 ≤ k ≤ 14, -27 ≤ l ≤ 27	-11 ≤ h ≤ 11, -28 ≤ k ≤ 37, -13 ≤ l ≤ 10	-12 ≤ h ≤ 13, -31 ≤ k ≤ 31, -20 ≤ l ≤ 20
Reflections collected	81470	15355	57514
Independent reflections	10248 [R_{int} = 0.0365, R_{sigma} = 0.0244]	5757 [R_{int} = 0.0254, R_{sigma} = 0.0465]	9185 [R_{int} = 0.0277, R_{sigma} = 0.0173]
Data/restraints/parameters	10248/0/504	5757/30/281	9185/6/458
Goodness-of-fit on F^2	1.018	0.924	1.080
Final R indexes [I>=2σ (I)]	R_1 = 0.0408, wR_2 = 0.0971	R_1 = 0.0372, wR_2 = 0.0847	R_1 = 0.0374, wR_2 = 0.1173
Final R indexes [all data]	R_1 = 0.0588, wR_2 = 0.1083	R_1 = 0.0623, wR_2 = 0.0889	R_1 = 0.0451, wR_2 = 0.1206
Largest diff. peak/hole / e Å^{-3}	0.44/-0.33	0.71/-0.35	0.80/-0.46
Absolute structure parameter	-	-	-
CCDC #	2166344	2166345	2166346

Table S5: Crystallographic details #4.

Compound	**7:Mes***	**8:Mes***	**9:^{Mes}Ter**
Empirical formula	$C_{21}H_{38}GaI_3P_2$	$C_{21}H_{38}Cl_{2.13}GaI_{0.86}P_2$	$C_{54}H_{68}Cl_6Ga_2P_4$
Formula weight	802.87	607.63	1193.10
Temperature/K	150(2)	150(2)	150(2)
Crystal system	monoclinic	monoclinic	triclinic
Space group	$P2_1/n$	$P2_1/n$	P-1
a/Å	9.1316(9)	8.9087(6)	12.9253(12)
b/Å	29.821(2)	29.337(2)	21.2504(19)
c/Å	10.5682(10)	10.4157(8)	24.984(2)
α/°	90	90	109.535(7)
β/°	91.854(8)	92.781(6)	97.030(7)
γ/°	90	90	90.092(7)
Volume/Å^3	2876.4(4)	2718.9(3)	6412.0(10)
Z	4	4	4
ρ_{calc}g/cm^3	1.854	1.484	1.236
μ/mm^{-1}	4.294	2.327	1.221
F(000)	1536	1229.0	2464.0
Crystal size/mm^3	0.2 × 0.18 × 0.06	0.37 × 0.12 × 0.10	0.2 × 0.18 × 0.1
Radiation	MoKα (λ = 0.71073)	MoKα (λ = 0.71073)	MoKα (λ = 0.71073)
2Θ range for data collection/°	2.732 to 50.996	4.154 to 50.996	3.096 to 51
Index ranges	-10 ≤ h ≤ 11, -32 ≤ k ≤ 36, -12 ≤ l ≤ 12	-10 ≤ h ≤ 10, -35 ≤ k ≤ 35, -12 ≤ l ≤ 12	-15 ≤ h ≤ 15, -25 ≤ k ≤ 25, -30 ≤ l ≤ 30
Reflections collected	22699	22538	71835
Independent reflections	5340 [R_{int} = 0.0321, R_{sigma} = 0.0320]	5049 [R_{int} = 0.0240, R_{sigma} = 0.0252]	23897 [R_{int} = 0.0798, R_{sigma} = 0.1210]
Data/restraints/parameters	5340/0/256	5049/25/272	23897/189/1147
Goodness-of-fit on F^2	1.054	1.103	0.873
Final R indexes [I>=2σ (I)]	R_1 = 0.0550, wR_2 = 0.1676	R_1 = 0.0472, wR_2 = 0.1211	R_1 = 0.0691, wR_2 = 0.1642
Final R indexes [all data]	R_1 = 0.0755, wR_2 = 0.1770	R_1 = 0.0600, wR_2 = 0.1245	R_1 = 0.1467, wR_2 = 0.1839
Largest diff. peak/hole / e Å^{-3}	1.47/-3.07	1.24/-0.56	0.97/-0.65
Absolute structure parameter	-	-	-
CCDC #	2166347	2166348	2166512

Table S6: Crystallographic details #5.

Compound	**10:Mes***	**11:Mes***
Empirical formula	$C_{21}H_{39}GaI_4P_2$	$C_{42}H_{78}Ga_4I_{10}O_2P_4$
Formula weight	930.78	2286.80
Temperature/K	150(2)	150(2)
Crystal system	monoclinic	triclinic
Space group	$P2_1/c$	P-1
a/Å	10.074(3)	10.1303(6)
b/Å	13.570(3)	12.8964(8)
c/Å	23.577(7)	14.0935(9)
α/°	90	81.618(2)
β/°	96.77(2)	81.678(2)
γ/°	90	71.362(2)
Volume/Å^3	3200.7(15)	1716.55(18)
Z	4	1
ρ_{calc}g/cm^3	1.932	2.212
μ/mm^{-1}	4.825	6.171
F(000)	1752.0	1060.0
Crystal size/mm^3	0.06 × 0.03 × 0.01	0.22 × 0.08 × 0.011
Radiation	MoKα (λ = 0.71073)	MoKα (λ = 0.71073)
2Θ range for data collection/°	3.468 to 53.998	2.938 to 57.754
Index ranges	-12 ≤ h ≤ 12, -17 ≤ k ≤ 17, -30 ≤ l ≤ 30	-13 ≤ h ≤ 13, -17 ≤ k ≤ 17, -19 ≤ l ≤ 19
Reflections collected	6978	69738
Independent reflections	6978 [R_{int} = 0.0435, R_{sigma} = 0.0735]	8990 [R_{int} = 0.0447, R_{sigma} = 0.0271]
Data/restraints/parameters	6978/0/269	8990/0/296
Goodness-of-fit on F^2	0.748	1.027
Final R indexes [I>=2σ (I)]	R_1 = 0.0307, wR_2 = 0.0546	R_1 = 0.0355, wR_2 = 0.0897
Final R indexes [all data]	R_1 = 0.0704, wR_2 = 0.0600	R_1 = 0.0482, wR_2 = 0.0971
Largest diff. peak/hole / e Å^{-3}	0.81/-0.72	3.02/-2.50
Absolute structure parameter	-	-
CCDC #	2166349	2166350

Table S7: Crystallographic details #6.

Compound	**12:Mes***	**12:^{Mes}Ter**	**12:^{Dip}Ter**
Empirical formula	$C_{21}H_{39}Cl_4GaP_2$	$C_{27}H_{35}Cl_4GaP_2$	$C_{33}H_{47}Cl_4GaP_2$
Formula weight	564.98	633.01	717.16
Temperature/K	150(2)	150(2)	150(2)
Crystal system	monoclinic	monoclinic	triclinic
Space group	$P2_1/n$	$P2_1/n$	P-1
a/Å	10.6965(3)	8.2634(4)	9.7565(3)
b/Å	10.6920(2)	13.3291(7)	11.7069(4)
c/Å	24.8307(8)	28.2426(13)	17.4299(6)
α/°	90	90	92.053(2)
β/°	101.014(3)	91.478(4)	104.767(2)
γ/°	90	90	104.411(2)
Volume/Å^3	2787.50(13)	3109.7(3)	1853.99(11)
Z	4	4	2
ρ_{calc}g/cm^3	1.346	1.352	1.285
μ/mm^{-1}	1.492	1.346	4.629
F(000)	1176.0	1304.0	748.0
Crystal size/mm^3	0.27 × 0.14 × 0.12	0.23 × 0.21 × 0.13	0.34 × 0.23 × 0.11
Radiation	MoKα (λ = 0.71073)	MoKα (λ = 0.71073)	CuKα (λ = 1.54178)
2Θ range for data collection/°	3.342 to 58.464	2.884 to 53	5.272 to 133.226
Index ranges	-14 ≤ h ≤ 14, -14 ≤ k ≤ 12, -34 ≤ l ≤ 33	-10 ≤ h ≤ 10, -16 ≤ k ≤ 16, -35 ≤ l ≤ 35	-11 ≤ h ≤ 11, -13 ≤ k ≤ 13, -20 ≤ l ≤ 20
Reflections collected	42166	42012	23411
Independent reflections	7539 [R_{int} = 0.0234, R_{sigma} = 0.0201]	6455 [R_{int} = 0.0278, R_{sigma} = 0.0202]	6527 [R_{int} = 0.0429, R_{sigma} = 0.0396]
Data/restraints/parameters	7539/0/269	6455/0/320	6527/24/451
Goodness-of-fit on F^2	0.987	1.164	1.023
Final R indexes [I>=2σ (I)]	R_1 = 0.0280, wR_2 = 0.0737	R_1 = 0.0483, wR_2 = 0.1351	R_1 = 0.0406, wR_2 = 0.1045
Final R indexes [all data]	R_1 = 0.0386, wR_2 = 0.0759	R_1 = 0.0596, wR_2 = 0.1378	R_1 = 0.0480, wR_2 = 0.1108
Largest diff. peak/hole / e Å^{-3}	0.50/-0.21	0.73/-0.31	0.50/-0.51
Absolute structure parameter	-	-	-
CCDC #	2166351	2166511	2166352

3 Syntheses of compounds

Additional Information. All starting materials synthesized by literature procedures (see table S1) were synthesized with slight modifications. All analytical data was in good agreement with those published in earlier works. In this work, the following abbreviations are used for the organic framework around P.

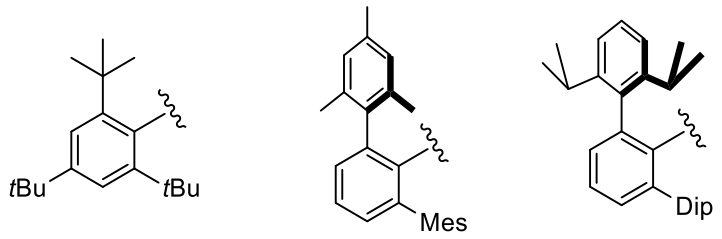

Mes* ^{Mes}Ter ^{Dip}Ter

Figure S17: *Structural motifs and their abbreviations relevant for this ESI.*

As the phospha-Wittig reagents are sensitive towards light, we recommend wrapping all flasks with tinfoil and switching off the lights in the laboratory and fume hoods. Especially the ^{Mes}Ter derivative is experienced to decompose quickly due to light sensitivity. Also, thermal instability is experienced, especially when adding Lewis acids. The respective Lewis acid-base adducts show an **extremely (!)** high sensitivity towards traces of moisture, which is why impurities in some cases could not be suppressed even with rigorous Schlenk techniques, freshly dried solvents and *J*-Young NMR tubes with PTFE valves. Therefore, in some cases, not all analytic data has been provided and/or impurities are marked with an arterisk/hashtag in the respective spectra. The provided NMR spectra were processed and analyzed with the MestReNova[9] software package. Resonances are depicted with the following abbreviations: s, singlet; d, doublet; t, triplet; q, quartet; hept, septet; dec, decet; m, multiplet; dd, doublet of doublets; dm, doublet of multiplets; doct, doublet of octets; ddt, doublet of doublet of triplets; tt, triplet of triplets; tm, triplet of multiplets; ps, pseudo; br, broad. IR spectra were

processed and analysed using either the OPUS[10] and/or the OMNIC[11] software package.

Important Note: The highly reactive nature of the compounds prevented the collection of satisfactory CHN-data. The deviations are currently in between 3 to 5% for both C and H values. Even though in very rare cases suitable values could be observed, we refuse to provide these because in our eyes there is no evidence beyond a reasonable doubt that the material is pure *at the point of measurement*. However, the state-of-the-art characterization such as with NMR spectroscopy (see displayed spectra) demonstrates the existence and in the cases of stable compounds analytical pureness of the herein published compounds if not stated otherwise. We are aware that Elemental Analysis is an important purity control, but reliable results were not obtained. As CHN analysis is unfortunately already prone to manipulations (see ref.[12]) we decided to not provide any values and provide high-resolution mass spectrometry data for all compounds.

3.1 Mes*P(H)$_2$O (1:Mes*)

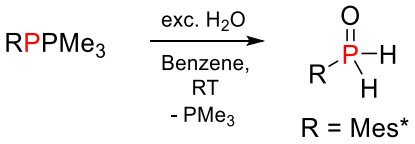

A 0.050 g portion of Mes*PPMe$_3$ (0.14 mmol, 1.0 eq) is dissolved in 3 mL of benzene. One drop of water (excess) is then carefully added to the solution. Upon stirring the solution for 30 min., the characteristic yellow colour fades and the reaction is then stopped. The solvent is removed under reduced pressure to obtain a beige powder. Careful(!) washing with 1 mL of *n*-pentane at -78°C followed by thorough drying *in vacuo* yields **1:Mes*** as a colorless powder (76%, 0.106 mmol, 0.032 g).

Mes*P(O)D$_2$ (1:Mes*-*d*$_2$)

Mes*PPMe$_3$ (0.018 g, 0.05 mmol) was dissolved in 0.6 mL of C$_6$D$_6$ followed by addition of one drop of D$_2$O. The reaction solution was shaken and regularly controlled by ^{1}H and ^{31}P{^{1}H} NMR spectroscopy which revealed conversion to Mes*P(O)D$_2$ (**1:Mes*-*d*$_2$**) accompanied by release of PMe$_3$.

^{1}H NMR (C$_6$D$_6$, 300 MHz, 298K): δ = 7.61 (d, $^1J_{PH}$ = 474.7 Hz, 2H, P(*H*)$_2$O), 7.48 (d, *J* = 4.1 Hz, 2H, C*H*$_{Ar}$), 1.53+1.52 (s, 18H, C*H*$_3$), 1.20 (s, 9H, C*H*$_3$) ppm. **^{13}C{^{1}H} NMR** (C$_6$D$_6$, 75.5 MHz, 298K): δ = 157.0 (d, $^2J_{P,C}$ = 8.5 Hz, *o*-*C*(CH$_3$)$_3$), 154.0 (d, $^4J_{PC}$ = 3.0 Hz, *p*-*C*(CH$_3$)$_3$), 126.9 (d, Ar*C*$_{ipso}$)*, 123.5 (d, $^3J_{PC}$ = 12.1 Hz, Ar*C*H), 38.8 (d, $^3J_{PC}$ = 3.7 Hz, *o*-*C*(CH$_3$)$_3$), 35.2 (*p*-*C*(CH$_3$)$_3$), 33.9 (*o*-C(*C*H$_3$)$_3$), 31.1 (s, *p*-C(*C*H$_3$)$_3$), ppm. * = overlap with C$_6$D$_6$ signal and assigned with a ^{1}H/^{13}C HMBC spectrum. **^{31}P{^{1}H} NMR** (C$_6$D$_6$, 122 MHz, 298K): δ = -13.28 (s, *P*(H)$_2$O) ppm. **^{31}P NMR** (C$_6$D$_6$, 122 MHz, 298K): δ = -13.28 (t, $^1J_{PH}$ = 475.0 Hz, *P*(H)$_2$O) ppm. **IR** (ATR, cm^{-1}): 2956 (s), 2870 (m), 2436 ν_{sym}(P-H) (m), 1598 (m), 1536 (w), 1463 (m), 1414 (m), 1364 (m), 1283 (m), 1238 (m), 1215 (s), 1176 (vs), 1163 (s), 1127 (m), 1063 (m), 1026 (s), 926 (m), 909 (m), 878 (m), 805 (m), 758 (m), 719 (m), 676 (w), 653 (w), 608 (m), 493 (w), 474 (m), 436 (w). **MS** (ESI-TOF): expected: m/z =

295.2191 $[M+H]^+$; found: m/z = 295.2182 $[M+H]^+$. **EA**: calculated: C 73.43, H 10.61; found: C 73.68, H 10.47.

Mes*P(O)D_2

^{1}H NMR (300 MHz, C_6D_6, 298 K): δ = 1.20 (s, 9H, *p*-$C_q(CH_3)_3P$), 1.50 (s, 18H, *o*-$C_q(CH_3)_3P$), 7.47 (d, *J* = 4.2 Hz, 2H, CH_{Aryl}) ppm.

^{31}P{^{1}H} (122 MHz, C_6D_6, 298 K): δ = -13.7 (p, $^1J_{P,D}$ = 73.0 Hz) ppm.

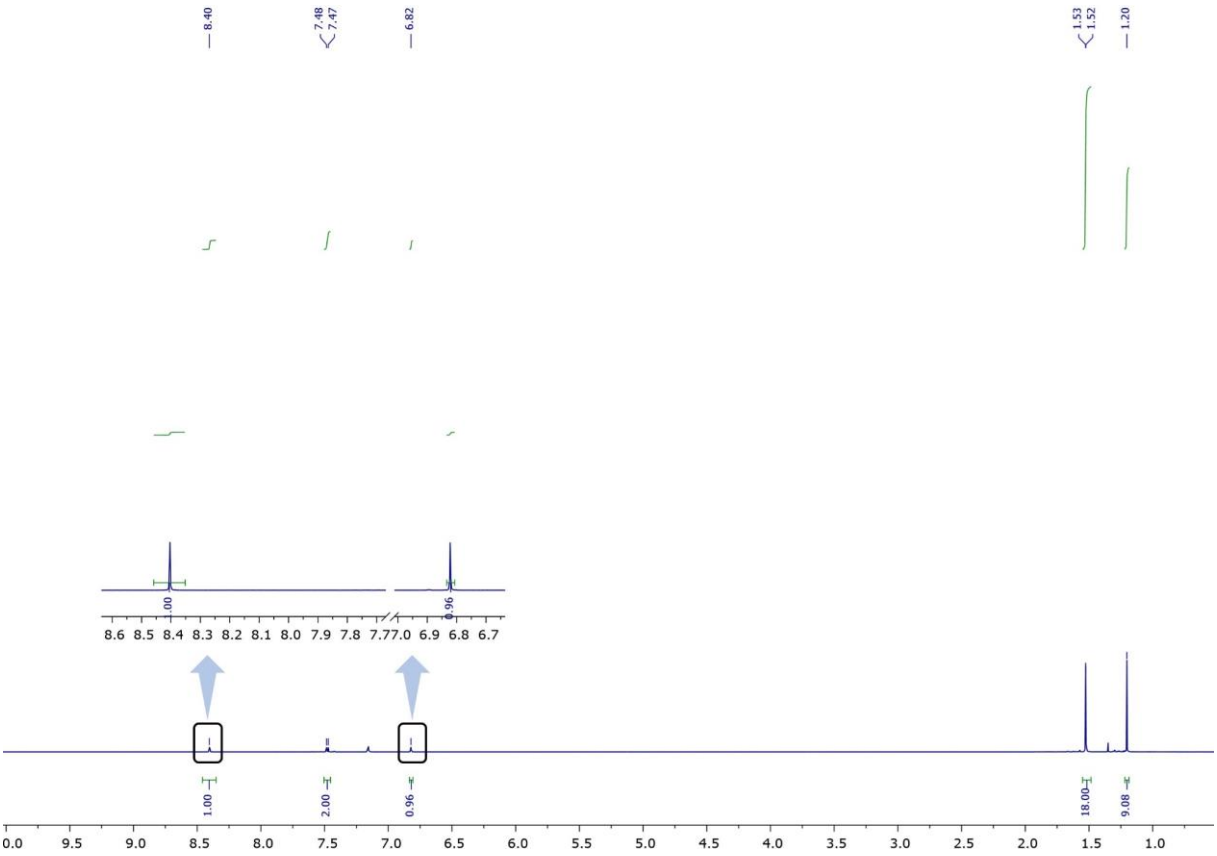

Figure S18: *^{1}H NMR of* ***1:Mes**** (given in ppm, C_6D_6, 300 MHz, 298K).

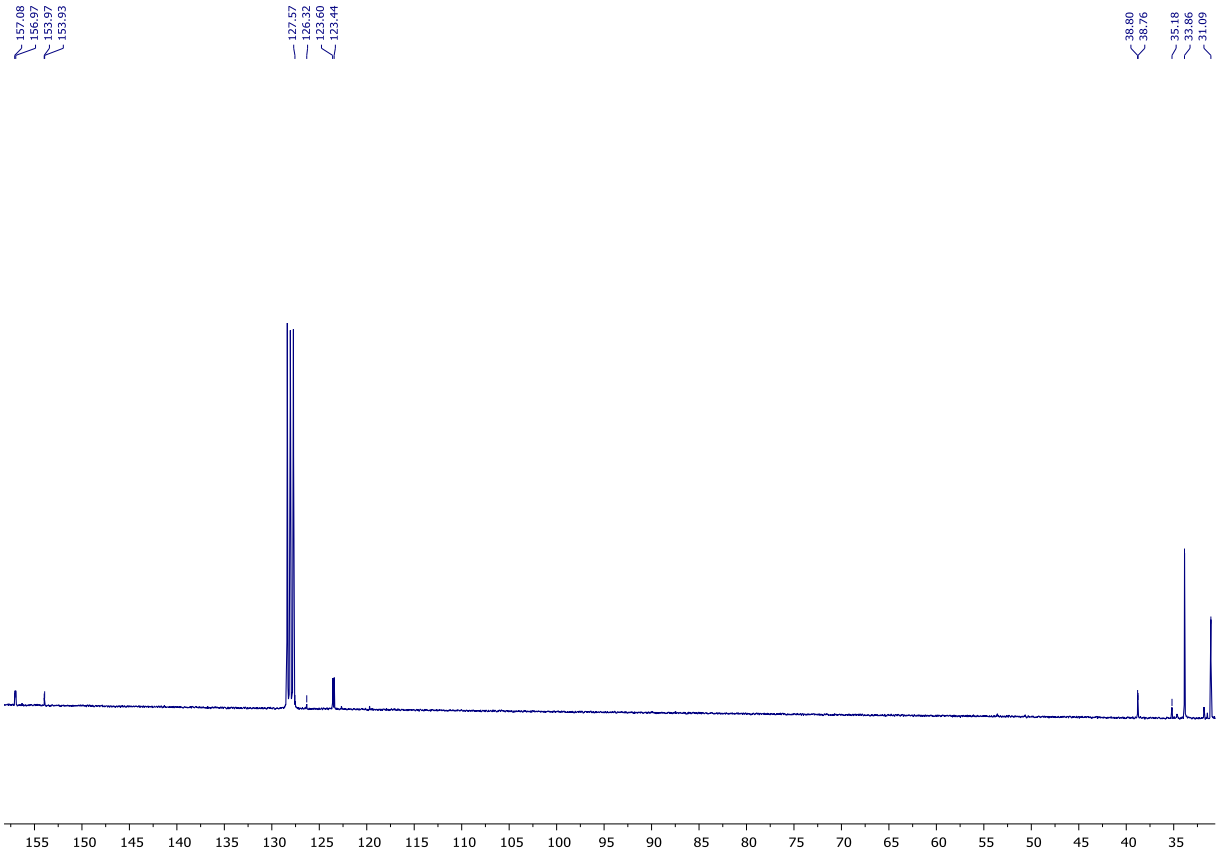

Figure S19: *$^{13}C\{^{1}H\}$ NMR of* ***1:Mes**** (given in ppm, C_6D_6, 75.5 MHz, 298K).

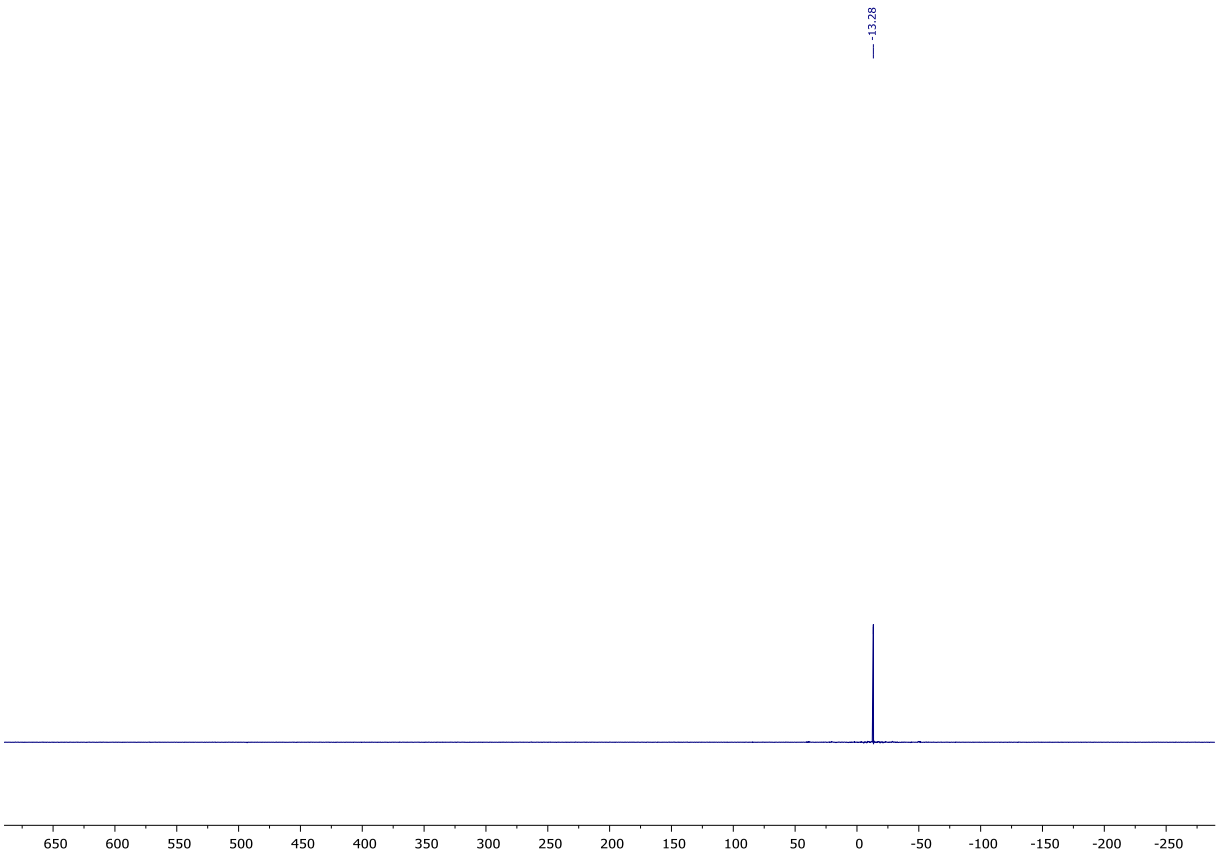

Figure S20: *$^{31}P\{^{1}H\}$ NMR of* ***1:Mes**** (given in ppm, C_6D_6, 122 MHz, 298K).

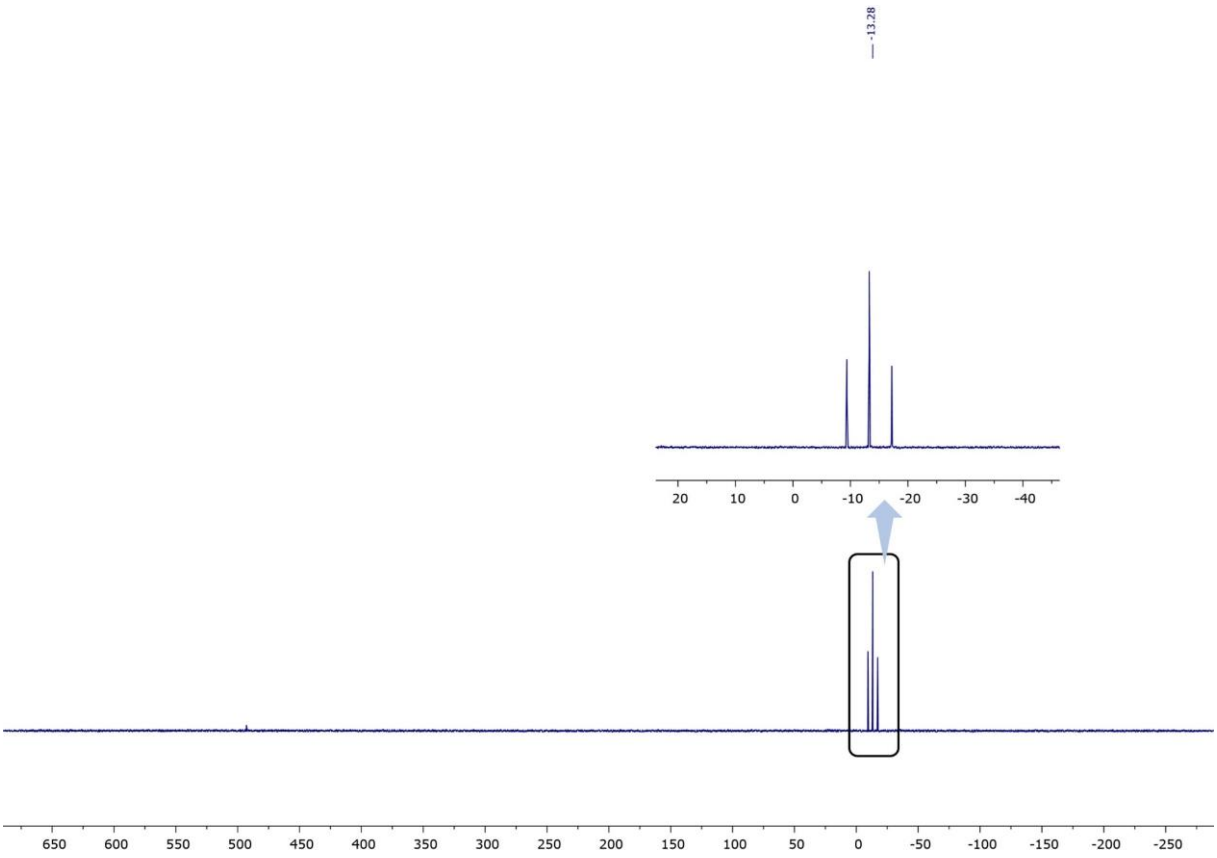

Figure S21: *^{31}P NMR of* ***1:Mes**** (given in ppm, C_6D_6, 122 MHz, 298K).

3.2 ^{Mes}TerP(H)$_2$O (1:^{Mes}Ter)

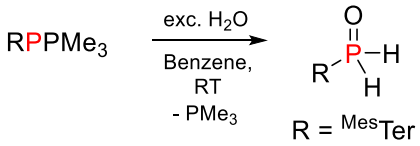

A 0.050 g portion of ^{Mes}TerPPMe$_3$ (0.12 mmol, 1.0 eq) is dissolved in 1.5 mL of benzene. One drop of water (excess) is then carefully added to the solution. Upon stirring the solution at ambient temperature overnight, the characteristic yellow colour fades and the reaction is then stopped. The solvent is removed under reduced pressure to obtain a beige powder. Careful(!) washing with 1 mL of *n*-pentane at ambient temperature followed by thorough drying *in vacuo* yields **1:^{Mes}Ter** as a slight beige powder (58%, 0.07 mmol, 0.025 g).

^{1}H NMR (C_6D_6, 300 MHz, 298K): δ = 7.18–7.12 (m, 1H, *p*-Ar*H*)*, 6.85–6.82 (m, 6H, *m*-*H* of Mes & *m*-Ar*H*), 6.69 (d, $^{1}J_{PH}$ = 476.5 Hz, 2H, P(*H*)$_2$O), 2.18 (s, 6H, *p*-C*H*$_3$ of Mes), 2.04 (s, 12H, *m*-C*H*$_3$ of Mes) ppm. *Overlap with C_6D_5H signal. **^{13}C{^{1}H} NMR** (C_6D_6, 75.5 MHz, 298K): δ = 146.5 (d, $^{1}J_{CP}$ = 11.0 Hz, Ar*C*$_{ipso}$), 138.0 (s, *p*–*C* of Mes), 136.6 (s, *m*–*C* of Mes), 136.4 (d, $^{2}J_{CP}$ = 5.9 Hz, *o*–Ar*C*), 133.3 (d, $^{3}J_{CP}$ = 1.3 Hz, Ar*C*$_q$ of Mes), 131.1 (s, *o*–*C* of Mes), 129.0 (d, $^{3}J_{CP}$ = 8.8 Hz, *m*–Ar*C*), 128.9 (s, *p*–Ar*C*), 21.2 (s, *p*-*C*H$_3$ of Mes), 21.1 (s, *m*-*C*H$_3$ of Mes) ppm. **^{31}P{^{1}H} NMR** (C_6D_6, 121.5 MHz, 298K): δ = -16.49 (s, *P*(H)$_2$O) ppm. **^{31}P NMR** (C_6D_6, 122 MHz, 298K): δ = -16.49 (t, $^{1}J_{PH}$ = 476.7 Hz, *P*(H)$_2$O) ppm. **IR** (ATR, cm^{-1}): 2965 (w), 2916 (w), 2858 (w), 2396 ν_{sym}(P-H) (w), 1612 (w), 1567 (w), 1482 (w), 1449 (s), 1377 (w), 1304 (w), 1244 (w), 1179 (s), 1167 (vs), 1124 (s), 1098 (w), 1085 (w), 1056 (w), 1022 (s), 1001 (w), 903 (w), 860 (w), 841 (s), 805 (s), 750 (s), 735 (m), 698 (s), 589 (m), 560 (w), 520 (m), 500 (m), 451 (m). **MS** (HR, ESI$^+$) calc. for $C_{24}H_{28}O_1P_1$ $[M+H]^+$ (found): 363.1878 (363.1880); calc. for $C_{24}H_{27}O_1P_1Na_1$ $[M+Na]^+$ (found): 385.1692 (385.1701).

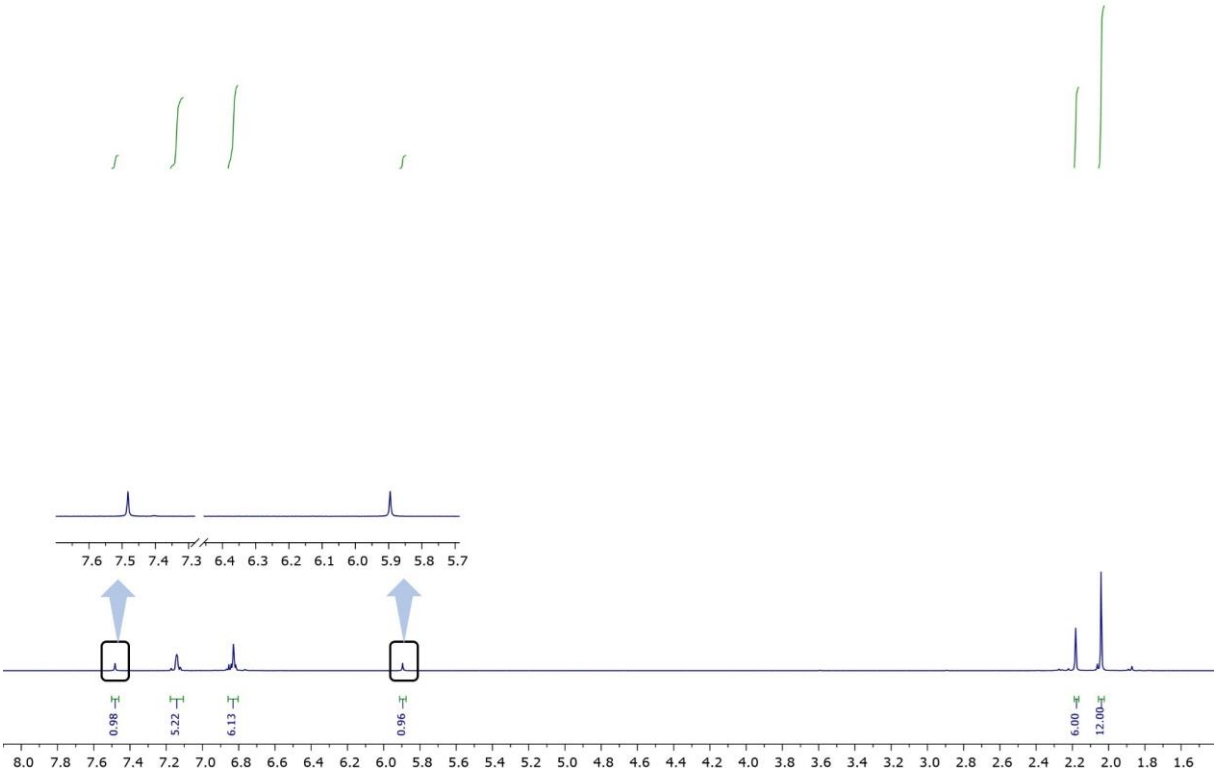

Figure S22: *^{1}H NMR of* ***1:^{Mes}Ter*** (given in ppm, C_6D_6, 300 MHz, 298K).

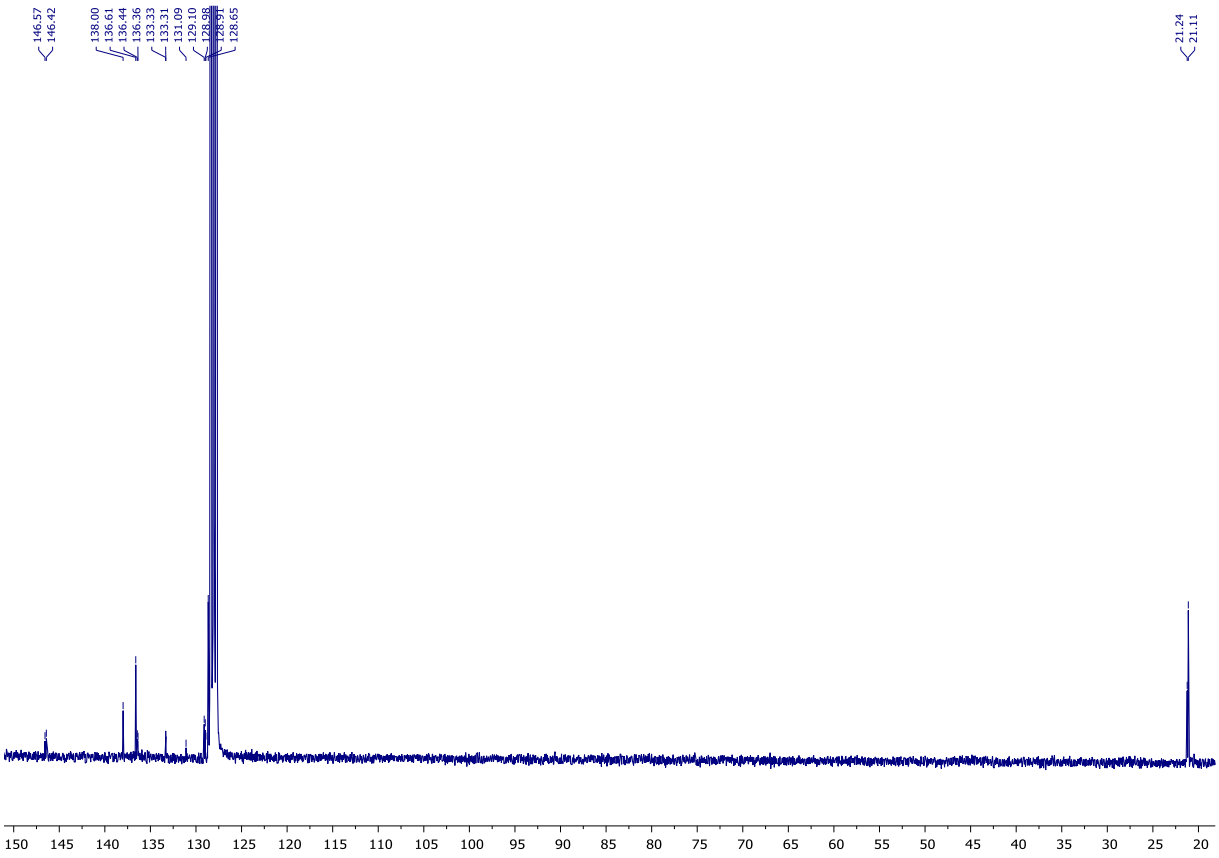

Figure S23: *$^{13}C\{^{1}H\}$ NMR of* ***1:^{Mes}Ter*** (given in ppm, C_6D_6, 75.5 MHz, 298K).

Figure S24: *$^{31}P\{^{1}H\}$ NMR of* ***1:^{Mes}Ter*** (given in ppm, C_6D_6, 122 MHz, 298K).

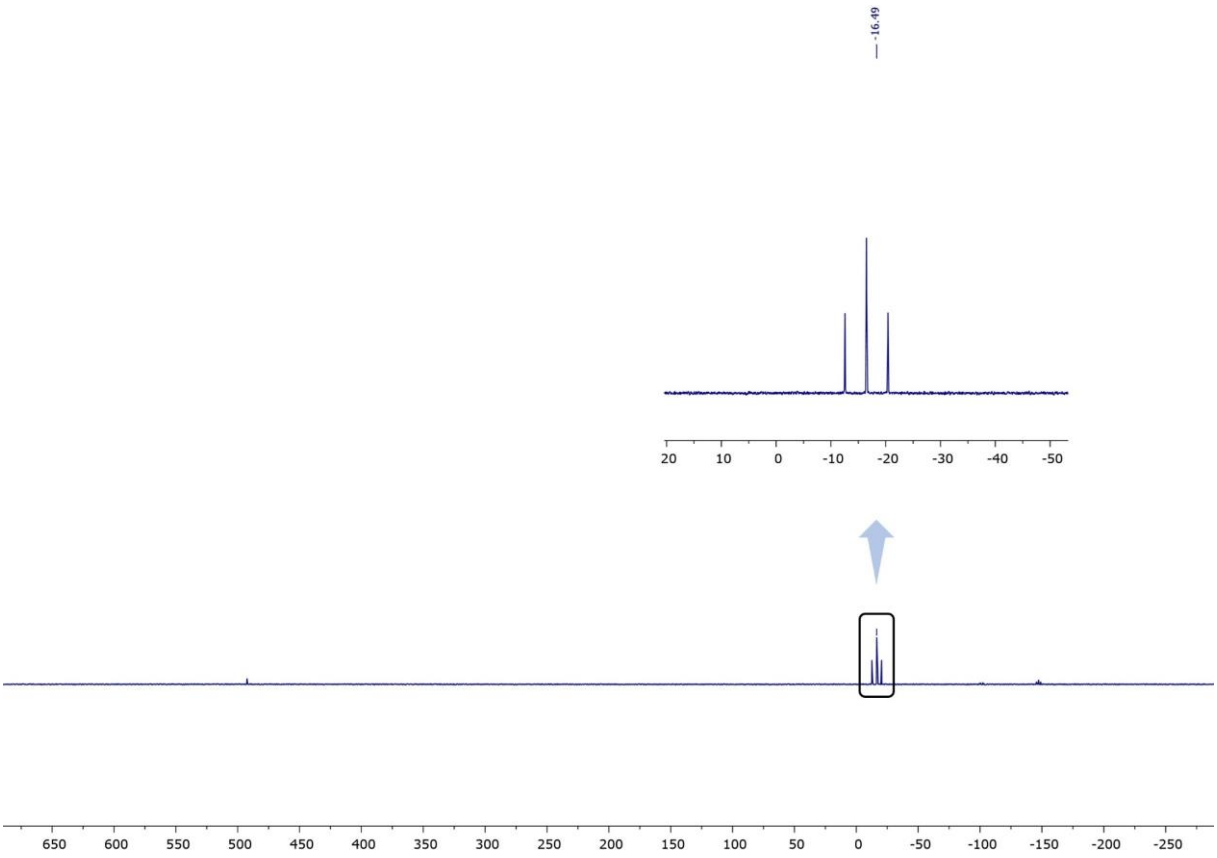

Figure S25: *^{31}P NMR of* ***1:^{Mes}Ter*** (given in ppm, C_6D_6, 122 MHz, 298K).

3.3 ^{Dip}TerP(H)$_2$O (1:^{Dip}Ter)

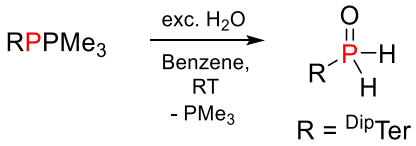

A 0.050 g portion of ^{Dip}TerPPMe$_3$ (0.1 mmol, 1.0 eq) is dissolved in 2 mL of benzene. One drop of water (excess) is then carefully added to the solution. Upon stirring the solution at ambient temperature overnight, the characteristic yellow colour fades and the reaction is then stopped. The solvent is removed under reduced pressure to obtain a beige powder. Careful(!) washing with 1 mL of *n*-pentane at -78°C followed by thorough drying *in vacuo* yields **1:^{Dip}Ter** as a slight beige powder (69%, 0.069 mmol, 0.031 g). By layering a C_6D_6 solution of **1:^{Dip}Ter** with *n*-pentane, suitable crystals for SC-XRD were obtained in the shape of colorless blocks.

^{1}H NMR (C_6D_6, 400 MHz, 298K): δ = 7.33–7.29 (m, 2H, *Ar*H), 7.18 (s, 2H, *Ar*H), 7.15–7.05 (m, 4H, *Ar*H)*, 6.85 (d, $^1J_{PH}$ = 476.6 Hz, 2H), 2.72 (hept, $^3J_{HH}$ = 6.8 Hz, C*H*(CH$_3$)$_2$, 2H), 1.25 (d, $^3J_{HH}$ = 6.9 Hz, CH(C*H*$_3$)$_2$, 12H), 1.04 (d, $^3J_{HH}$ = 6.8 Hz, CH(C*H*$_3$)$_2$, 12H). *overlap with C_6D_5H signal. **^{13}C{^{1}H} NMR** (C_6D_6, 101 MHz, 298K): δ = 147.4 (s, *o*–C$_{Dip}$),145.4 (d, $^1J_{CP}$ = 10.7 Hz, *ipso*–C$_{Aryl}$), 136.2 (d, $^3J_{CP}$ = 6.1 Hz, *ipso*–C of Dip), 131.8 (s, *p*–C$_{Aryl}$), 131.6 (d, $^3J_{CP}$ = 1.7 Hz, *m*–C$_{Aryl}$), 129.9 (d, $^2J_{CP}$ = 8.7 Hz, *o*–C$_{Aryl}$),129.7 (s, *p*-C of Dip), 123.3 (s, *m*–C of Dip), 31.4 (s, *C*H(CH$_3$)$_2$), 25.4 (s, CH(*C*H$_3$)$_2$), 22.9 (s, CH(*C*H$_3$)$_2$) ppm. **^{31}P{^{1}H} NMR** (C_6D_6, 162 MHz, 298K): δ = -16.27 (s, *P*(H)$_2$O) ppm. **^{31}P NMR** (C_6D_6, 122 MHz, 298K): δ = -16.27 (d, $^1J_{PH}$ = 476.7 Hz, *P*(H)$_2$O) ppm. **IR** (ATR, cm^{-1}): 2958 (s), 2925 (m), 2867 (m), 2359 ν_{sym}(P-H) (w), 1593 (w), 1577 (w), 1566 (w), 1459 (m), 1382 (m), 1362 (m), 1327 (w), 1310 (w), 1250 (w), 1194 (s), 1125 (w), 1103 (w), 1087 (w), 1055 (m), 1032 (s), 1002 (w), 967 (w), 935 (w), 900 (w), 883 (w), 829 (w), 805 (s), 756 (vs), 706 (m), 687 (w), 610 (w), 587 (w), 566 (w), 527 (w), 511 (w), 463 (w), 437 (s). **MS** (HR, ESI$^+$) calc. for $C_{30}H_{40}O_1P_1$ [M+H]$^+$ (found): 447.2817 (447.2824); calc. for $C_{30}H_{39}Na_1O_1P_1$ [M+Na]$^+$ (found): 469.2631 (469.2641).

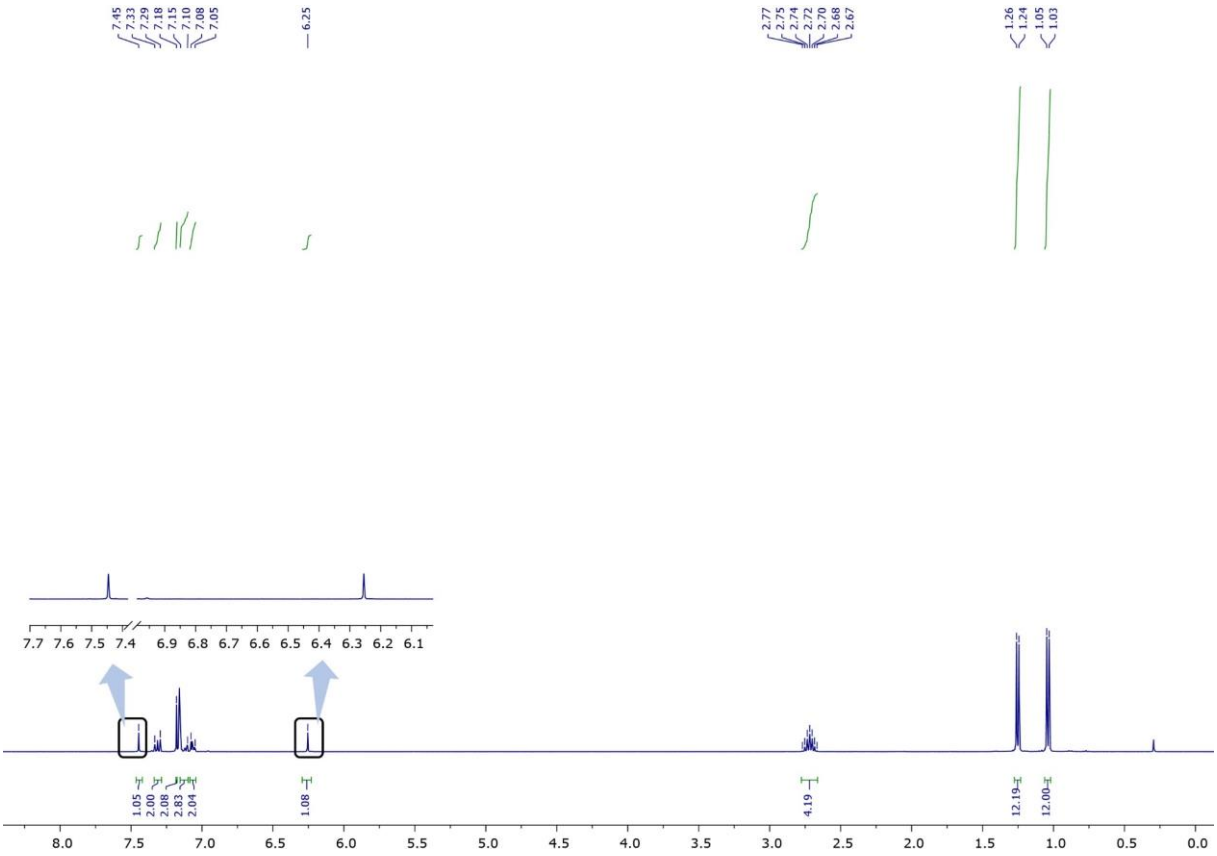

Figure S26: *^{1}H NMR of* ***1:^{Dip}Ter*** (given in ppm, C_6D_6, 400 MHz, 298K).

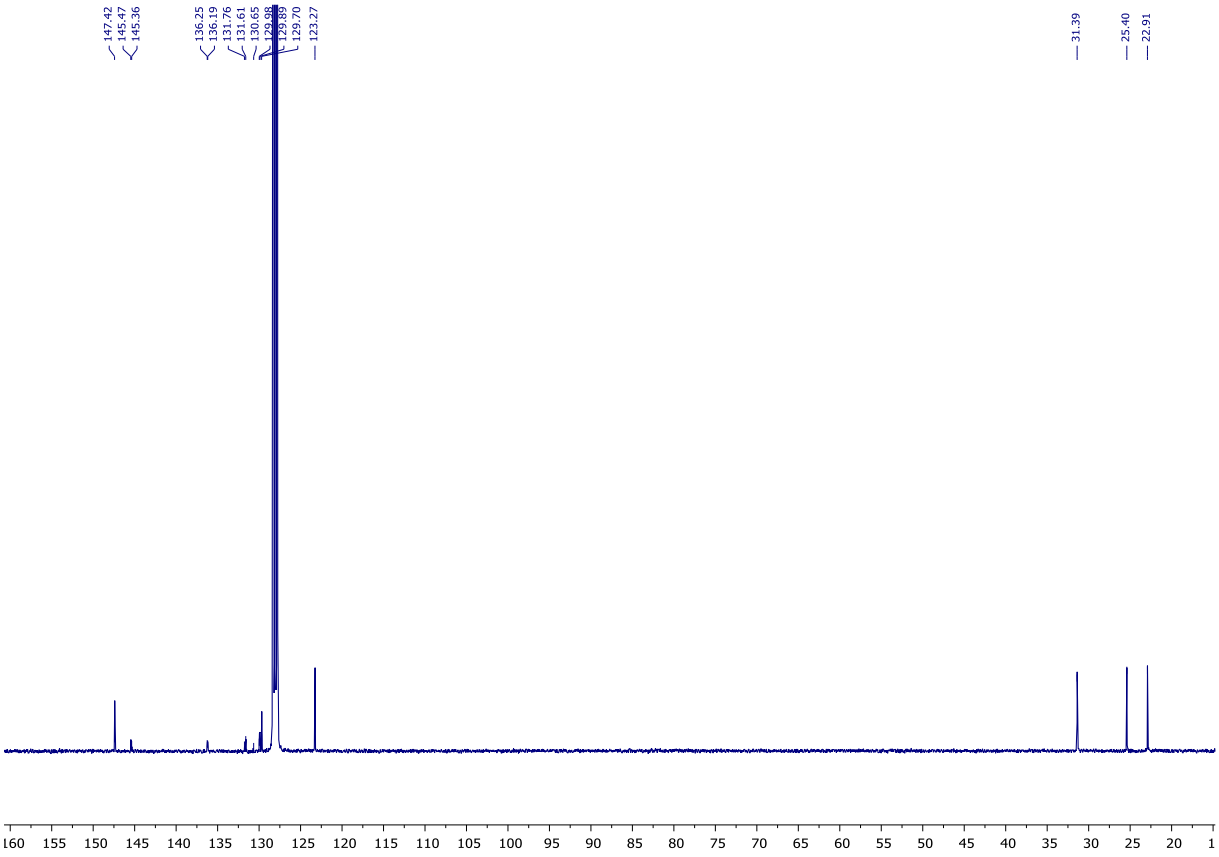

Figure S27: *$^{13}C\{^{1}H\}$ NMR of* ***1:^{Dip}Ter*** (given in ppm, C_6D_6, 101 MHz, 298K).

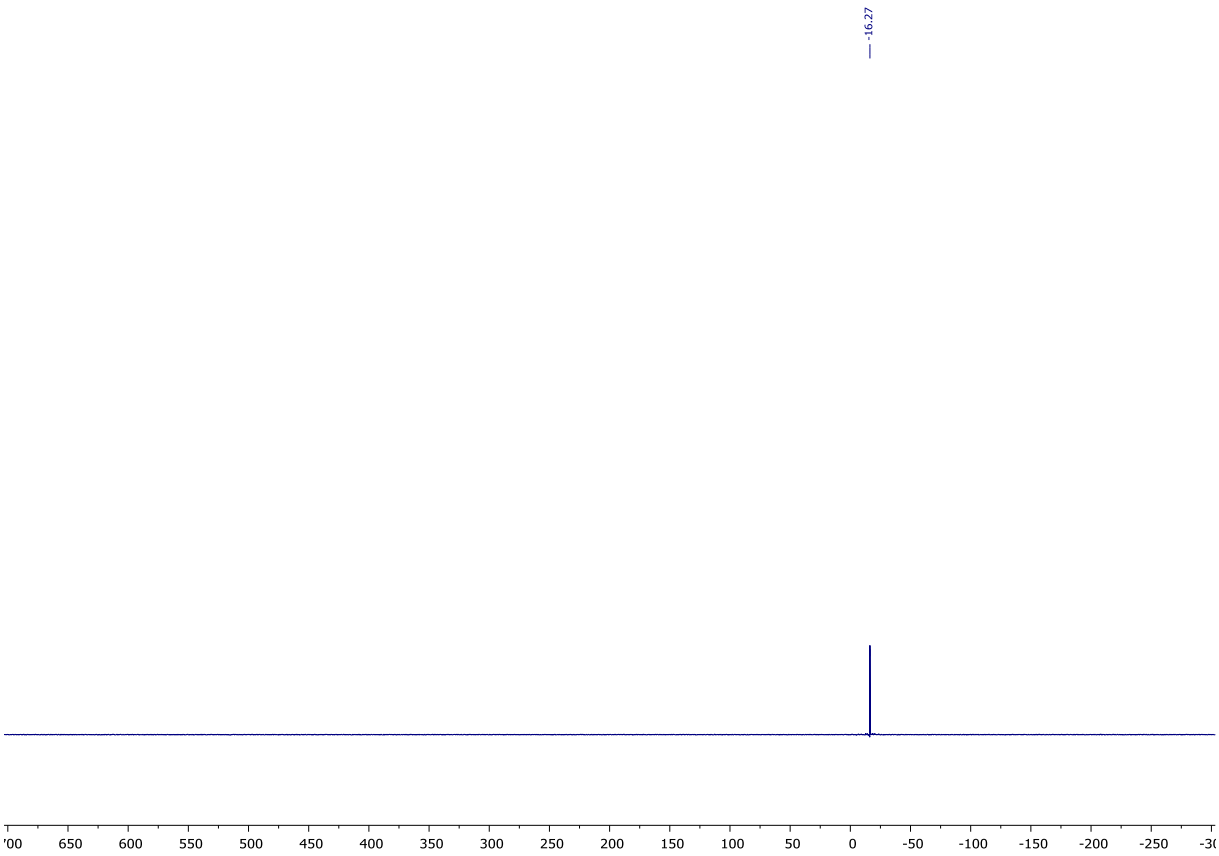

Figure S28: *$^{31}P\{^{1}H\}$ NMR of* ***1:^{Dip}Ter*** (given in ppm, C_6D_6, 162 MHz, 298K).

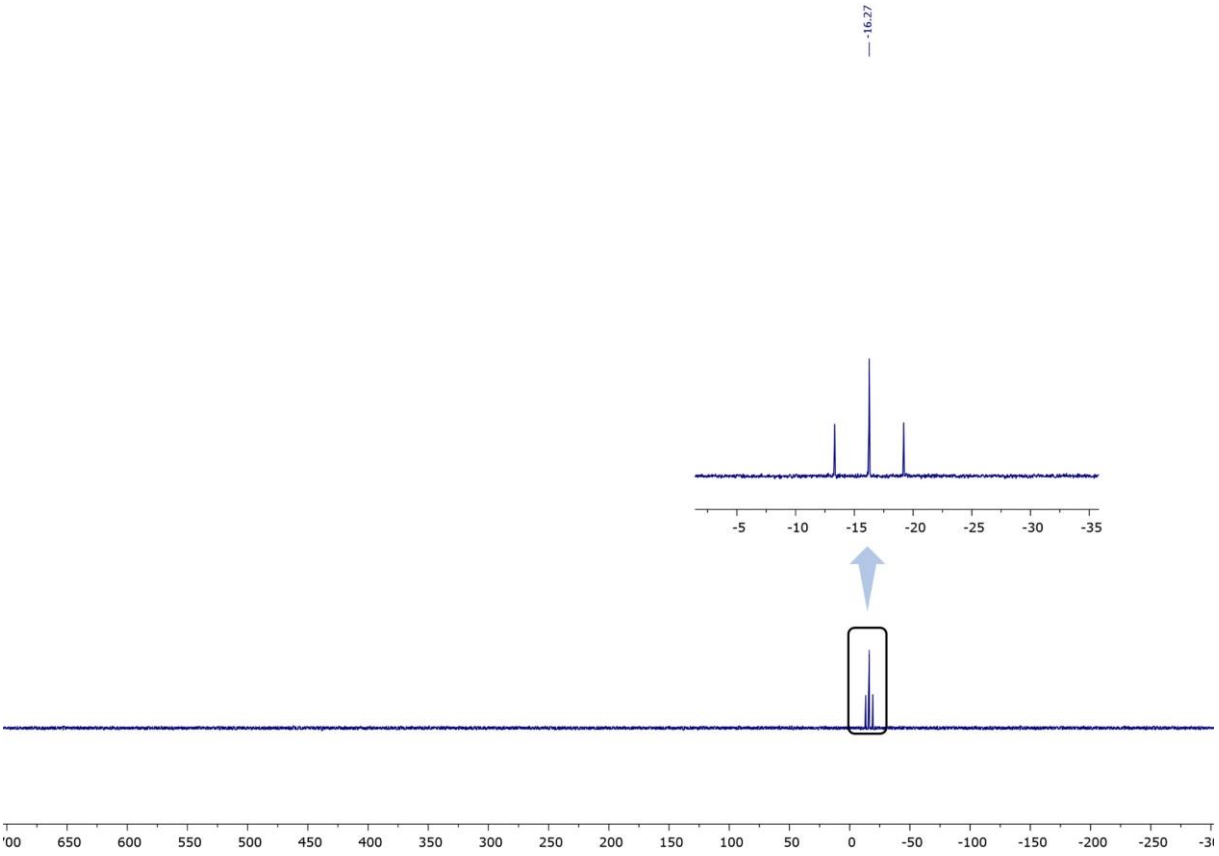

Figure S29: *^{31}P NMR of* ***1:^{Dip}Ter*** (given in ppm, C_6D_6, 162 MHz, 298K).

3.4 Mes*P(H)O–P(H)Mes* (2:Mes*)

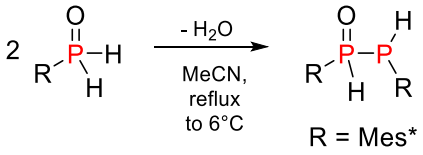

A 20 mg portion of **1:Mes*** is suspended in 2 mL of MeCN. Heating the solution to reflux for 5 min. with a heatgun and slow cooling to 6°C yields a few, small colorless needles of **2:Mes*** suitable for SC-XRD. For crystallographic details see table S2.

3.5 [Mes*P(H)$_2$OGaCl$_3$] (3:Mes*)

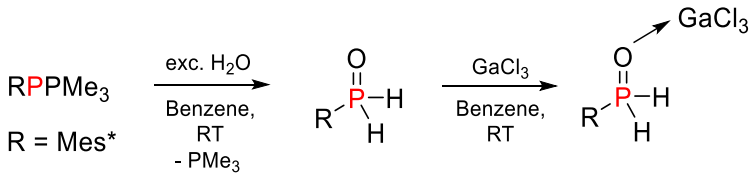

A 0.050 g portion of Mes*PPMe$_3$ (0.14 mmol, 1.0 eq) is dissolved in 1.5 mL of benzene. One drop of water (excess) is then carefully added to the solution. Upon stirring the solution for 30 min., a characteristic yellow colour fades and the reaction is then stopped. The solvent is removed under reduced pressure to obtain a beige powder which is then thoroughly(!) dried *in vacuo*. Subsequently, 0.025 of GaCl$_3$ (0.14 mmol, 1.0 eq) are added. The mixture is dissolved in 1.5 mL of benzene and stirred for 15 min. The solvent is then again removed under reduced pressure and the residue is washed with 2 mL of n-pentane. After drying, dissolving in 1 mL of DCM and placing the solution at -32°C, **3:Mes*** is obtained in the form of colorless, crystalline blocks (60%, 0.084 mmol, 0.040 g).

^{1}H NMR (CD_2Cl_2, 300 MHz, 298K): δ = 8.01 (d, $^1J_{PH}$ = 530.5 Hz, 2H, P(*H*)$_2$O), 7.63 (d, J = 5.6 Hz, 2H, C*H*$_{Ar}$), 1.60+1.59 (s, 18H, C*H*$_3$), 1.34 (s, 9H, C*H*$_3$) ppm. **^{13}C{^{1}H} NMR** (CD_2Cl_2, 75.5 MHz, 298K): δ = 159.8 (d, $^2J_{P,C}$ = 10.1 Hz, *o*-*C*(CH$_3$)$_3$),154.0 (d, $^4J_{PC}$ = 3.1 Hz, *p*-*C*(CH$_3$)$_3$), 125.4 (d, $^3J_{PC}$ = 13.9 Hz, Ar*C*H), 39.3 (d, $^3J_{PC}$ = 3.9 Hz, *o*-*C*(CH$_3$)$_3$), 36.1 (s, *p*-*C*(CH$_3$)$_3$), 34.2 (s, *o*-C(*C*H$_3$)$_3$), 31.1 (s, *p*-C(*C*H$_3$)$_3$), not observed: (Ar*C*$_{ipso}$). **^{31}P{^{1}H} NMR** (CD_2Cl_2, 122 MHz, 298K): δ = 1.21 (s, *P*(H)$_2$O) ppm. **^{31}P NMR** (CD_2Cl_2, 122 MHz, 298K): δ = 1.21 (t, $^1J_{PH}$ = 530.5 Hz, *P*(H)$_2$O) ppm. **IR** (ATR, cm^{-1})*: 2964 (m), 1594 (m), 1533 (w), 1488 (w), 1468 (w), 1404 (w), 1370 (m), 1238 (w), 1213 (w), 1193 (w), 1163 (w), 1086 (vs), 1047 (s), 1015 (s), 923 (w), 886 (w), 783 (w), 758 (w), 710 (w), 656 (w), 624 (m), 531 (s), 496 (w), 441 (w).* P-H stretching vibration is supressed and thus not observed (see also ref.[13]). **MS** (HR, ESI$^+$); under ESI$^+$ MS conditions, only ligand **1:Mes*** was observed: calc. for $C_{18}H_{31}O_1P_1$ [M+H]$^+$ (found): 295.2191 (295.2194); calc. for $C_{18}H_{31}Na_1O_1P_1$ [M+Na$^+$] (found) 317.2004 (317.2012).

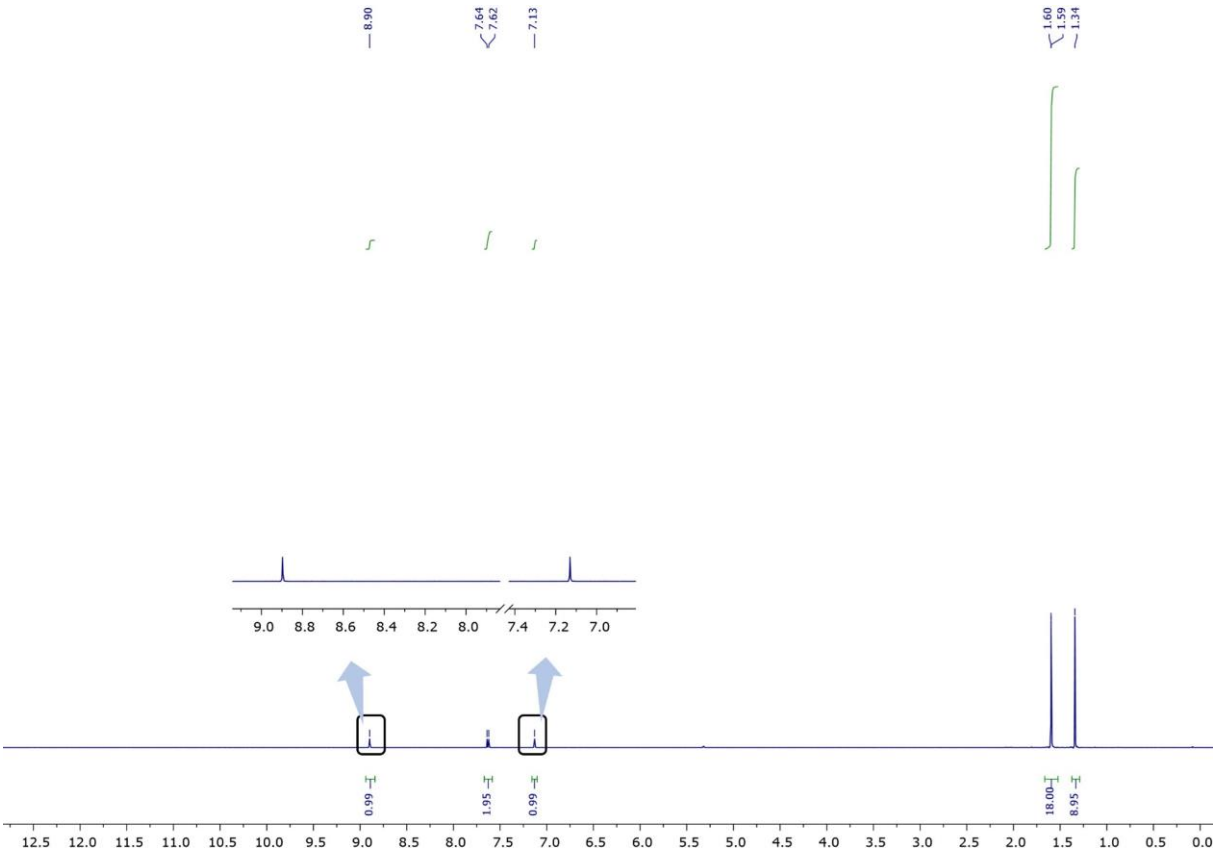

Figure S30: *^{1}H NMR of* ***3:Mes**** (given in ppm, CD_2Cl_2, 300 MHz, 298K).

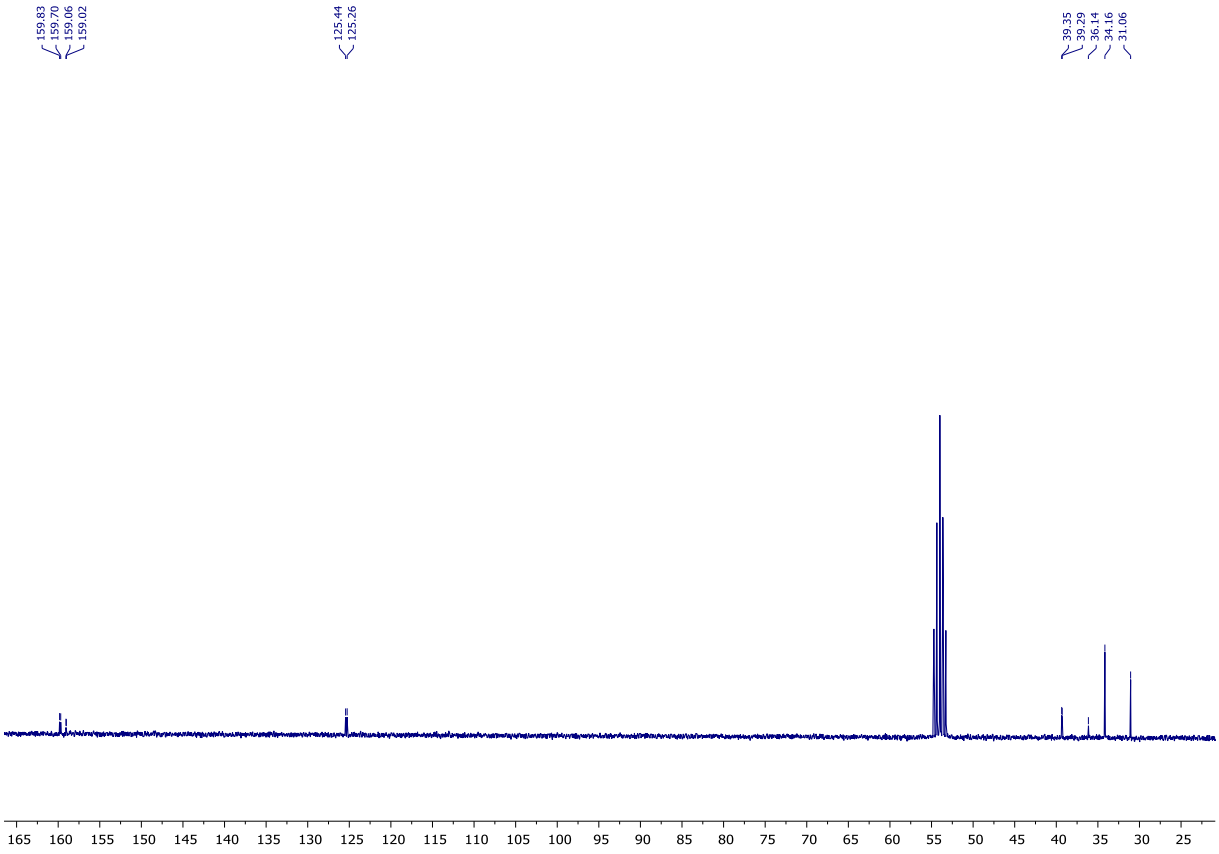

Figure S31: *$^{13}C\{^{1}H\}$ NMR of* ***3:Mes**** (given in ppm, CD_2Cl_2, 75.5 MHz, 298K).

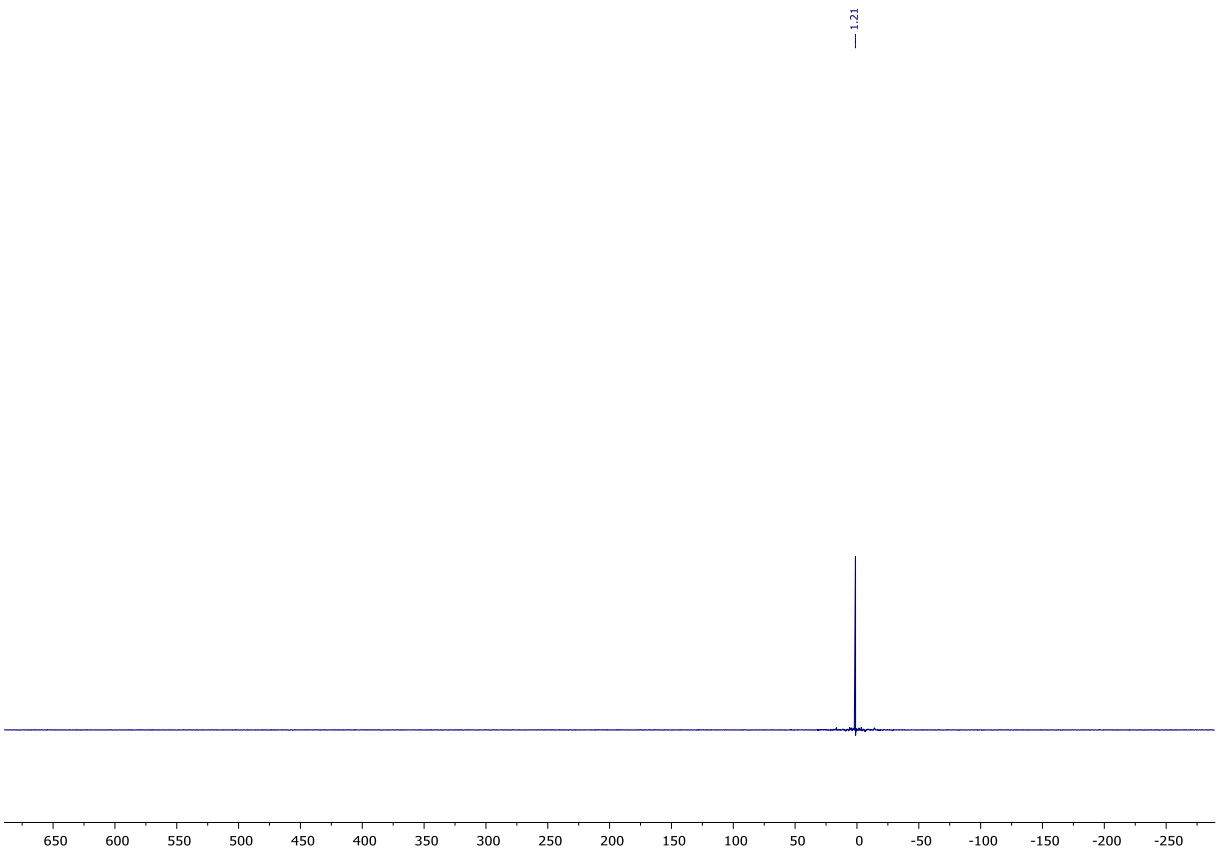

Figure S32: *$^{31}P\{^{1}H\}$ NMR of* ***3:Mes**** (given in ppm, CD_2Cl_2, 122 MHz, 298K).

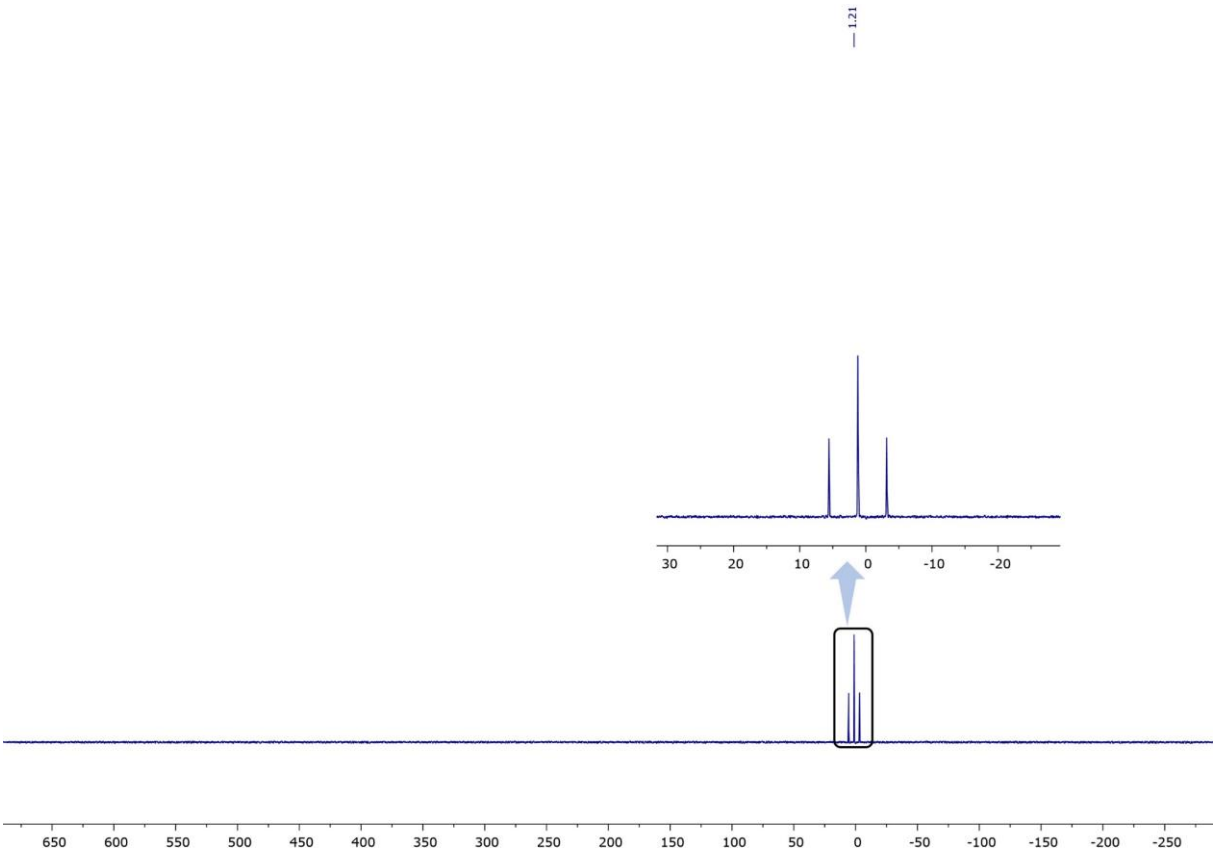

Figure S33: *^{31}P NMR of* ***3:Mes**** (given in ppm, CD_2Cl_2, 122 MHz, 298K).

3.6 [Mes^{Ter}P(H)$_2$OGaCl$_3$] (3:^{Mes}Ter)

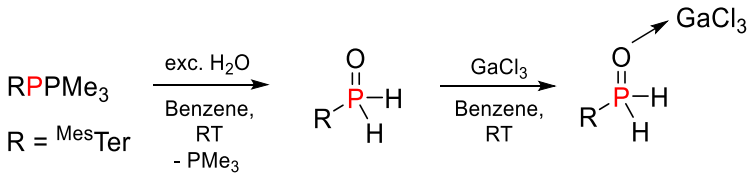

A 0.050 g portion of ^{Mes}TerPPMe$_3$ (0.118 mmol, 1.0 eq) is dissolved in 1.5 mL of benzene. Subsequently, two small drops of water are carefully added to the solution. After stirring overnight, the solvent is removed under reduced pressure and the obtained slight beige powder is thoroughly dried *in vacuo*. Then, 0.021 g of GaCl$_3$ (0.118 mmol, 1.0 eq) are added, and the mixture is dissolved in 2.5 mL benzene. After stirring for another 45 min., the solvent is again removed under reduced pressure and the obtained white powder is extracted with 2 mL of DCM. After filtration, the solvent is again removed under reduced pressure and the crude product suspended in 1.8 mL of benzene. Heating the suspension up to 80°C using a heat-gun gives a clear solution which is then placed at 6°C for recrystallization. After a few days, colorless block-shaped crystals of **3:^{Mes}Ter** are obtained (0.046 g, 0.085 mmol, 72%).

^{1}H NMR (CD_2Cl_2, 300 MHz, 298K): δ = 7.99–7.93 (m, 1H, *p*-Ar*H*), 7.43–7.39 (m, 2H, *m*-Ar*H*), 7.03 (m, 4H, *m*-*H* of Mes), 6.84 (d, $^1J_{PH}$ = 533.2 Hz, 2H, P(*H*)$_2$O), 2.36 (s, 6H, *p*-C*H*$_3$ of Mes), 1.99 (s, 12H, *m*-C*H*$_3$ of Mes) ppm. **^{13}C{^{1}H} NMR** (CD_2Cl_2, 75.5 MHz, 298K): δ = 149.0 (d, $^2J_{CP}$ = 13.2 Hz, *o*–Ar*C*), 140.1 (s, *p*–*C* of Mes), 137.5 (s, *p*–Ar*C*), 136.6 (s, *o*–*C* of Mes), 134.1 (d, $^3J_{CP}$ = 6.8 Hz, Ar*C*$_q$ of Mes), 130.6 (d, $^3J_{CP}$ = 10.4 Hz, *m*–Ar*C*), 129.5 (*m*–*C* of Mes), 120.7 (d, $^1J_{CP}$ = 123.5 Hz, Ar*C*$_{ipso}$), 21.3 (s, *p*-*C*H$_3$ of Mes), 20.9 (s, *m*-*C*H$_3$ of Mes) ppm. **^{31}P{^{1}H} NMR** (CD_2Cl_2, 162 MHz, 298K): δ = 3.62 (s, *P*(H)$_2$O) ppm. **^{31}P NMR** (CD_2Cl_2, 122 MHz, 298K): δ =3.63 (pstt, $^1J_{PH}$ = 532.5 Hz, *J* = 4.2 Hz, *P*(H)$_2$O)* ppm. *Unknown fine-coupling observed here giving a pseudo triplet of triplets. **IR** (ATR, cm^{-1})**: 2977.33 (w), 2919.56 (w), 2855.31 (w), 1609.32 (m), 1564.70 (m), 1451.43 (s), 1380.88 (w), 1302.53 (vw), 1268.19 (vw), 1180.02 (w), 1134.82 (s), 1072.61 (s), 1053.12 (s), 1011.85 (s), 994.62 (s), 893.35 (m), 851.28 (s), 843.60 (s), 813.01 (s), 755.95 (m), 737.13 (m), 680.91 (s), 578.10 (s), 561.62(m), 533.44 (s), 500.28 (w), 446.62 (s). **P-H stretching

vibration is supressed and thus not observed. **MS** (HR, ESI^+); under ESI^+ MS conditions, only ligand **1:^{Mes}Ter** was observed: calc. for $C_{24}H_{28}O_1P_1$ $[M+H]^+$ (found): 363.1878 (363.1881); calc. for $C_{24}H_{27}O_1P_1Na_1$ $[M+Na]^+$ (found): 385.1692 (385.1702).

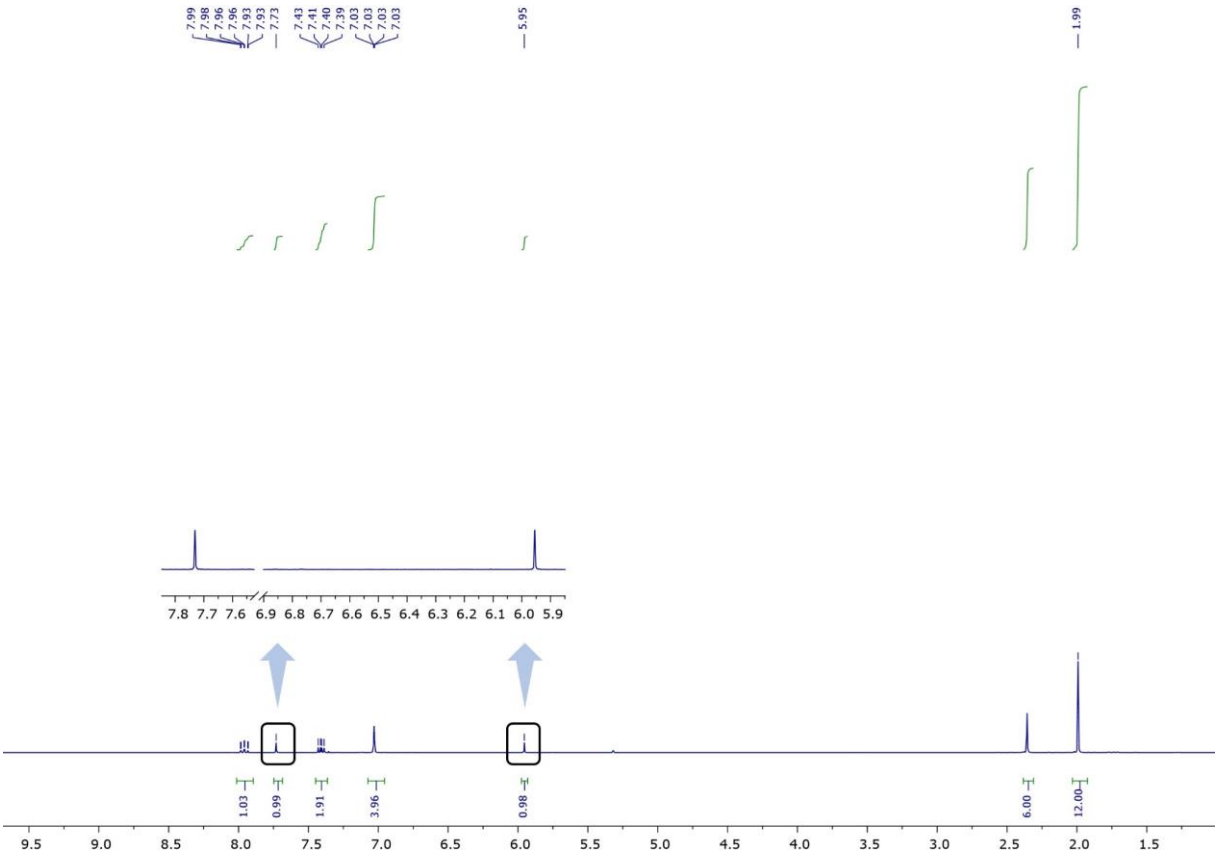

Figure S34: *^{1}H NMR of* ***3:^{Mes}Ter*** (given in ppm, CD_2Cl_2, 300 MHz, 298K).

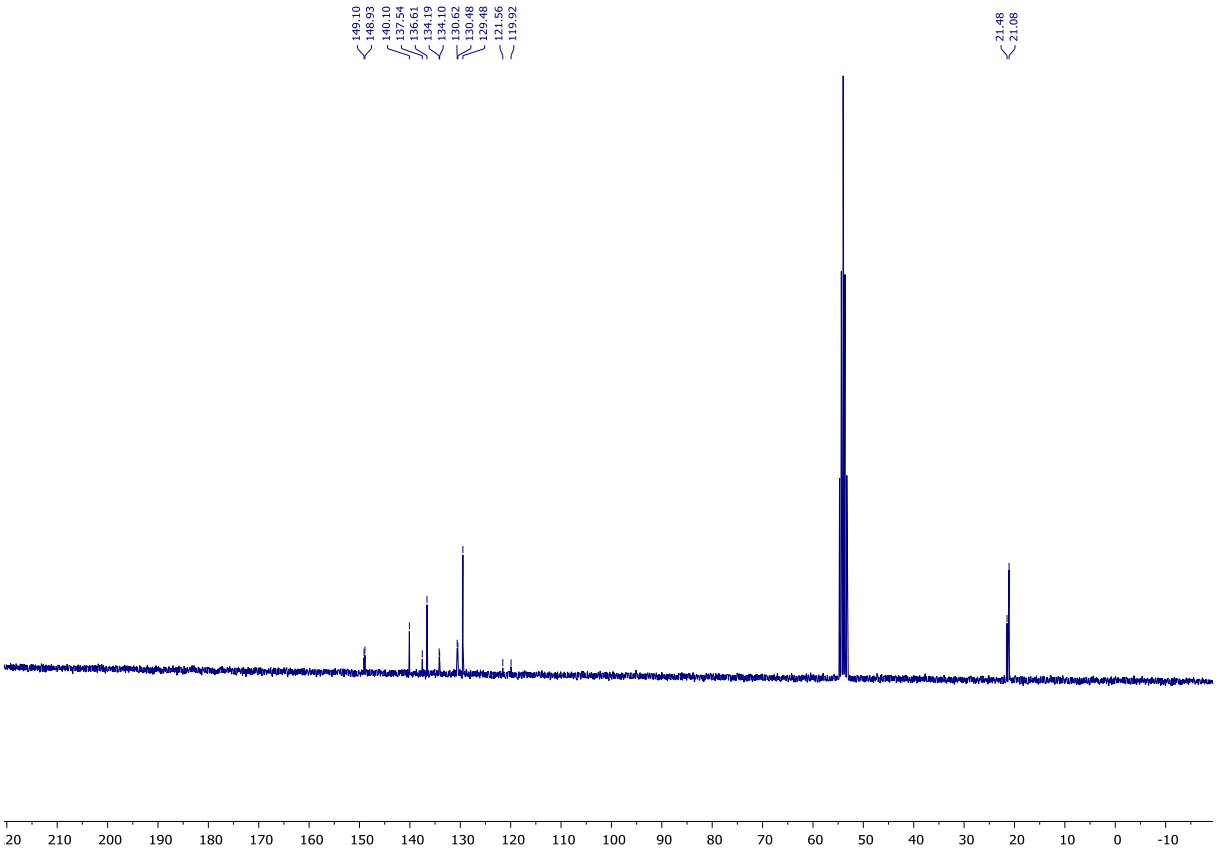

Figure S35: *$^{13}C\{^{1}H\}$ NMR of* ***3:^{Mes}Ter*** (given in ppm, CD_2Cl_2, 75.5 MHz, 298K).

Figure S36: *$^{31}P\{^{1}H\}$ NMR of* ***3:^{Mes}Ter*** (given in ppm, CD_2Cl_2, 122 MHz, 298K).

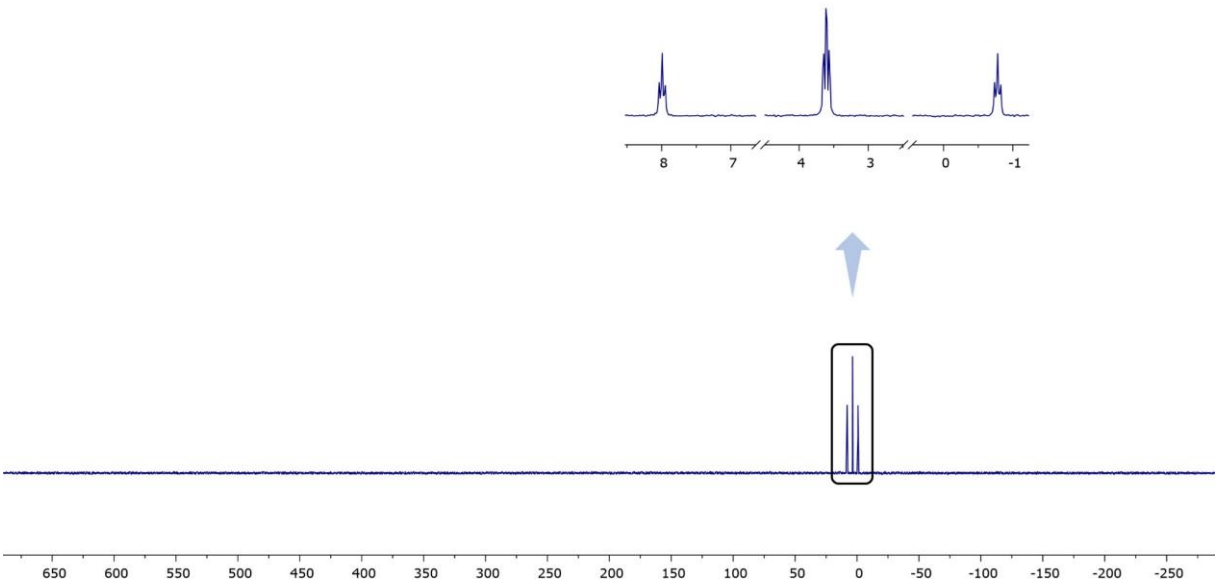

Figure S37: *^{31}P NMR of* ***3:^{Mes}Ter*** (given in ppm, CD_2Cl_2, 122 MHz, 298K).

3.7 [Mes*P(H)$_2$OGaI$_3$] (4:Mes*)

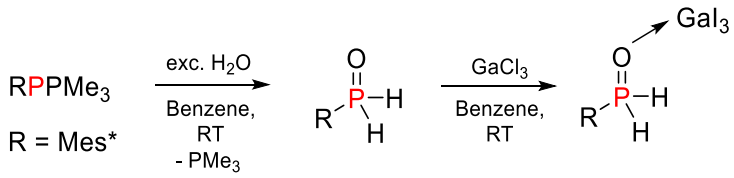

A 0.050 g portion of Mes*PPMe$_3$ (0.14 mmol, 1.0 eq) is dissolved in 2 mL of benzene. Two drops of water (excess) are then carefully added to the solution. Upon stirring the solution for 30 min., a characteristic yellow colour fades and the reaction is then stopped. The solvent is removed under reduced pressure to obtain a beige powder which is then thoroughly(!) dried *in vacuo*. Subsequently, 0.063 of GaI$_3$ (0.14 mmol, 1.0 eq) are added. The mixture is dissolved in 4 mL of benzene and stirred for 10 min. The solvent is then again removed under reduced pressure to obtain a colorless grease. The grease is dissolved on 2 mL of *n*-pentane and is vigorously stirred for 5 min. Over time, **4:Mes*** precipitates from the solution as a white powder. Carefully decanting the solvent off and drying the powder *in vacuo* finally yields **4:Mes*** as a crystalline, pale-white powder (0.127 mmol, 0.095 g, 91%). Block-shaped crystals suitable for SC-XRD were obtained from a layered **4:Mes*** DCM/n-Pentane mixture (1:6) at -32°C.

^{1}H NMR (CD_2Cl_2, 300 MHz, 298K): δ = 8.00 (d, $^1J_{PH}$ = 527.8 Hz, 2H, P(*H*)$_2$O), 7.63 (d, *J* = 5.6 Hz, 2H, C*H*$_{Ar}$), 1.61+1.61 (s, 18H, C*H*$_3$),1.35 (s, 9H, C*H*$_3$) ppm. **^{13}C{^{1}H} NMR** (CD_2Cl_2, 75.5 MHz, 298K): δ = 159.64 (d, $^2J_{P,C}$ = 10.1 Hz, *o*-*C*(CH$_3$)$_3$), 158.9 (d, $^4J_{PC}$ = 3.2 Hz, *p*-*C*(CH$_3$)$_3$), 125.29 (d, $^3J_{PC}$ = 13.9 Hz, ArCH), 112.88 (d, $^1J_{CP}$ = 107.5 Hz, ArC$_{ipso}$), 39.49 (d, $^3J_{PC}$ = 3.8 Hz, *o*-*C*(CH$_3$)$_3$), 36.1 (s, *p*-*C*(CH$_3$)$_3$), 34.3 (s, *o*-C(*C*H$_3$)$_3$), 31.1 (s, *p*-C(*C*H$_3$)$_3$). **^{31}P{^{1}H} NMR** (CD_2Cl_2, 122 MHz, 298K): δ = -1.85 (s, *P*(H)$_2$O) ppm. **^{31}P NMR** (CD_2Cl_2, 122 MHz, 298K): δ = -1.85 (t, $^1J_{PH}$ = 527.8 Hz, *P*(H)$_2$O) ppm. **IR** (ATR, cm^{-1})*: 2960.33 (s), 2865.08 (w), 1590.92 (m), 1530.45 (w), 1464.90 (m), 1401.17 (w), 1368.40 (m), 1236.66 (w), 1209.70 (w), 1191.13 (w), 1160.45 (w), 1079.07 (vs), 1037.75 (s), 1007.20 (vs), 919.52 (w), 887.43 (w), 808.29 (vw), 756.08 (w), 709.29 (m), 655.23 (w), 625.90 (m), 525.99 (s), 486.84 (m), 436.04 (w), 416.81 (vw). * P-H stretching vibration is supressed and thus not observed. **MS** (HR, ESI$^+$); under ESI$^+$ MS conditions, only ligand **1:Mes*** was observed:

calc. for $C_{18}H_{31}O_1P_1$ $[M+H]^+$ (found): 295.2191 (295.2189); calc. for $C_{18}H_{31}Na_1O_1P_1$ $[M+Na^+]$ (found) 317.2004 (317.2010).

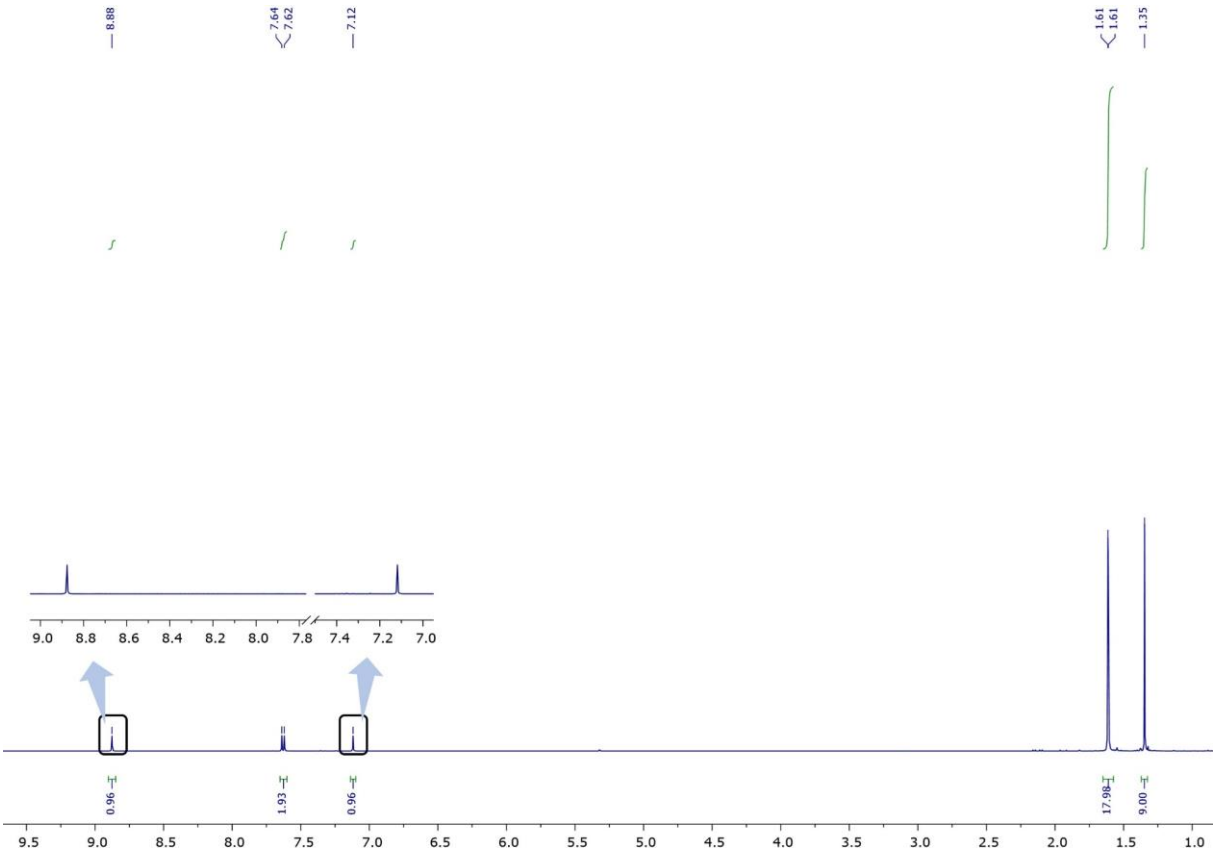

Figure S38: *^{1}H NMR of* ***4:Mes**** (given in ppm, CD_2Cl_2, 300 MHz, 298K).

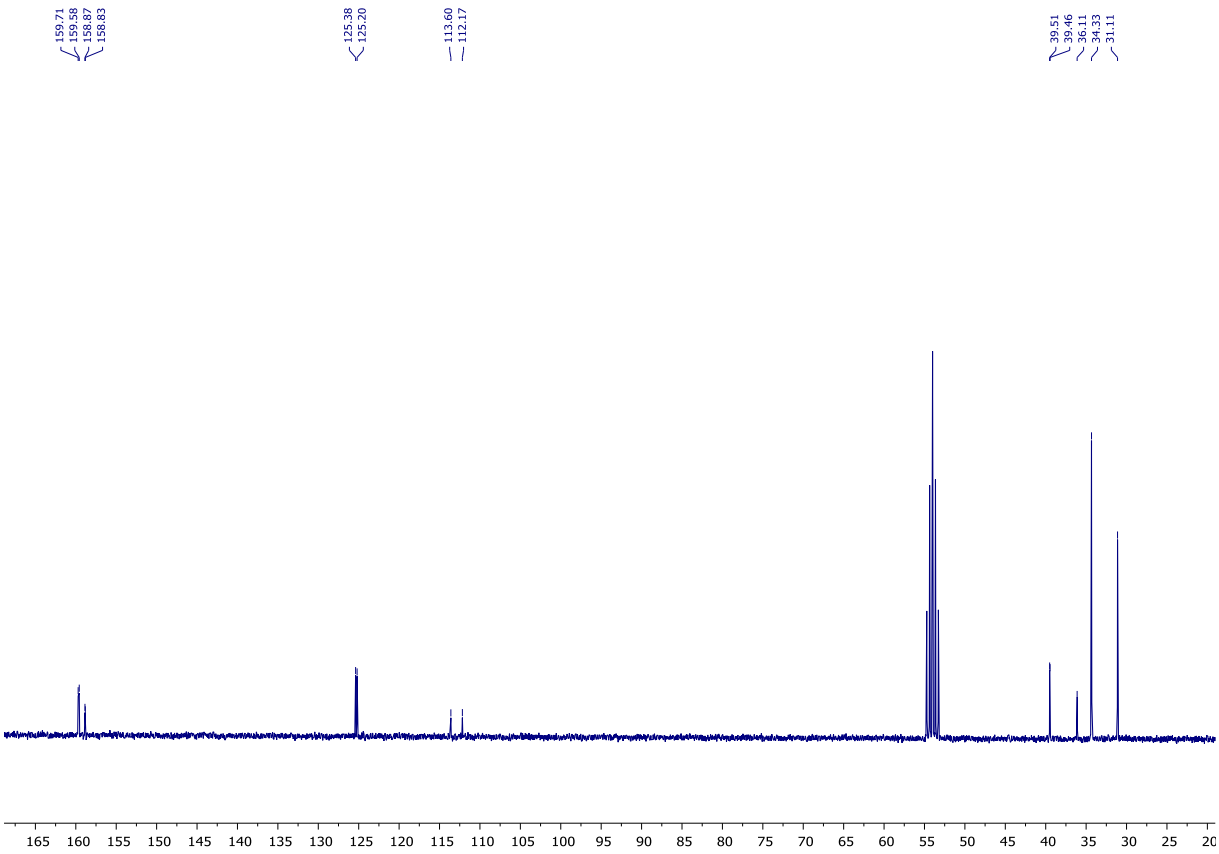

Figure S39: *$^{13}C\{^{1}H\}$ NMR of* ***4:Mes**** (given in ppm, CD_2Cl_2, 75.5 MHz, 298K).

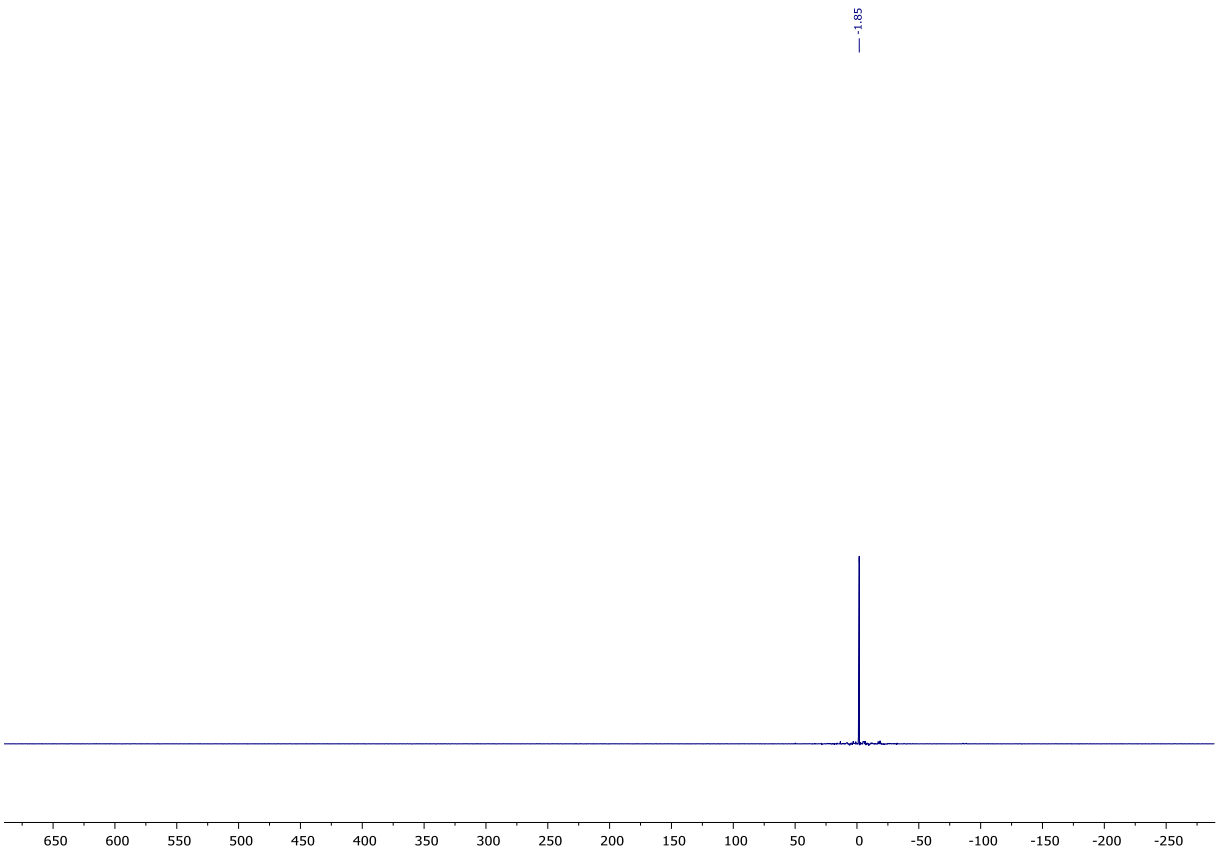

Figure S40: *$^{31}P\{^{1}H\}$ NMR of* ***4:Mes**** (given in ppm, CD_2Cl_2, 122 MHz, 298K).

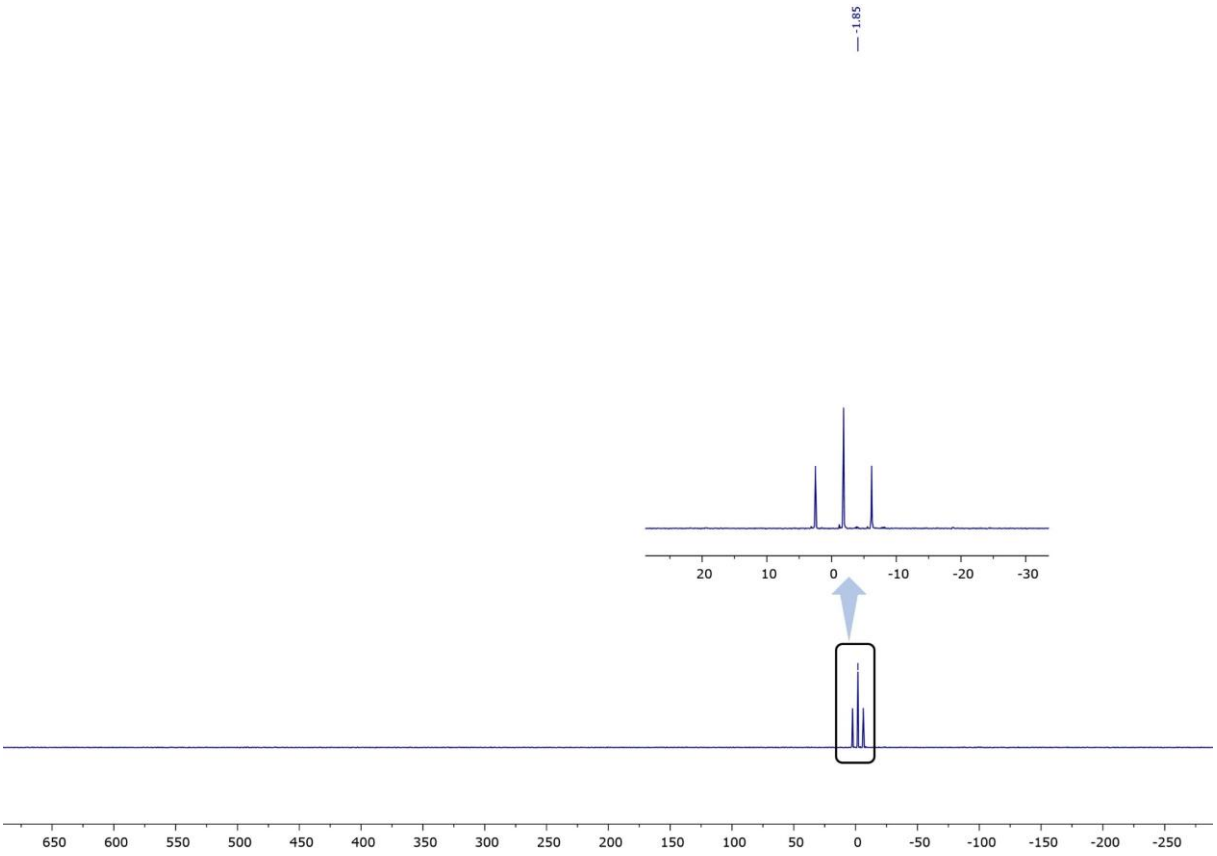

Figure S41: *^{31}P NMR of* ***4:Mes**** (given in ppm, CD_2Cl_2, 122 MHz, 298K).

3.8 [^{Mes}TerP(H)$_2$OGaI$_3$] (4:^{Mes}Ter)

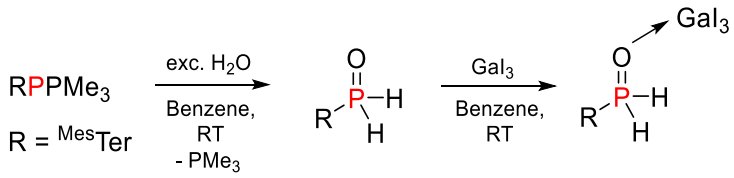

A 0.050 g portion of ^{Mes}TerPPMe$_3$ (0.118 mmol, 1.0 eq) is dissolved in 1.5 mL of benzene. Subsequently, two small drops of water are carefully added to the solution. After stirring overnight, the solvent is removed under reduced pressure and the obtained slight beige powder is thoroughly dried *in vacuo*. Then, 0.054 g of GaI$_3$ (0.118 mmol, 1.0 eq) are added, and the mixture is dissolved in 2 mL benzene. After stirring for another 30 min., the solvent is again removed under reduced pressure and the obtained white powder is extracted with 2 mL of DCM. After filtration, the solvent is again removed under reduced pressure and the crude product dissolved in 0.5 mL of benzene. Concentrating the solution until saturation is reached, yields block-shaped crystals at 6°C among traces of a white powder. Decanting off the supernatant and recrystallizing the obtained crystals from benzene at 6°C again followed by washing with 2 mL of *n*-hexane yields pure **4:^{Mes}Ter** as colourless blocks (0.037 g, 0.046 mmol, 39%).

^{1}H NMR (CD_2Cl_2, 400 MHz, 298K): δ = 7.98–7.94 (m, 1H, *p*-Ar*H*), 7.43–7.37 (m, 2H, *m*-Ar*H*), 7.02-7.03 (m, 4H, *m*-*H* of Mes), 6.70 (d, $^1J_{PH}$ = 529.9 Hz, 2H, P(*H*)$_2$O), 2.35 (s, 6H, *p*-C*H*$_3$ of Mes), 2.01 (s, 12H, *m*-C*H*$_3$ of Mes) ppm. **^{13}C{^{1}H} NMR** (CD_2Cl_2, 110 MHz, 298K): δ = 149.0 (d, $^2J_{CP}$ = 13.0 Hz, *o*–Ar*C*), 140.0 (s, *p*–*C* of Mes), 137.3 (s, *p*–Ar*C*), 136.5 (s, *o*–*C* of Mes), 134.3 (d, $^3J_{CP}$ = 6.8 Hz, ArC_q of Mes), 130.4 (d, $^3J_{CP}$ = 10.4 Hz, *m*–Ar*C*), 129.6 (*m*–*C* of Mes), 120.1 (d, $^1J_{CP}$ = 123.4 Hz, ArC_{ipso}), 21.5 (s, *p*-CH_3 of Mes), 21.2 (s, *m*-CH_3 of Mes) ppm. **^{31}P{^{1}H} NMR** (CD_2Cl_2, 162 MHz, 298K): δ = -1.47 (s, *P*(H)$_2$O) ppm. **^{31}P NMR** (CD_2Cl_2, 162 MHz, 298K): δ =-1.47 (*ps*-tm, $^1J_{PH}$ = 529.9 Hz, *P*(H)$_2$O)* ppm. *Unknown fine-coupling observed here giving a pseudo triplet of multiplets. **IR** (ATR, cm^{-1}): 2972.83 (w), 2913.22 (m), 2853.64 (w), 1609.28 (m), 1565.57 (m), 1451.36 (m), 1434.48 (m), 1394.43 (w), 1378.80 (m), 1300.49 (w), 1267.97 (m), 1180.77 (w), 1132.85

(w), 1070.51 (s), 1048.75 (vs), 1009.96 (s), 991.42 (s), 951.31 (s), 888.97 (w), 847.11 (s), 811.47 (s), 755.60 (m), 736.10 (m), 709.19 (w), 679.75 (m), 578.69 (m), 559.78 (m), 525.93 (s), 499.04 (m), 453.21 (m), 439.03 (s). **MS** (HR, ESI^+); under ESI^+ MS conditions, only ligand **1:^{Mes}Ter** was observed: calc. for $C_{24}H_{28}O_1P_1$ $[M+H]^+$ (found): 363.1878 (363.1880); calc. for $C_{24}H_{27}O_1P_1Na_1$ $[M+Na]^+$ (found): 385.1692 (385.1695).

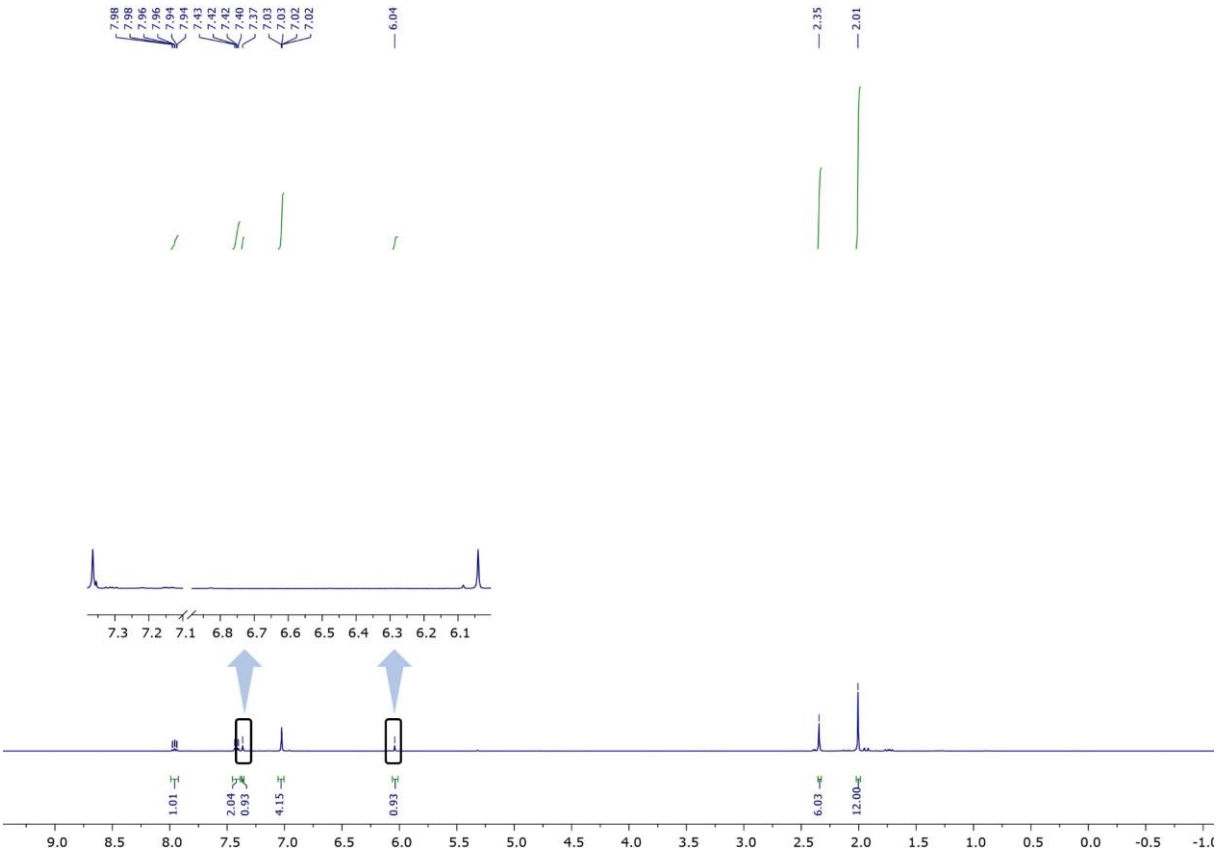

Figure S42: *^{1}H NMR of* ***4:^{Mes}Ter*** (given in ppm, CD_2Cl_2, 400 MHz, 298K).

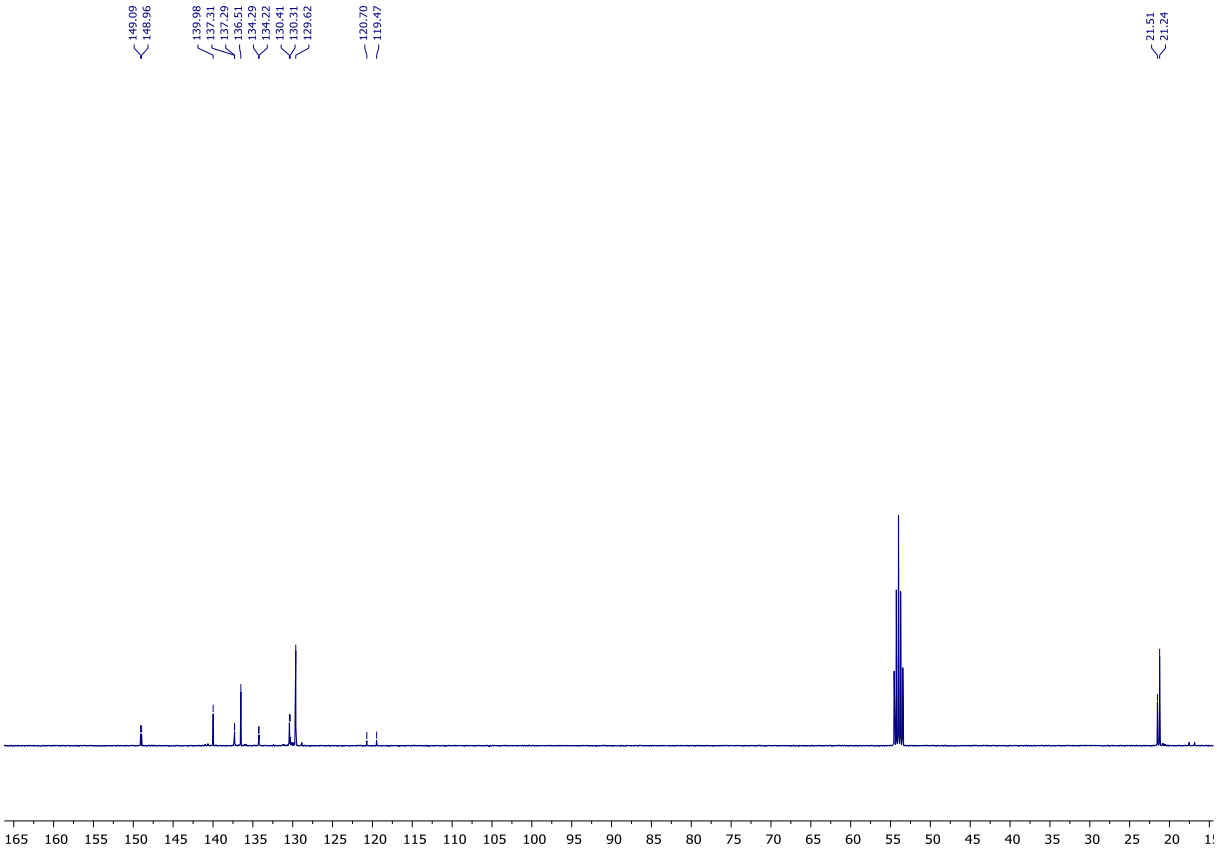

Figure S43: *$^{13}C\{^{1}H\}$ NMR of* ***4:^{Mes}Ter*** (given in ppm, CD_2Cl_2, 110 MHz, 298K).

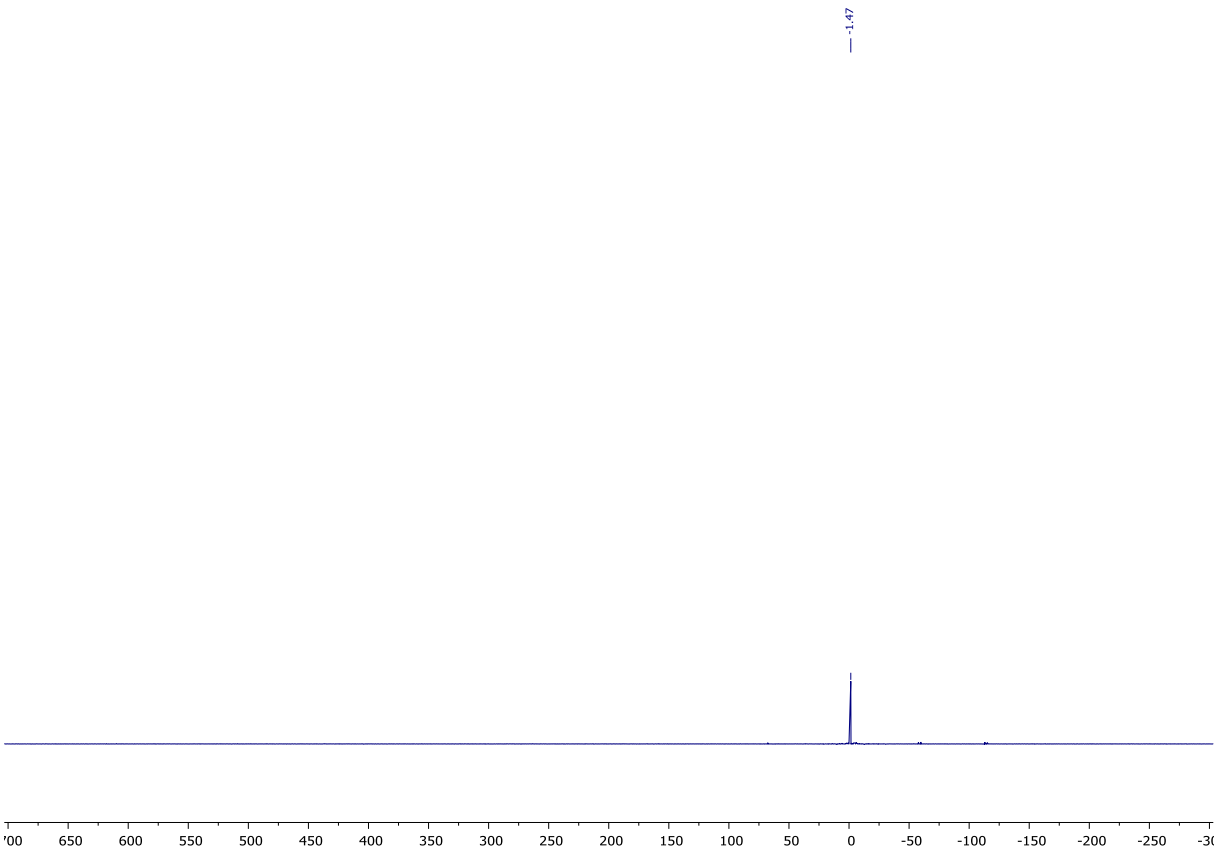

Figure S44: *$^{31}P\{^{1}H\}$ NMR of* ***4:^{Mes}Ter*** (given in ppm, CD_2Cl_2, 162 MHz, 298K).

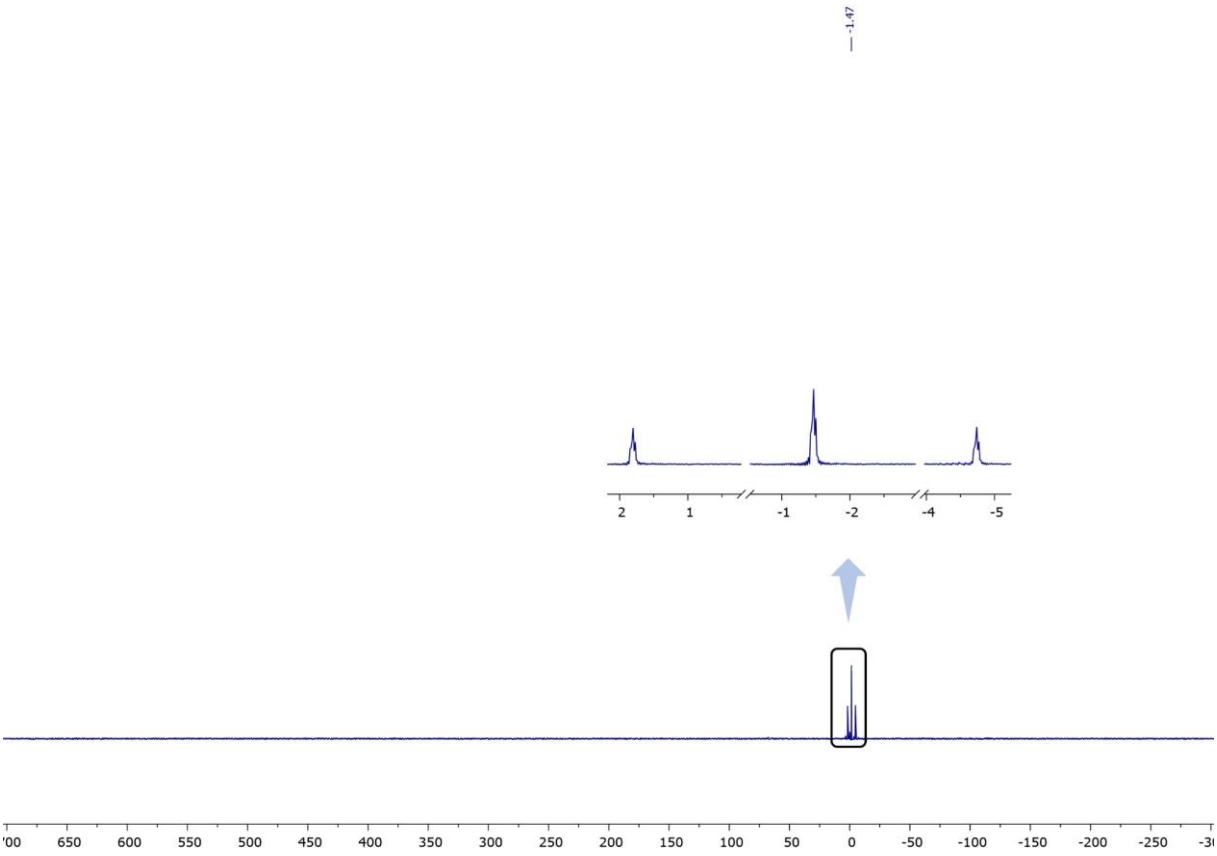

Figure S45: *^{31}P NMR of* ***4:^{Mes}Ter*** (given in ppm, CD_2Cl_2, 162 MHz, 298K).

3.9 [Mes*P(H)$_2$OB(C$_6$F$_5$)$_3$] (5:Mes*)

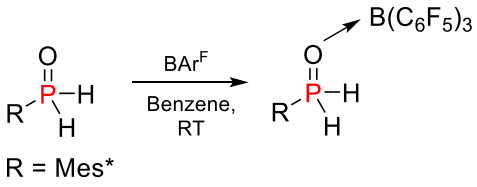

A 0.075 g portion of Mes*P(O)H$_2$ (0.255 mmol, 1.0 eq) and 0.130 g B(C$_6$F$_5$)$_3$ (0.255 mmol, 1.0 eq) were dissolved in 3 mL of benzene. The reaction mixture was stirred for three hours at room temperature. All volatile components were then removed under vacuum. The remaining slightly yellow solid was washed with *n*-pentane (2 × 4 mL) and dried under vacuum to give **5:Mes*** as a colorless solid (50%, 0.128 mmol, 0.103 g). Block-shaped crystals suitable for SC-XRD were obtained by layering a C$_6$D$_6$ solution of **5:Mes*** with *n*-pentane and subsequent slow evaporation.

^{1}H NMR (C$_6$D$_6$, 300 MHz, 298K): δ = 7.30 (d, $^1J_{PH}$ = 542.8 Hz, 2H, P(*H*)$_2$O), 7.22 (d, *J* = 4.2 Hz, 2H, C*H*$_{Ar}$), 1.13 (s, 9H, C*H*$_3$), 0.93 (s, 18H, C*H*$_3$) ppm. **^{11}B{^{1}H} NMR** (96 MHz, C$_6$D$_6$, 298 K): δ = 0.0 (brs, *B*(C$_6$F$_5$)$_3$) ppm.**^{13}C{^{1}H} NMR** (C$_6$D$_6$, 75.5 MHz, 298K): δ =158.8 (d, $^2J_{P,C}$ = 8.0 Hz, *o*-*C*(CH$_3$)$_3$), 158.0 (d, $^4J_{PC}$ = 3.3 Hz, *p*-*C*(CH$_3$)$_3$), 124.8 (d, $^3J_{PC}$ = 12.6 Hz, ArCH), 38.6 (d, $^3J_{PC}$ = 3.3 Hz, *o*-*C*(CH$_3$)$_3$), 35.3 (s, *p*-*C*(CH$_3$)$_3$), 32.4 (s, *o*-C(*C*H$_3$)$_3$), 30.6 (s, *p*-C(*C*H$_3$)$_3$), not observed: (Ar*C*$_{ipso}$). **^{19}F{^{1}H} NMR** (282 MHz, C$_6$D$_6$, 298 K): δ = -163.6 to -163.8 (m, 6F, *m*-F$_{Ar}$B), -157.2 (t, $^3J_{FF}$ = 20.7 Hz, 3F, *p*-F$_{Ar}$B), -133.8 to -134.0 (m, 6F, *o*-F$_{Ar}$B); ($\Delta\delta$ $^{19}F_{m,p}$ = 6.5 Hz) ppm. **^{31}P{^{1}H} NMR** (C$_6$D$_6$, 122 MHz, 298K): δ = 6.1 (hept, $^4J_{PF}$ = 7.2 Hz, *P*(H)$_2$O) ppm. **^{31}P NMR** (C$_6$D$_6$, 122 MHz, 298K): δ = 6.1 (t, $^1J_{PH}$ = 543.1 Hz, *P*(H)$_2$O) ppm.

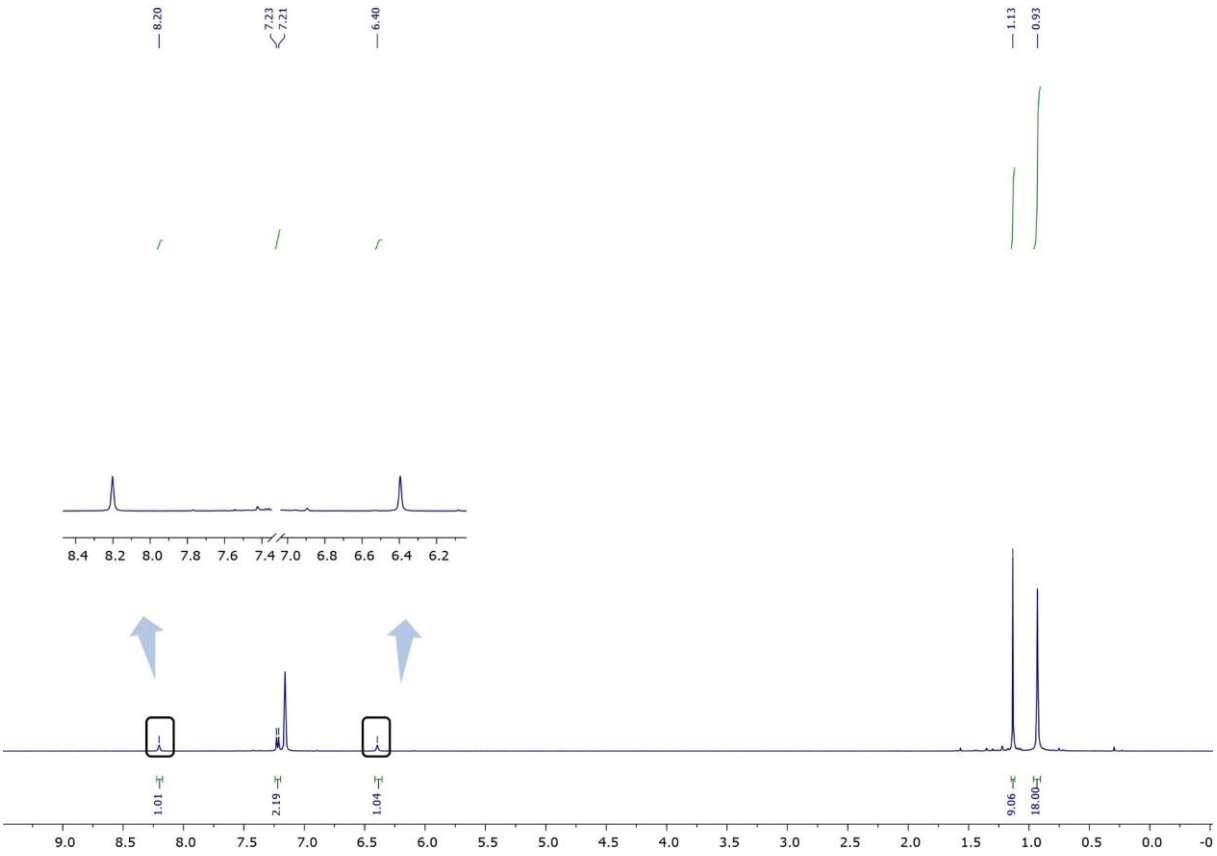

Figure S46: *^{1}H NMR of* ***5:Mes**** (given in ppm, C_6D_6, 300 MHz, 298K).

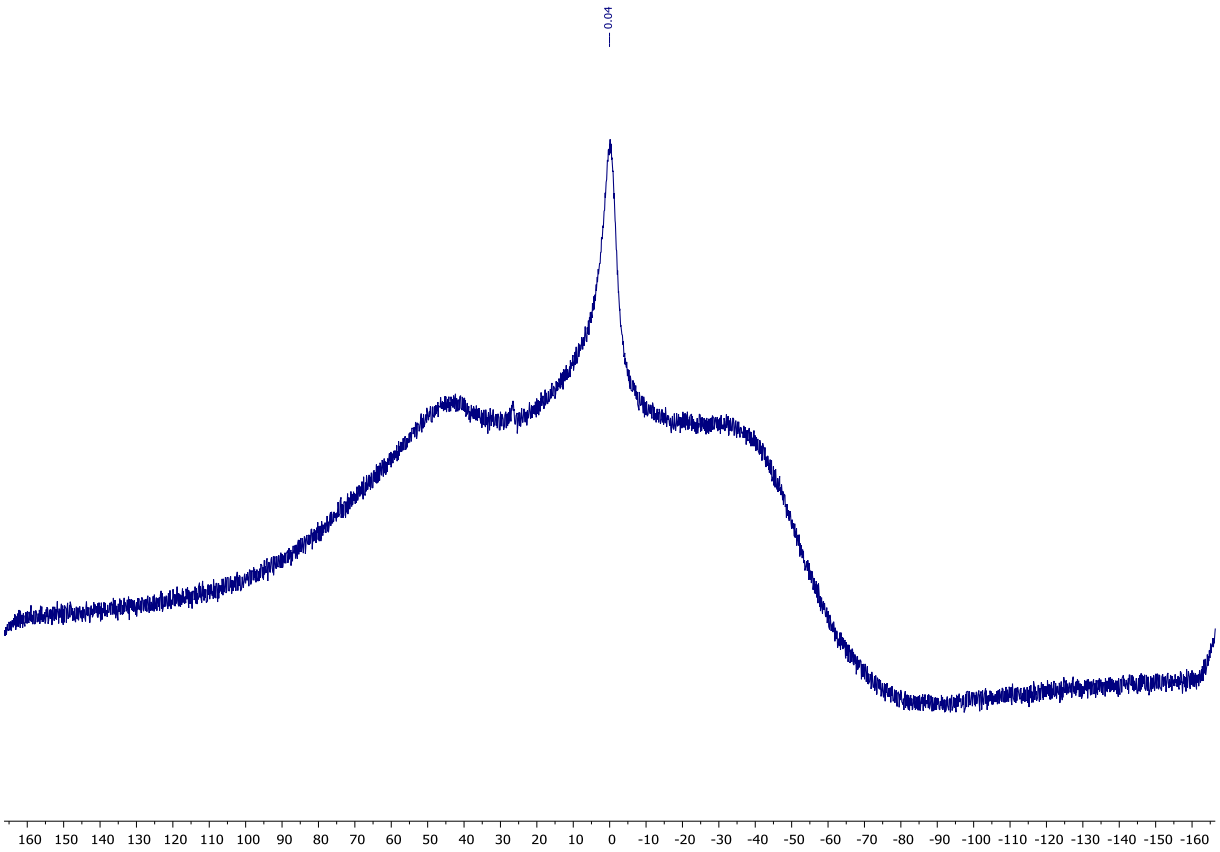

Figure S47: *$^{11}B\{^{1}H\}$ NMR of* ***5:Mes**** (given in ppm, C_6D_6, 96 MHz, 298K).

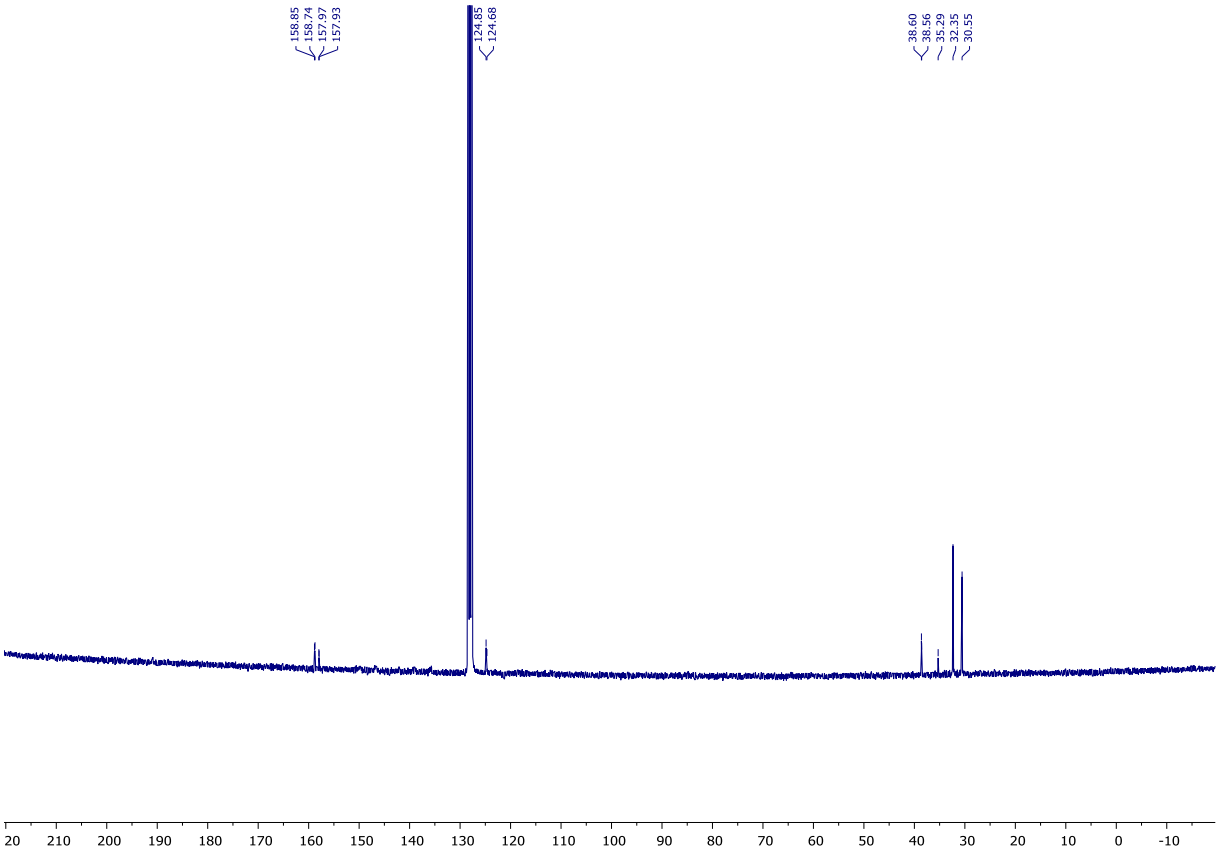

Figure S48: *$^{13}C\{^{1}H\}$ NMR of* ***5:Mes**** (given in ppm, C_6D_6, 75.5 MHz, 298K).

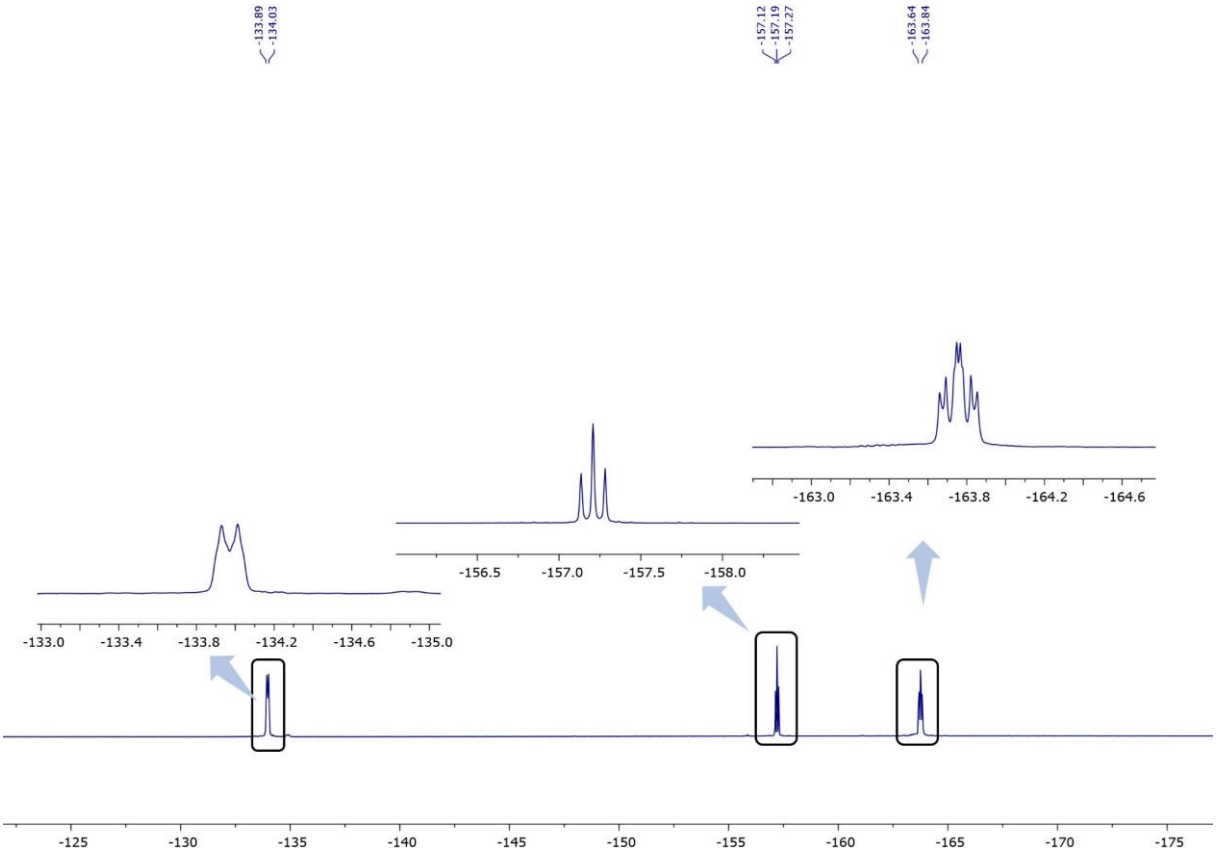

Figure S49: *^{19}F NMR of* ***5:Mes**** (given in ppm, C_6D_6, 282 MHz, 298K).

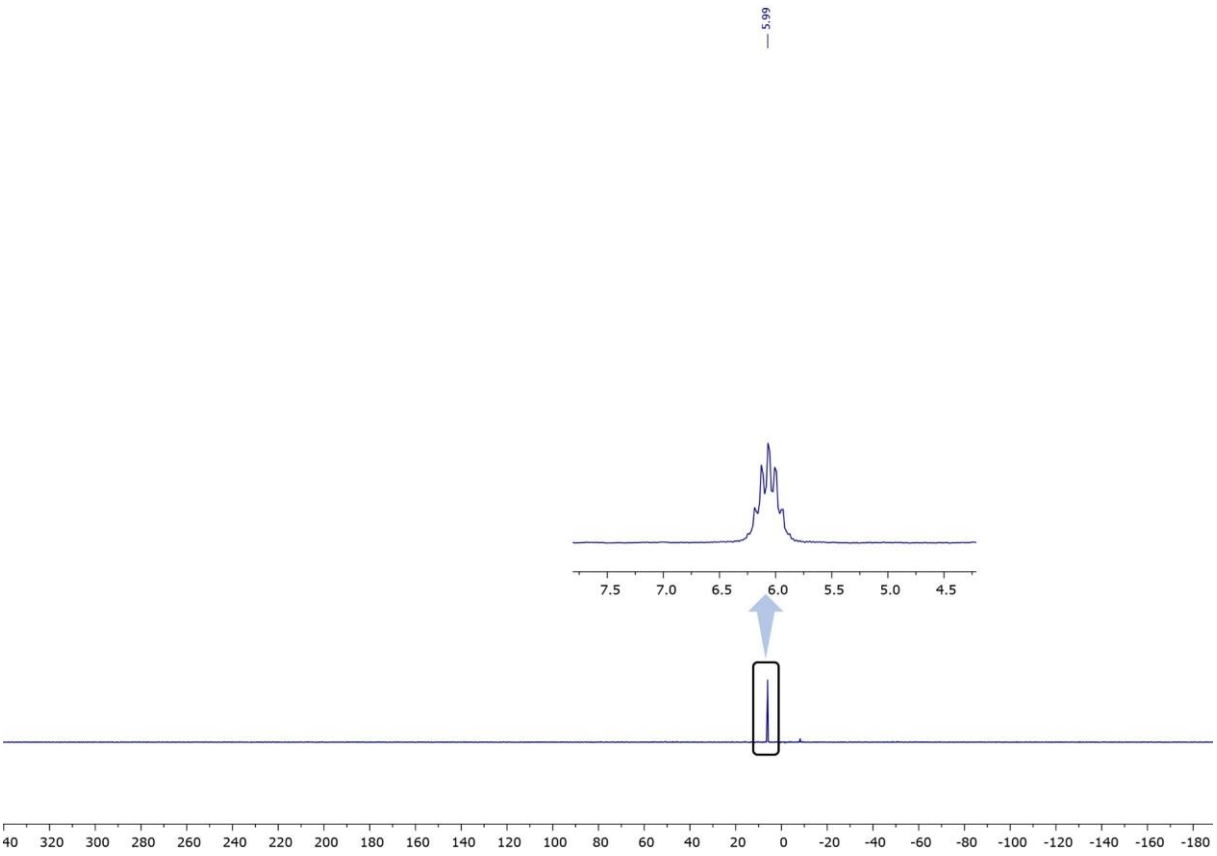

Figure S50: *$^{31}P\{^{1}H\}$ NMR of* ***5:Mes**** (given in ppm, C_6D_6, 122 MHz, 298K).

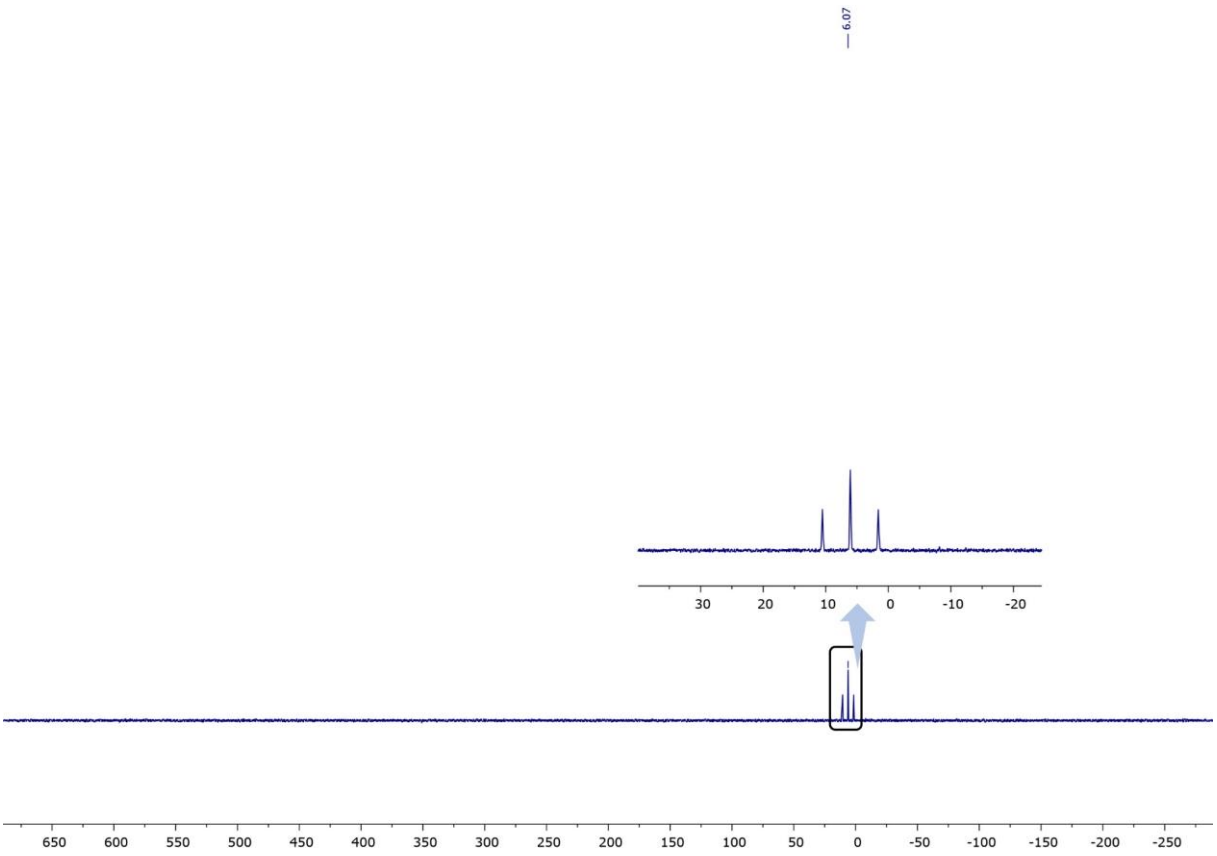

Figure S51: *^{31}P NMR of* ***5:Mes**** (given in ppm, C_6D_6, 122 MHz, 298K).

3.10 [Mes*P(PMe$_3$)GaCl$_3$] (6:Mes*)

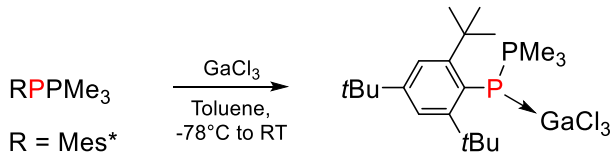

A 100 mg portion of Mes*PPMe$_3$ (0.283 mmol, 1.0 eq) together with 0.050 g of GaCl$_3$ (0.283 mmol, 1.0 eq) are placed in a Schlenk tube. At -78°C, 5 mL of toluene are added, and the obtained suspension is stirred for 20 min. at that temperature. The cooling bath is then removed, and the suspension is stirred for another 20 min. The solvent is then filtered off and the white precipitate is thoroughly dried *in vacuo*. A pale-white powder is obtained with **6:Mes*** as the main product (crude yield: 0.110 g). The contamination with [Mes*P(H)(PMe$_3$)][An] (An = anion) is experienced to be up to 20% at this stage. To obtain analytically pure material, meticulous recrystallization is necessary. The crude product is therefor suspended in 1.5 mL of freshly dried, and distilled toluene. Subsequently, just as much freshly dried, and distilled DCM is added until a clear colorless solution is obtained. Placing the solution at -78°C precipitates pure **6:Mes*** as a (micro-)crystalline powder after a few days (0.040 mmol, 0.021 g, 14%). A few crystals suitable for SC-XRD are obtained from the crude product after dissolving in DCM and placing a concentrated solution at -32°C.

^{1}H NMR (CD_2Cl_2, 400 MHz, 298K): δ = 7.46 (dd, J = 3.5, 0.8 Hz, 2H, CH_{Ar}), 1.63 (s, 18H, CH_3), 1.53 (dd, $^2J_{PH}$ = 12.8 Hz, $^3J_{PH}$ = 3.5 Hz, 9H, CH_3 of PMe_3), 1.30 (s, 9H, CH_3) ppm. **^{13}C{^{1}H} NMR** (CD_2Cl_2, 101 MHz, 298K): δ = 161.8 (s, *o*-$C(CH_3)_3$)*, 153.4 (s, *p*-$C(CH_3)_3$)*, 123.2–123.1 (m, ArCH), 39.4 (d, $^3J_{PC}$ = 3.5 Hz, *o*-$C(CH_3)_3$), 35.5 (s, *p*-$C(CH_3)_3$), 34.6 (d, $^{ts}J_{PC}$ = 6.2 Hz, *o*-$C(CH_3)_3$), 31.4 (s, *p*-$C(CH_3)_3$), 14.3 (dd, $^1J_{CP}$ = 44.2 Hz, $^2J_{CP}$ = 9.3 Hz, CH_3 of PMe_3), (not observed: (ArC_{ipso}) ppm. * Assigned with ^{1}H/^{13}C HMBC spectrum. **^{31}P{^{1}H} NMR** (CD_2Cl_2, 162 MHz, 298K): δ = 21.32 (d, $^1J_{PP}$ = 395.4 Hz, R-P*P*Me_3), -95.48 (*br*-d, $^1J_{PP}$ = 395.8 Hz, R-*P*PMe_3) ppm. **^{31}P NMR** (CD_2Cl_2, 162 MHz, 298K): δ = 21.36 (dm, $^1J_{PP}$ = 395.4 Hz, R-P*P*Me_3)**, -95.48 (*br*-d, $^1J_{PP}$ = 396.2 Hz, R-*P*PMe_3)** ppm. ** poor signal to noise ratio, proton coupling could not be resolved properly, resonances assigned as

doublet of multiplets. **IR** (ATR, cm^{-1}): 2961 (s), 2870 (m), 1593 (m), 1532 (w), 1466 (m), 1401 (m), 1364 (s), 1296 (w), 1237 (m), 1212 (m), 1179 (s), 1127 (m), 1096 (s), 1061 (w), 1010 (s), 960 (vs), 903 (w), 879 (m), 857 (w), 783 (w), 750 (s), 718 (m), 676 (w), 652 (w), 637 (m), 613 (w), 520 (m), 467 (w), 439 (w).

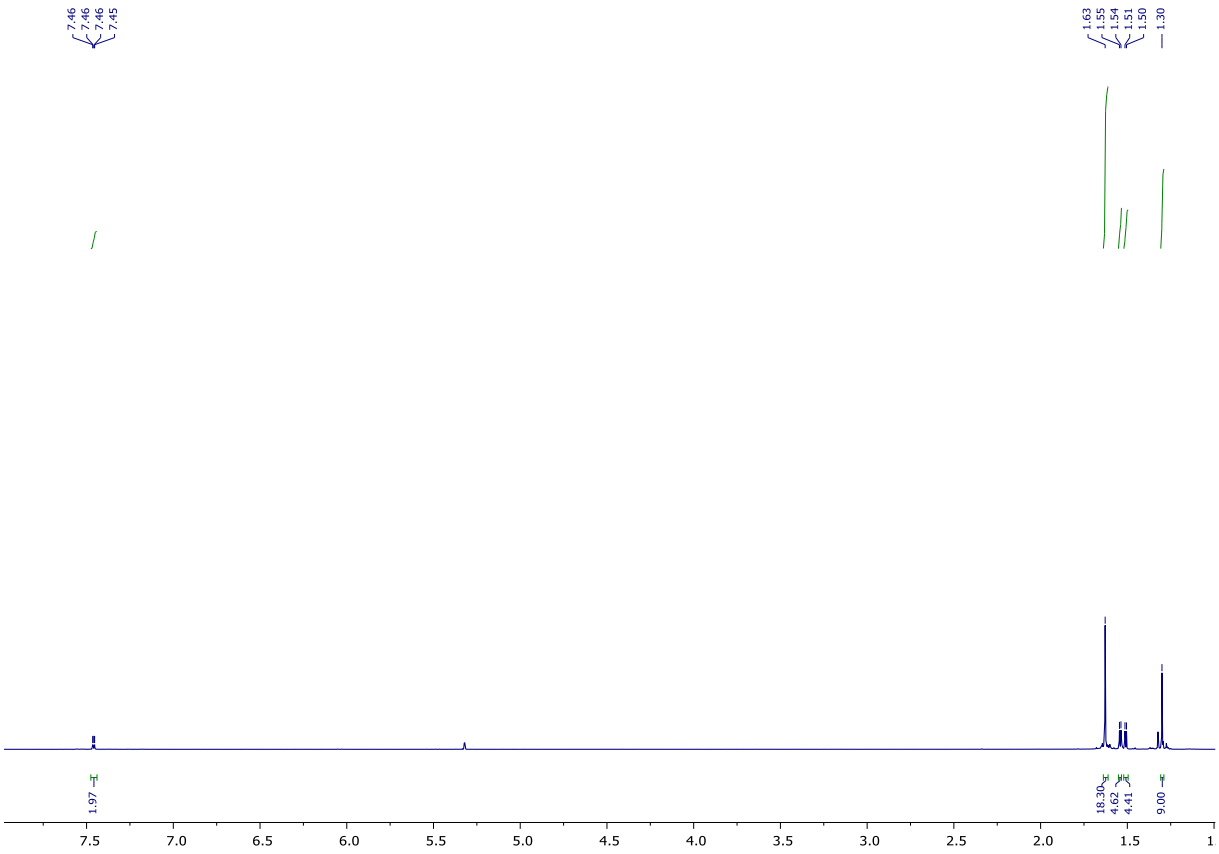

Figure S52: *^{1}H NMR of* ***6:Mes**** (given in ppm, CD_2Cl_2, 400 MHz, 298K).

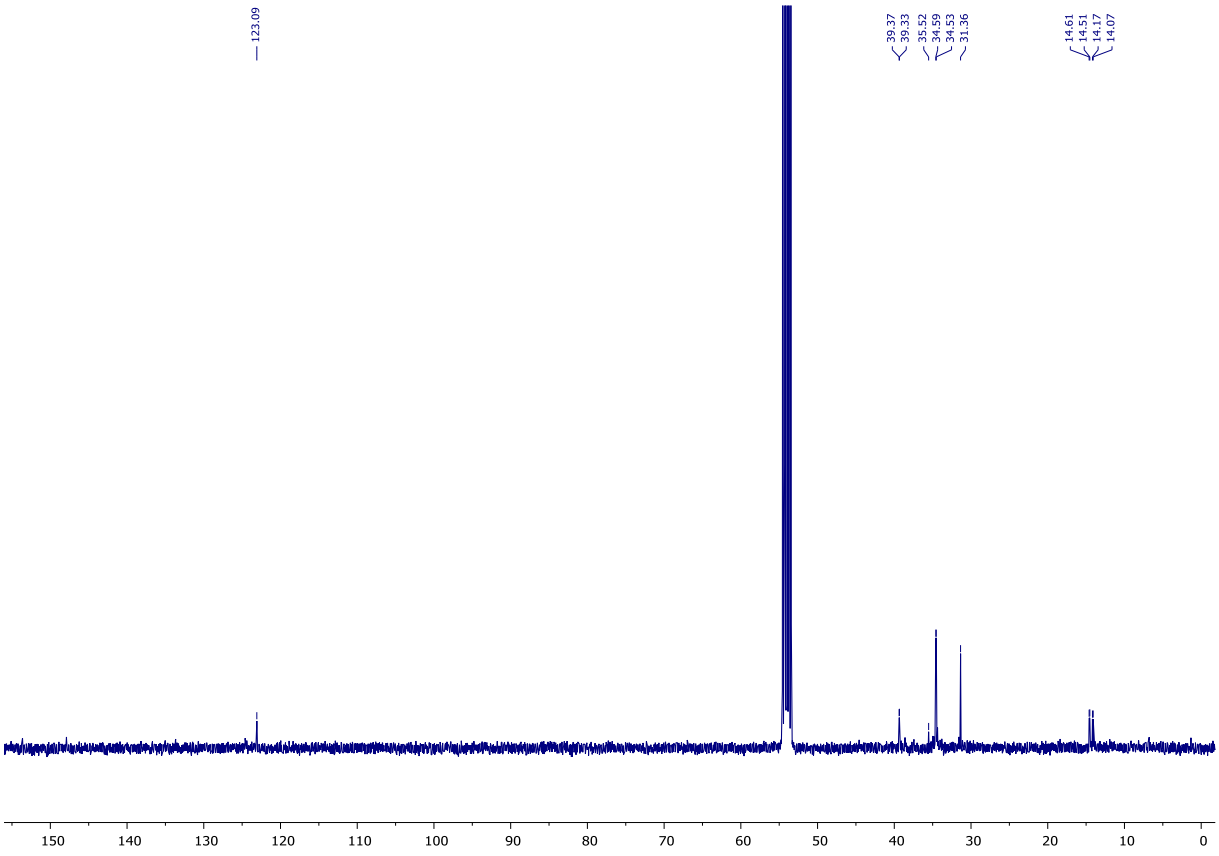

Figure S53: *$^{13}C\{^{1}H\}$ NMR of* ***6:Mes**** (given in ppm, CD_2Cl_2, 101MHz, 298K).

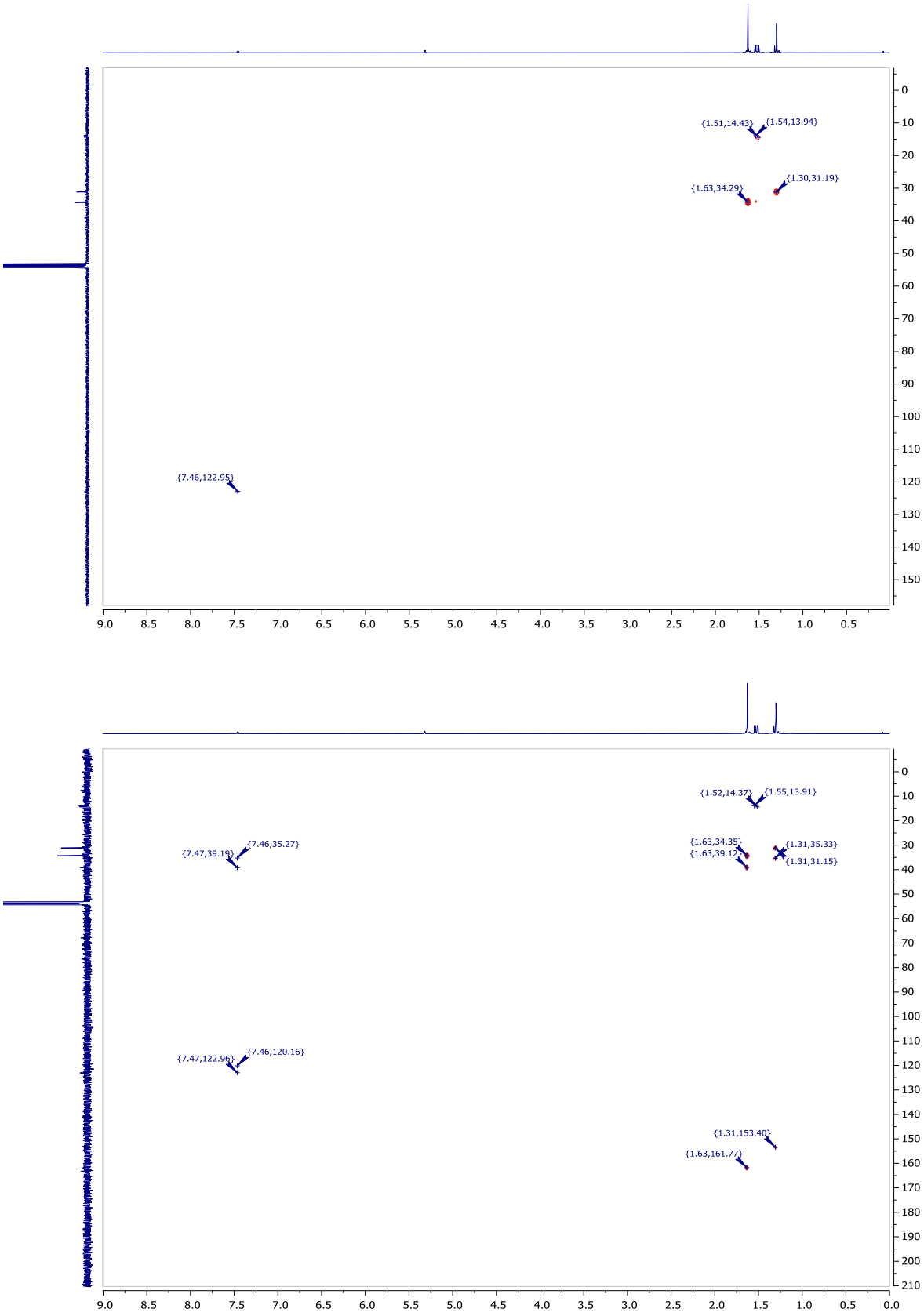

Figure S54: *1H-^{13}C NMR HSQC(top) and HMBC (bottom) spectrum of* ***6:Mes****.*

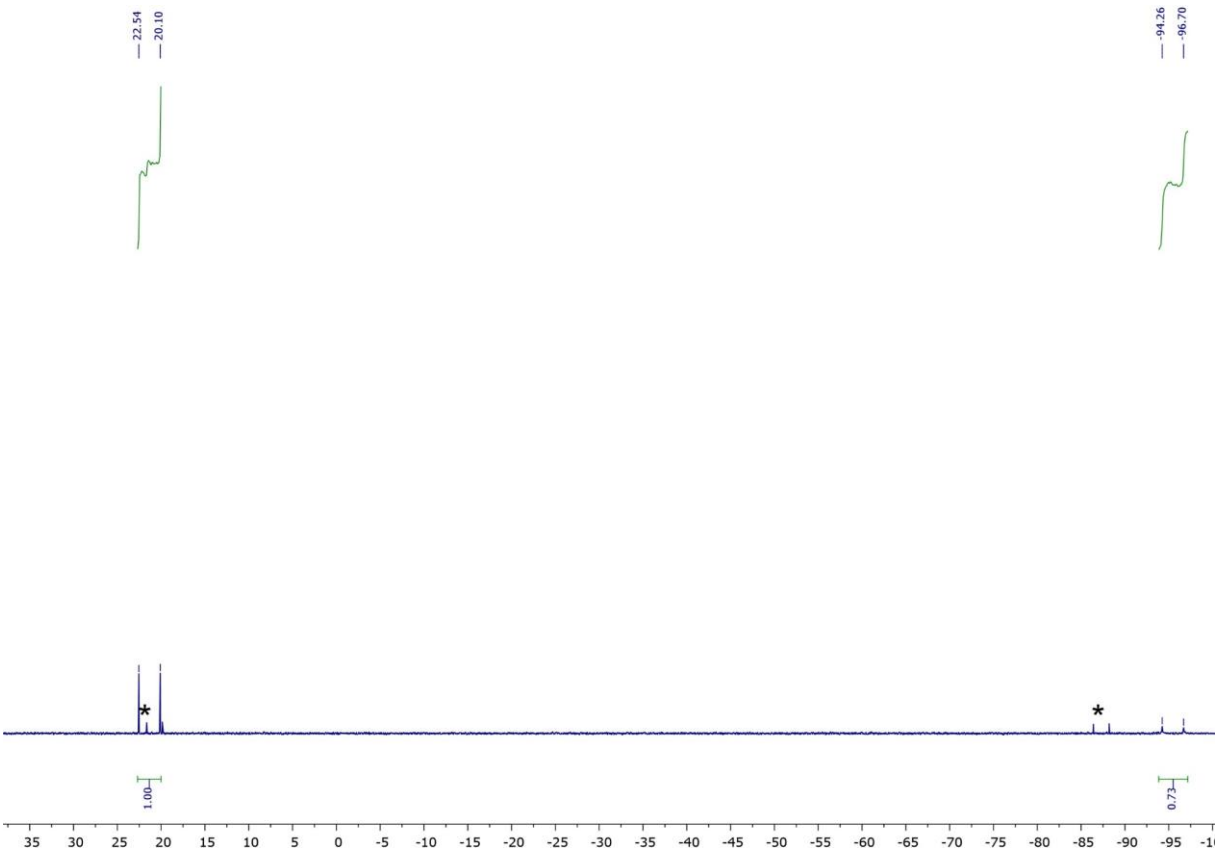

Figure S55: *$^{31}P\{^{1}H\}$ NMR of* ***6:Mes**** (given in ppm, CD_2Cl_2, 162 MHz, 298K). *: trace amounts of [Mes*P(H)PMe_3][An].

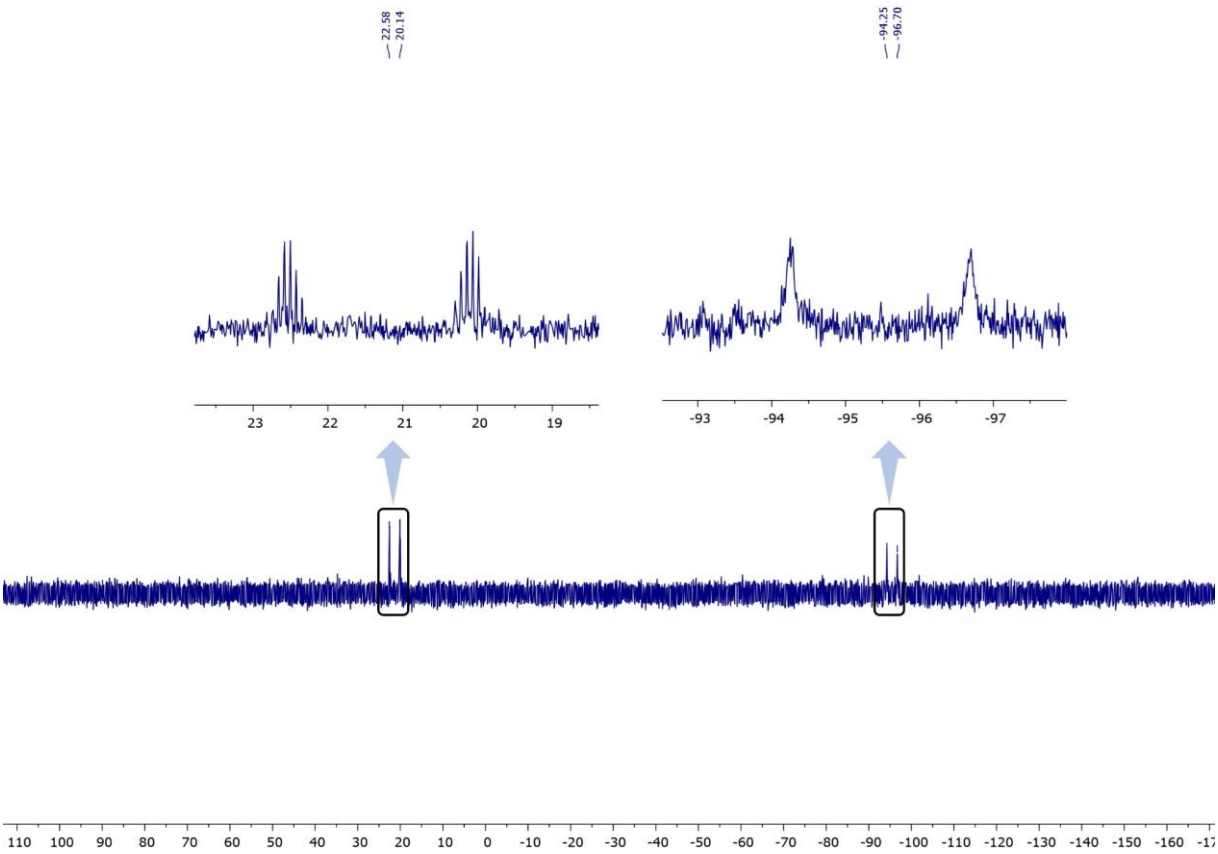

Figure S56: *^{31}P NMR of* ***6:Mes**** (given in ppm, CD_2Cl_2, 162 MHz, 298K).

3.11 [^{Dip}TerP(PMe$_3$)GaCl$_3$] (6:^{Dip}Ter)

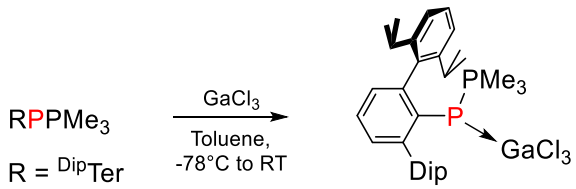

A 0.050 g portion of ^{Dip}TerPPMe$_3$ (0.1 mmol, 1.0 eq) together with 0.017 g of GaCl$_3$ are placed in a Schlenk tube. At -78°C, 3 mL of toluene are added, and the obtained suspension is stirred for 30 min. Then cooling is stopped, and the cold solvent is filtered off. The residue is thoroughly dried in vacuo to obtain 55 mg of crude **6:^{Dip}Ter**. The compound can be recrystallized in 20 mg batches. For this purpose, crude **6:^{Dip}Ter** is suspended in 1.5 mL of *n*-heptane. Just as much DCM is added until everything has dissolved and a clear solution is obtained. At -32°C, 5 mg of extremely(!) sensitive **6:^{Dip}Ter**·xDCM is obtained. The amount of single crystals were just enough for SC-XRD and IR spectroscopy (<0.007 mmol, <0.005 g, <7%: first batch).

^{31}P{^{1}H} NMR (CD_2Cl_2, 122 MHz, 298K, crude): δ = 12.87 (d, $^1J_{PP}$ = 412.5 Hz, R-P*P*Me$_3$), -85.73 (*br*-d, $^1J_{PP}$ = 411.9 Hz, R-*P*PMe$_3$) ppm. **IR** (ATR, pure, cm^{-1}): 3064.87 (w), 2957.15 (s), 2925.42 (m), 2867.02 (m), 1591.54 (w), 1557.03 (w), 1463.13 (m), 1423.70 (m), 1383.63 (m), 1362.40 (m), 1311.62 (m), 1288.66 (m), 1249.32 (m), 1180.62 (w), 1125.06 (w), 1056.16 (w), 1039.26 (w), 950.22 (vs), 856.93 (w), 822.10 (m), 803.81 (s), 755.18 (vs), 678.44 (m), 658.62 (w), 579.45 (m), 469.91 (w), 430.28 (w), 408.64 (w).

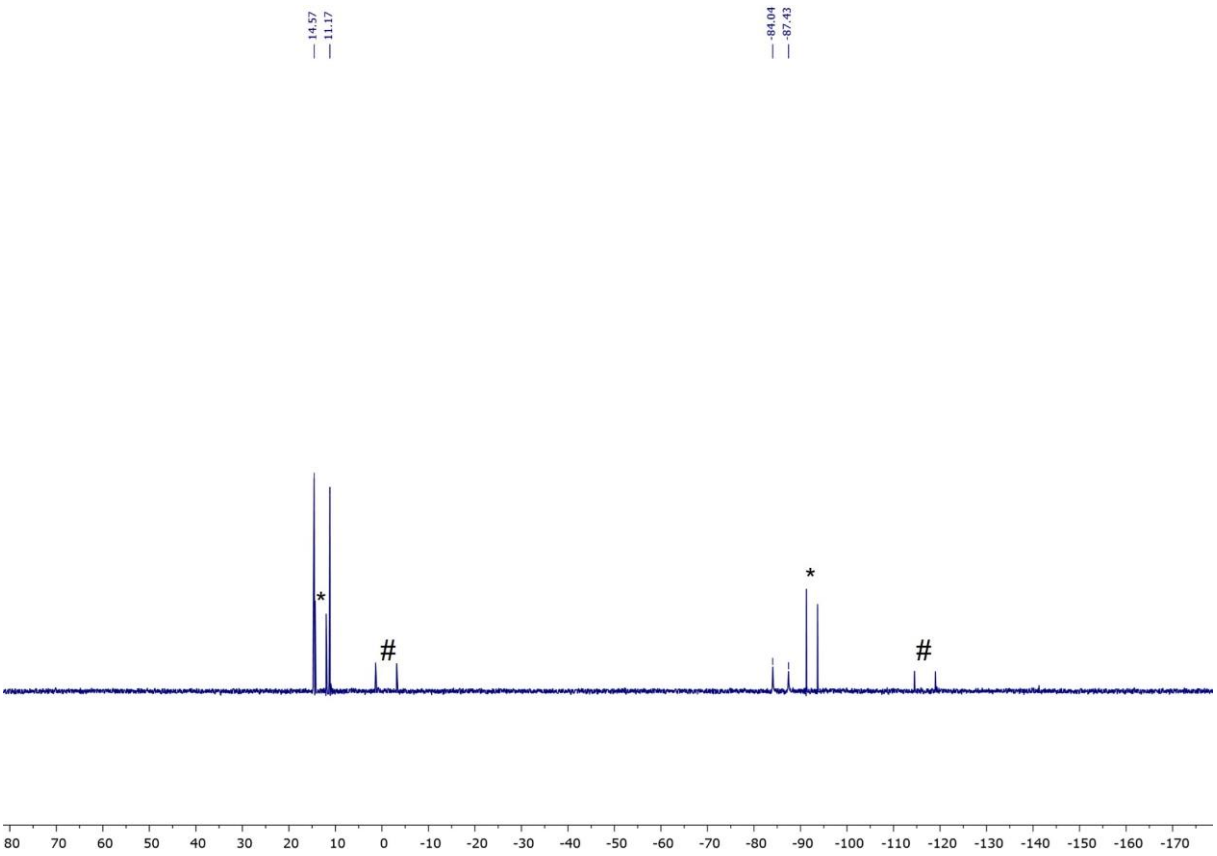

Figure S57: *$^{31}P\{^{1}H\}$ NMR of crude* ***6:^{Dip}Ter*** (given in ppm, CD_2Cl_2, 122 MHz, 298K). *[^{Dip}TerP(H)PMe_3][An]. #^{Dip}Ter$PPMe_3$ (through decomposition in solution).

3.12 [Mes*P(PMe$_3$)GaI$_3$] (7:Mes*)

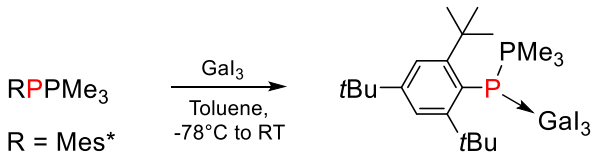

A 0.150 g portion of Mes*PPMe$_3$ (0.43 mmol, 1.0 eq) together with 0.194 g of GaI$_3$ (0.43 mmol, 1.0 eq) are placed in a Schlenk flask. Upon cooling to -78°C, 5 mL of toluene are added. The obtained suspension is stirred for 30 min. at that temperature and cooling is stopped. After stirring for another 30 min at ambient temperature, the solvent is filtered off. The remaining residue is thoroughly washed with 5 mL of benzene and is dried *in vacuo*. Dissolving the crude product in 5 mL of DCM, layering with 8 mL of *n*-hexane and placing the flask at 6°C yields large yellow block-shaped crystals after three days. After decanting and drying in vacuo, **7:Mes*** is obtained as slight yellow crystalline blocks which are suitable for SC-XRD (0.163 mmol, 0.131 g, 38%).

^{1}H NMR (CD_2Cl_2, 400 MHz, 298K): δ = 7.47 (dd, J = 3.4 Hz, J = 0.8 Hz, 2H, CH_{Ar}), 1.69 (s, 18H, CH_3), 1.61 (dd, $^2J_{PH}$ = 12.7 Hz, $^3J_{PH}$ = 3.1 Hz, 9H, CH_3 of PMe$_3$), 1.30 (s, 9H, CH_3) ppm. **^{13}C{^{1}H} NMR** (CD_2Cl_2, 101 MHz, 298K): δ = 161.4 (dd, $^3J_{CP}$ = 12.9 Hz, $^4J_{CP}$ = 6.1 Hz, *o*-*C*(CH$_3$)$_3$), 153.6–153.5 (m, *p*-*C*(CH$_3$)$_3$)*, 123.4 (dd, $^3J_{CP}$ = 7.6 Hz, $^4J_{CP}$ = 2.9 Hz, ArCH), 122.6 (dd, $^1J_{CP}$ = 53.9 Hz, $^2J_{CP}$ = 9.8 Hz, ArC_{ipso}), 39.4 (d, $^3J_{PC}$ = 2.5 Hz, *o*-*C*(CH$_3$)$_3$), 35.6 (s, *p*-*C*(CH$_3$)$_3$), 34.6 (d, $^{ts}J_{PC}$ = 5.9 Hz, *o*-C(*C*H$_3$)$_3$), 31.4 (s, *p*-C(*C*H$_3$)$_3$), 14.7 (dd, $^1J_{CP}$ = 43.8 Hz, $^2J_{CP}$ = 8.7 Hz, *C*H$_3$ of PMe$_3$) ppm. *Unknown C-P coupling. **^{31}P{^{1}H} NMR** (CD_2Cl_2, 162 MHz, 298K): δ = 21.67 (d, $^1J_{PP}$ = 423.0 Hz, R-P*P*Me$_3$), -86.37 (*br*-d, $^1J_{PP}$ = 423.1 Hz, R-*P*PMe$_3$) ppm. **^{31}P NMR** (CD_2Cl_2, 162 MHz, 298K): δ = 21.36 (*ps*-doct, $^1J_{PP}$ = 395.4 Hz, $^2J_{PH}$ = 12.6 Hz, R-P*P*Me$_3$)**, -86.38 (*br*-d, $^1J_{PP}$ = 422.6 Hz, R-*P*PMe$_3$)** ppm. **Expected doublet of decets could not be resolved. **IR** (ATR, cm^{-1}): 2952 (s), 2908 (m), 2865 (m), 1582 (w), 1519 (w), 1463 (m), 1402 (s), 1353 (m), 1310 (w), 1291 (m), 1235 (m), 1208 (m), 1126 (m), 949 (vs), 875 (s), 855 (m), 747 (s), 673 (m), 650 (w), 593 (w), 574 (w), 504 (w), 462 (w), 435 (w), 407 (m).

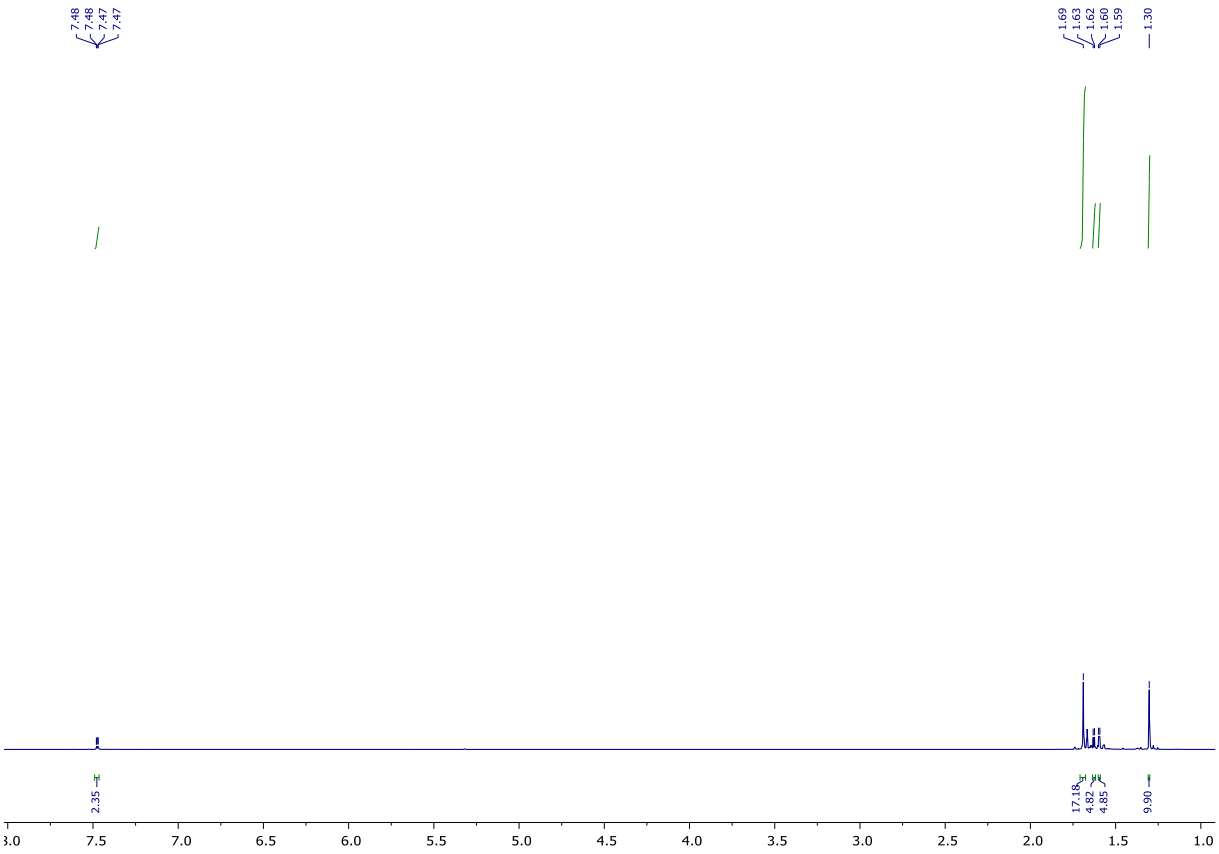

Figure S58: *^{1}H NMR of* ***7:Mes**** (given in ppm, CD_2Cl_2, 400 MHz, 298K).

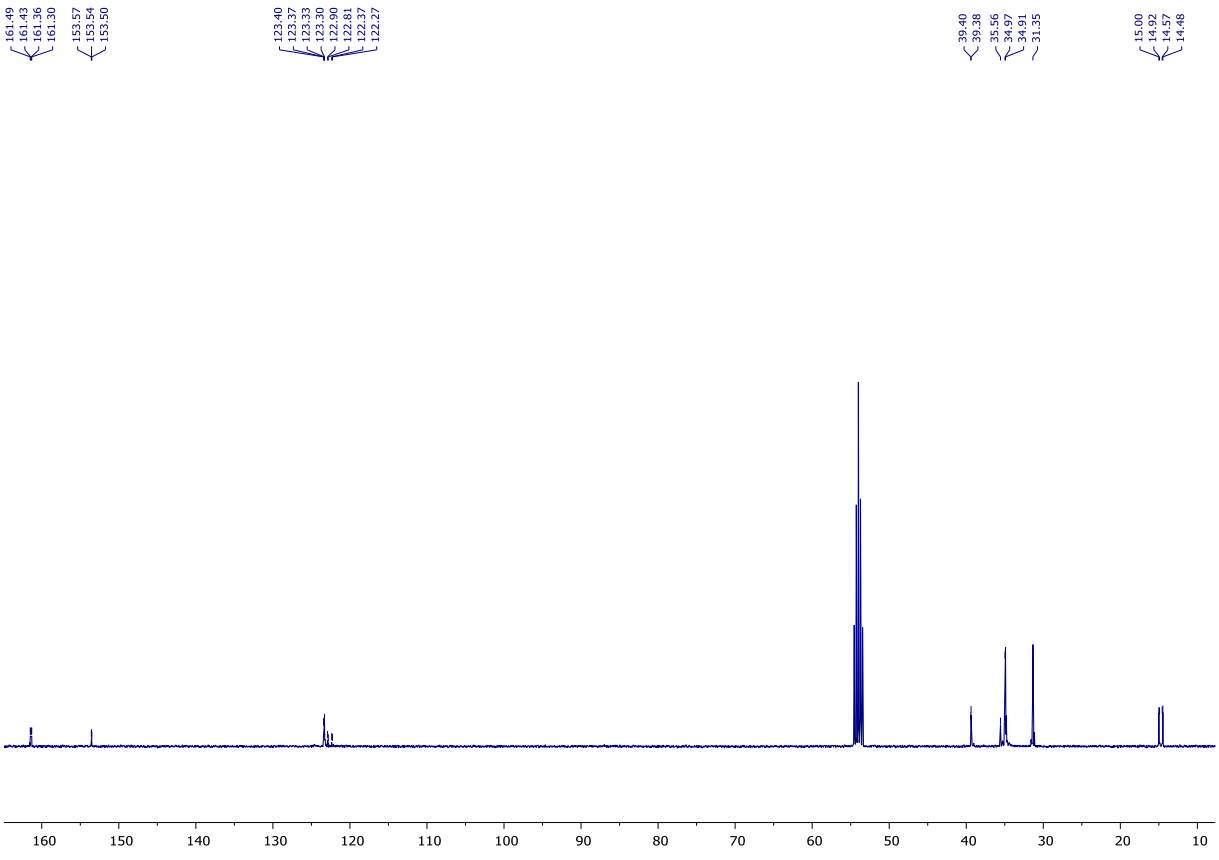

Figure S59: *$^{13}C\{^{1}H\}$ NMR of* ***7:Mes**** (given in ppm, CD_2Cl_2, 101MHz, 298K).

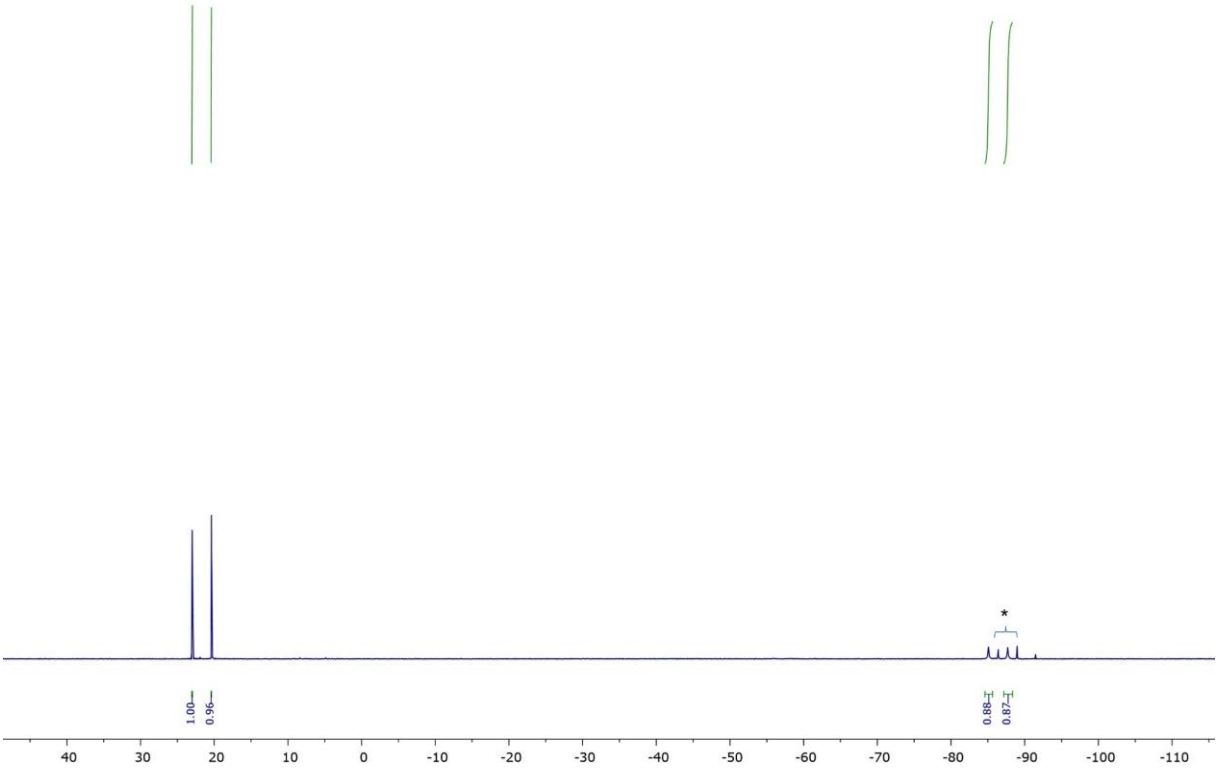

Figure S60: *$^{31}P\{^{1}H\}$ NMR of* ***7:Mes**** (given in ppm, CD_2Cl_2, 162 MHz, 298K). *traces of an unknown decomposition product.

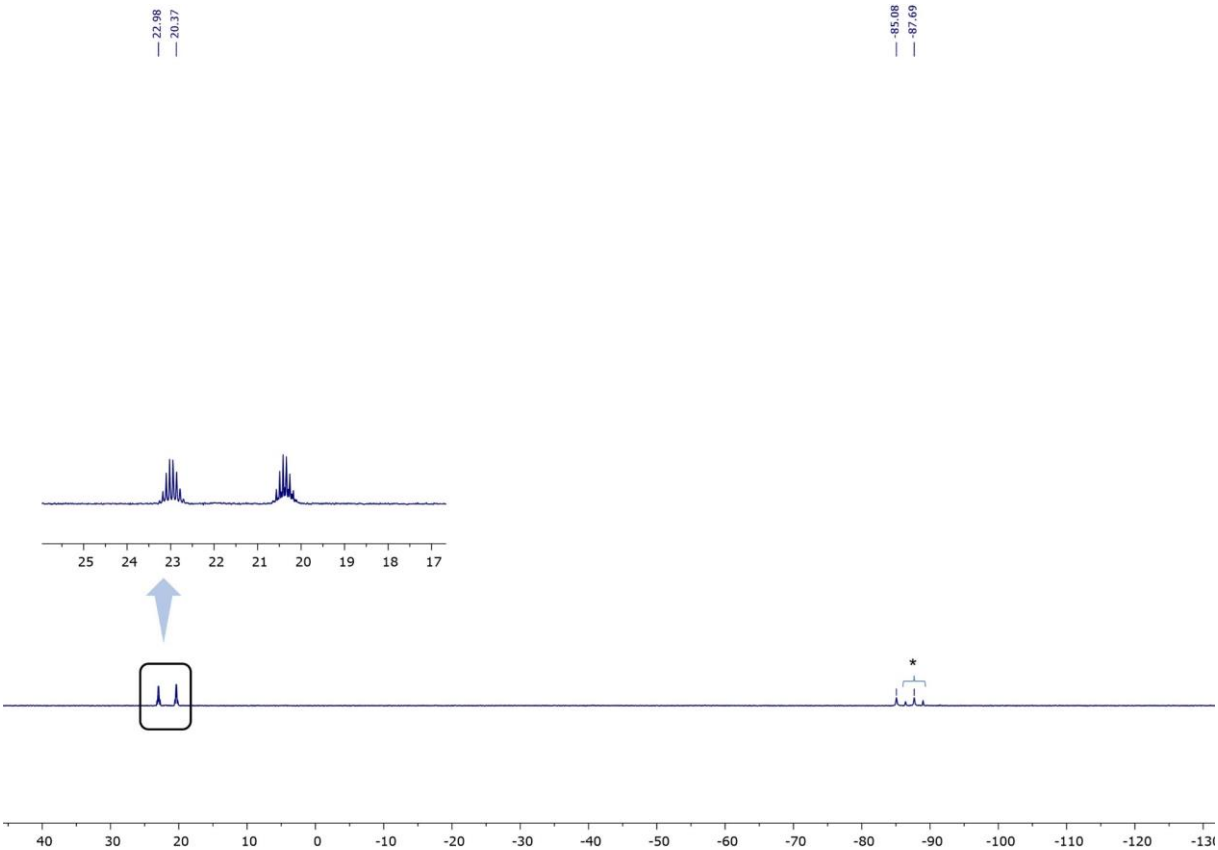

Figure S61: *^{31}P NMR of* ***7:Mes**** (given in ppm, CD_2Cl_2, 162 MHz, 298K). *traces of an unknown decomposition product.

3.13 Mes*P(PMe$_3$)–GaCl$_x$I$_{3-x}$ (8:Mes*)

After dissolving **7:Mes*** in DCM and stirring the solution vigorously in DCM, the recrystallization does afford a few platelet-shaped crystals of **8:Mes*** when placing an *n*-hexane layered solution at -32°C for several days.

3.14 [(^{Mes}TerP(PMe$_3$))$_2$GaCl$_2$]GaCl$_4$ (9:^{Mes}Ter)

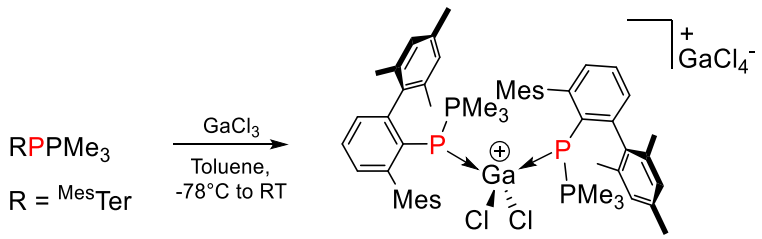

A 0.100 g portion of ^{Mes}TerPPMe$_3$ (0.238 mmol, 1.0 eq) and 0.042 of GaCl$_3$ (0.238 mmol, 1.0 eq) are placed in a Schlenk tube. At -78°C, 5 mL of toluene are added. The resulting suspension is stirred for one hour at that temperature. The cooling bath is then removed, and the obtained white suspension is stirred for another 20 min. at ambient temperature. The solvent is carefully filtered off to obtain 0.120 g of crude **9:^{Mes}Ter**. The best obtained batch showed a contamination of about 7% of [^{Mes}TerP(H)PMe$_3$][An] (estimated by means of ^{31}P NMR) – *no analytically pure material could be obtained*, even employing freshly dried and distilled solvents as well as meticulous Schlenk techniques. A few small colourless platelets of **9:^{Mes}Ter** for SC-XRD can be grown. For this purpose, 4 mL of *n*-heptane are added to the crude product. Just as much DCM is then added until a colorless, clear solution is obtained. Placing the solution at -32°C yields platelet-shaped crystals after a few days.

^{1}H NMR (CD_2Cl_2, 300 MHz, 298K): δ = 7.54–7.48 (m, 1H, *p*-Ar*H*), 7.09–7.05 (m, 4H, *m*-*H* of Mes), 6.97 (*br*-s, 2H, *m*-Ar*H*), 2.35 (s, 6H, *p*-C*H*$_3$ of Mes), 2.27 (*br*-s, 6H, *m*-C*H*$_3$ of Mes), 1.99 (*br*-s, 6H, *m*-C*H*$_3$ of Mes), 1.46 (dd, $^2J_{PH}$ = 12.9 Hz, $^3J_{PH}$ = 4.8 Hz, 9H, C*H*$_3$ of PMe$_3$) ppm. **^{31}P{^{1}H} NMR** (CD_2Cl_2, 122 MHz, 298K): δ = 13.13 (d, $^1J_{PP}$ = 410.3 Hz, R-P*P*Me$_3$), -86.37 (*br*-d, $^1J_{PP}$ = 408.6 Hz, R-*P*PMe$_3$) ppm. **^{31}P NMR** (CD_2Cl_2, 122 MHz, 298K): δ = 13.13 (*ps*-doct, $^1J_{PP}$ = 411.9 Hz, $^2J_{PH}$ = 12.9 Hz, R-P*P*Me$_3$)**, -84.87 (*br*-d, $^1J_{PP}$ = 410.4 Hz, R-*P*PMe$_3$)** ppm. **Expected doublet of decets could not be resolved.

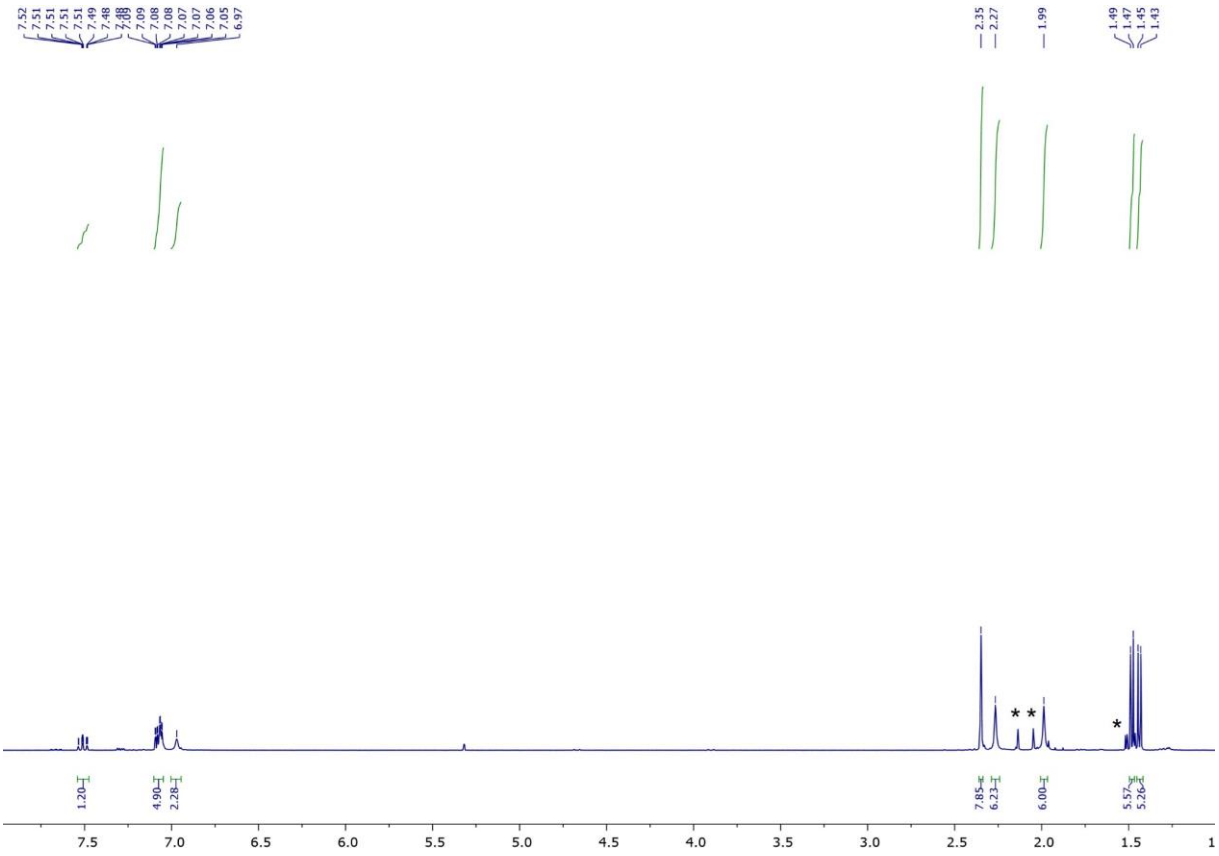

Figure S62: *^{1}H NMR of* ***9:^{Mes}Ter*** (given in ppm, CD_2Cl_2, 300 MHz, 298K). *[^{Mes}TerP(H)PMe$_3$][An].

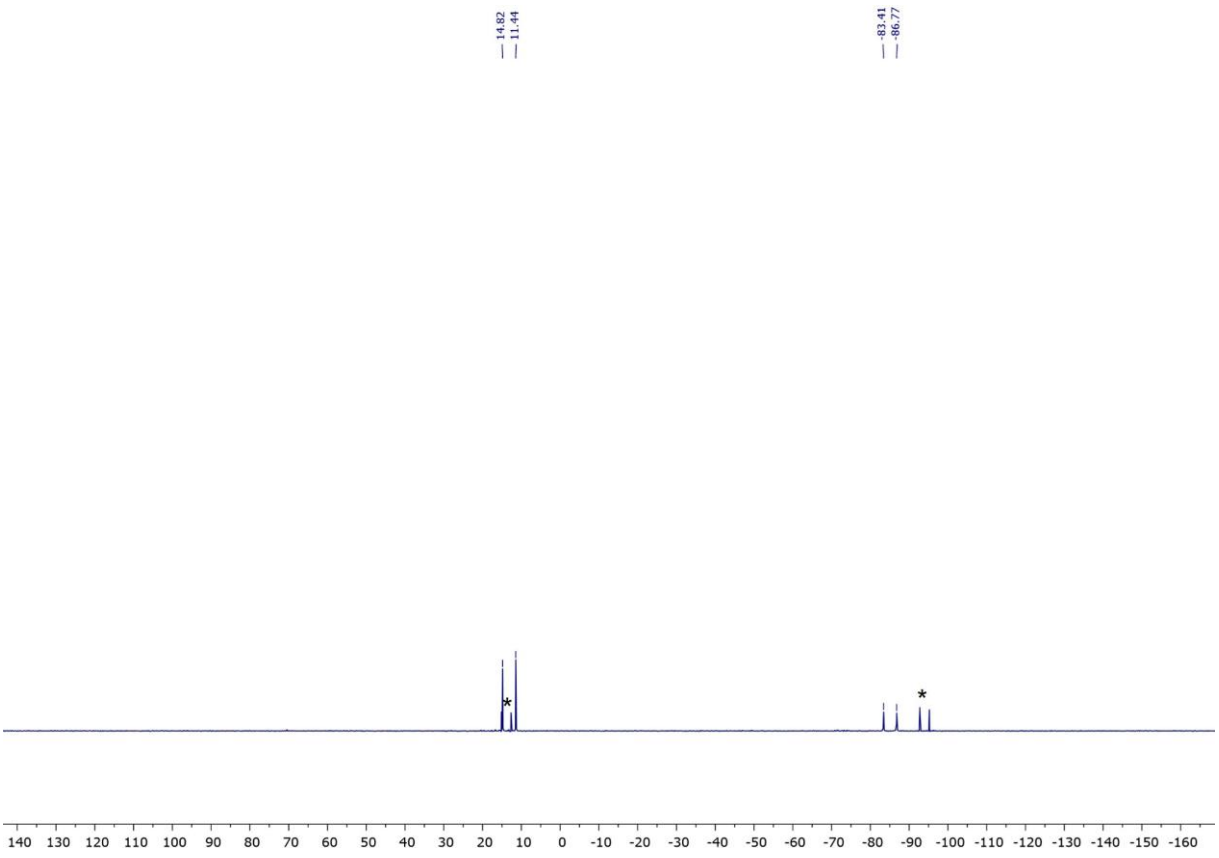

Figure S63: *$^{31}P\{^{1}H\}$ NMR of* ***9:^{Mes}Ter*** (given in ppm, CD_2Cl_2, 122 MHz, 298K). *[^{Mes}TerP(H)PMe$_3$][An].

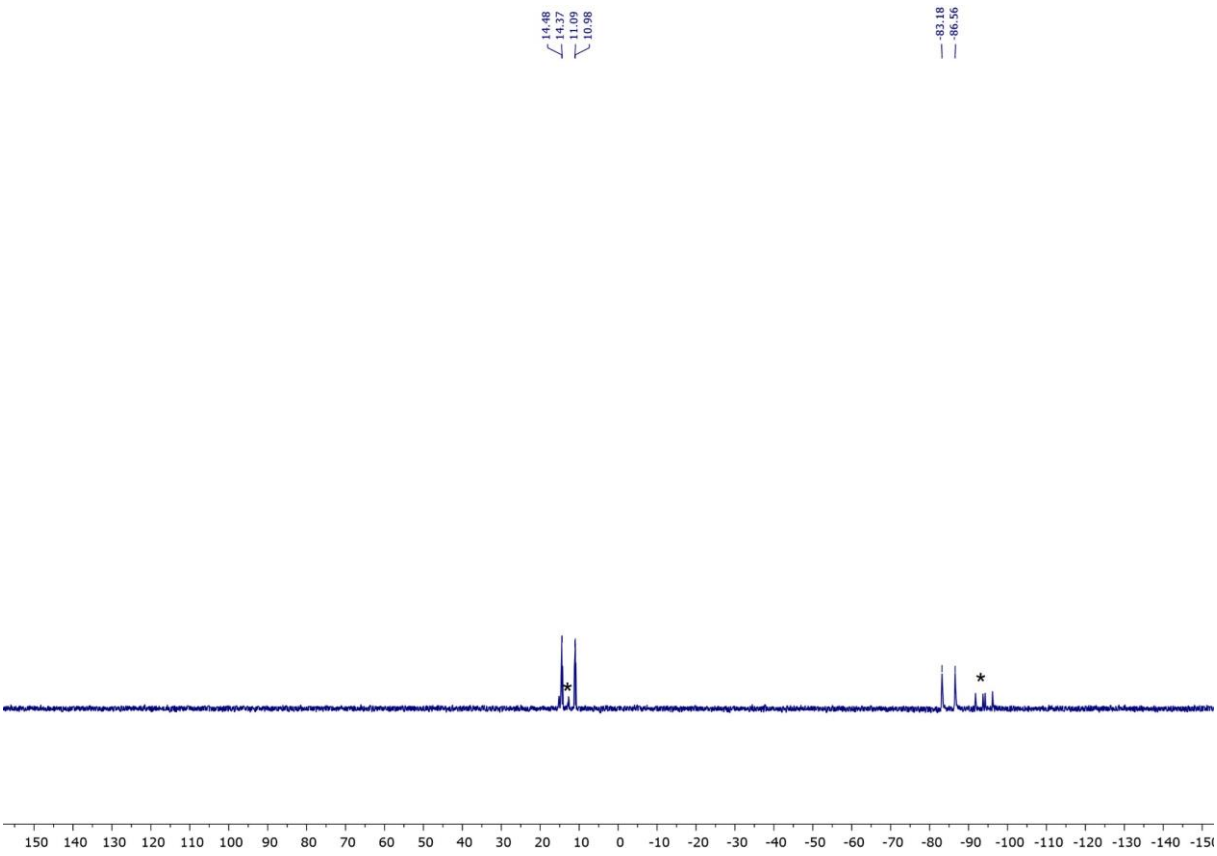

Figure S64: *^{31}P NMR of* ***9:^{Mes}Ter*** (given in ppm, CD_2Cl_2, 122 MHz, 298K). *[^{Mes}TerP(H)PMe_3][An].

3.15 [Mes*P(H)(PMe$_3$)]GaI$_4$ (10:Mes*)

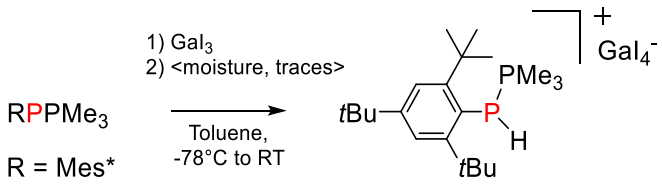

A 0.075 g portion of Mes*PPMe$_3$ (0.075 g, 0.21 mmol, 1.0 eq) together with GaI$_3$ (0.096 g, 0.21 mmol, 1.0 eq) are cooled to -78°C. Then, 4 mL of toluene are added, and the obtained suspension is stirred for 5 min. at that temperature. The cooling bath is removed, and the suspension is stirred for a further hour at ambient temperature (wrap flask with tin-foil!). The solvent is then filtered off and the residue is thoroughly washed with 3 mL of moisture contaminated *n*-hexane. After drying the crude product *in vacuo*, the residue is dissolved in 1.5 mL of DCM. The obtained solution is then layered with 5 mL of n-hexane and subsequently placed at -32°C. After a few days, a few block-shaped crystals of **10:Mes*** were obtained among powdery material. Careful sorting of the single crystals allowed an NMR spectroscopic investigation. Crystals were just enough for SC-XRD and ^{1}H / ^{31}P/^{31}P{^{1}H} NMR.

^{1}H NMR (CD_2Cl_2, 400 MHz, 298K): δ = 7.55 (s, 1H, C*H*$_{Ar}$), 7.53 (d, J = 5.4 Hz, 1H, C*H*$_{Ar}$), 5.80 (dd, $^{1}J_{PH}$ = 226.0 Hz, $^{2}J_{PH}$ = 9.3 Hz, 1H, P(*H*)PMe$_3$), 1.69 (dd, $^{2}J_{PH}$ = 13.2 Hz, $^{3}J_{PH}$ = 1.9 Hz, 9H, C*H*$_3$ of PMe$_3$), 1.61 (s, 9H, C*H*$_3$), 1.54 (s, 9H, C*H*$_3$), 1.33 (s, 9H, C*H*$_3$) ppm. **^{31}P{^{1}H} NMR** (CD_2Cl_2, 122 MHz, 298K): δ = 20.87 (d, $^{1}J_{PP}$ = 291.8 Hz, R-P(H)*P*Me$_3$), -87.00 (d, $^{1}J_{PP}$ = 290.7 Hz, R-*P*(H)PMe$_3$) ppm. **^{31}P NMR** (CD_2Cl_2, 122 MHz, 298K): δ = 20.87 (dm, $^{1}J_{PP}$ = 292.6 Hz, R-P(H)*P*Me$_3$)*, -87.00 (dd, $^{1}J_{PP}$ = 291.3 Hz, $^{1}J_{PH}$ = 226.0 Hz, R-*P*(H)PMe$_3$) ppm. * An expected doublet of decet of doublets could not be resolved.

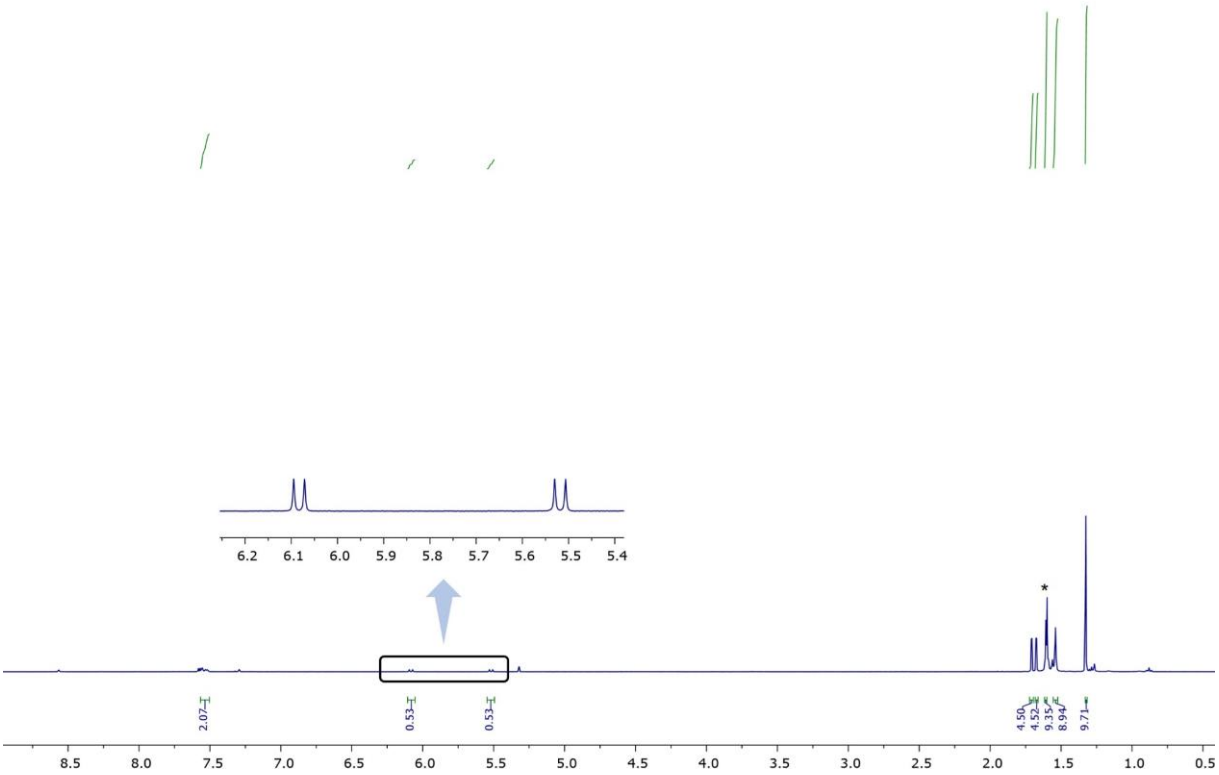

Figure S65: *^{1}H NMR of* ***10:Mes**** (given in ppm, CD_2Cl_2, 400 MHz, 298K). *Unknown decomposition product.

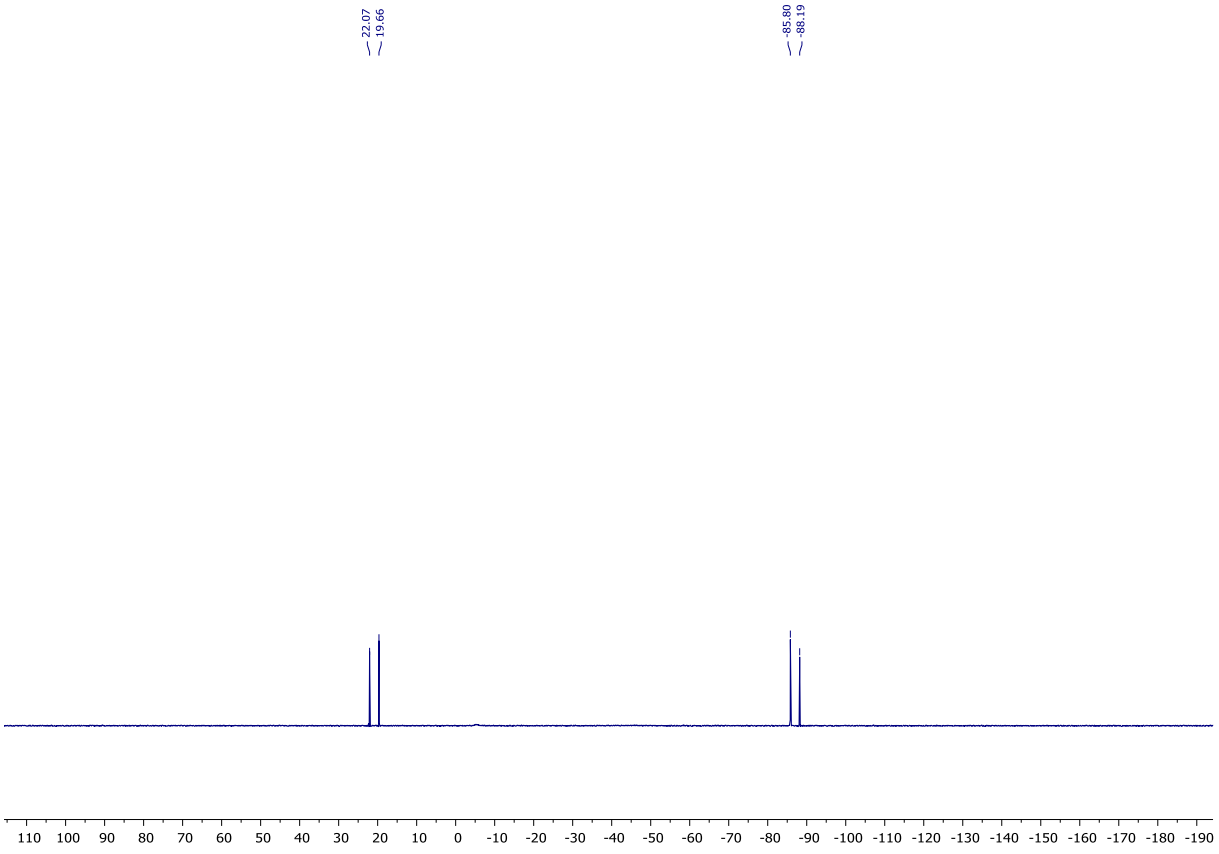

Figure S66: *$^{31}P\{^{1}H\}$ NMR of* ***10:Mes**** (given in ppm, CD_2Cl_2, 122 MHz, 298K).

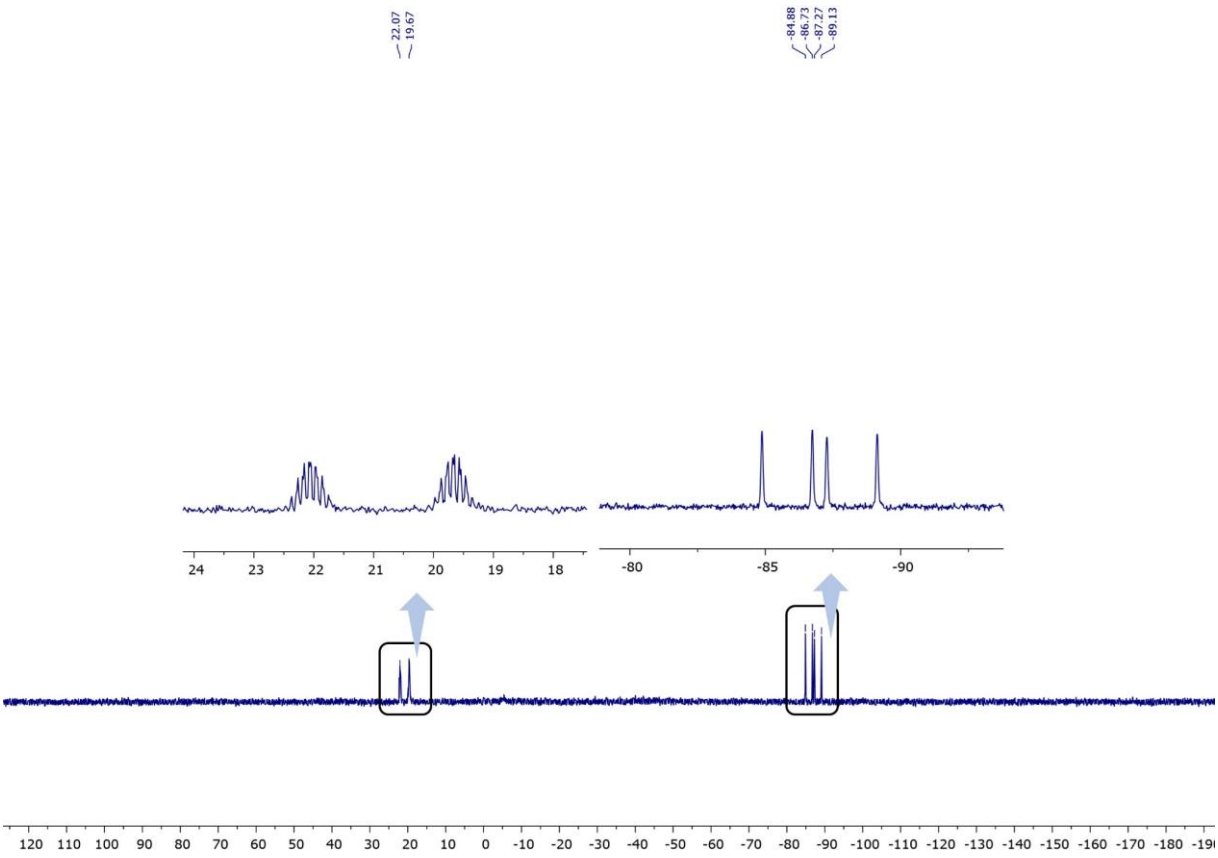

Figure S67: *^{31}P NMR of* ***10:Mes**** (given in ppm, CD_2Cl_2, 122 MHz, 298K).

3.16 $[Mes^*P(H)(PMe_3)]_2Ga_4O_2I_{10}$ (11:Mes*)

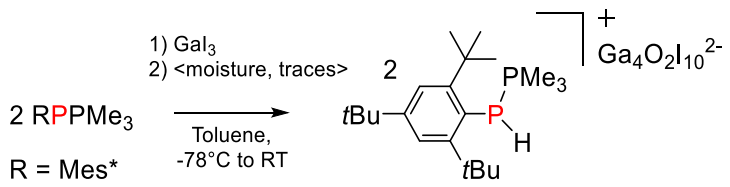

When recrystallizing the crude product of the synthesis of **10:Mes*** from a layered DCM/*n*-hexane(non-absolute) solution (1:2) at 6°C, a few very small platelet-shaped crystals of **11:Mes*** can be obtained for SC-XRD (see table S6 for details).

3.17 [Mes*P(H)(PMe$_3$)]GaCl$_4$ (12:Mes*)

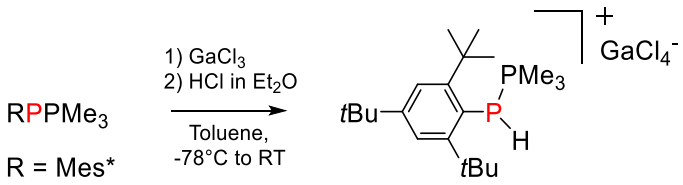

A 150 mg portion of Mes*PPMe$_3$ (0.43 mmol, 1.0 eq) together with 0.076 g of GaCl$_3$ (0.43 mmol, 1.0 eq) are placed in a Schlenk tube. Upon cooling at -78°C, 5 mL of toluene are added, and the obtained suspension is stirred for 30 min. at that temperature. The cooling bath is then removed, and 0.22 mL of 2M HCl in Et$_2$O (0.43 mmol of HCl, 1.0 eq) are immediately added to the solution. After stirring for another 30 min. at ambient temperature, the solvent filtered off and the obtained residue is washed with 5 mL of benzene. Then, the obtained colorless residue is dissolved in 5 mL of DCM. The slight cloudy solution is filtered, and the obtained colorless solution is layered with 8 mL of -hexane. The respective flask is kept at 6°C overnight and is then placed at -32°C. After two days, large colorless platelet-shaped crystals of **10:Mes*** are obtained which are suitable for SC-XRD (0.19 mmol, 0.110 g, 45% – first batch). After decanting the solution and placing again at -32°C, a second batch of crystals is obtained after a few days. Combining the crystals yields 0.150 g of **10:Mes*** (0.27 mmol, 62% – combined yield).

^{1}H NMR (CD_2Cl_2, 400 MHz, 298K): δ = 7.55 (s, 1H, CH_{Ar}), 7.52 (d, J = 5.2 Hz, 1H, CH_{Ar}), 5.77 (dd, $^1J_{PH}$ = 226.3 Hz, $^2J_{PH}$ = 9.3 Hz, 1H, P(H)PMe$_3$), 1.63 (dd, $^2J_{PH}$ = 13.3 Hz, $^3J_{PH}$ = 1.9 Hz, 9H, CH_3 of PMe$_3$), 1.60 (s, 9H, CH_3), 1.53 (s, 9H, CH_3), 1.32 (s, 9H, CH_3) ppm. **^{13}C{^{1}H} NMR** (CD_2Cl_2, 101 MHz, 298K): δ =159.2 (d, $^3J_{CP}$ = 7.1 Hz, o-C(CH$_3$)$_3$), 159.1-158.9 (m, o-C(CH$_3$)$_3$)*, 154.6 (d, J = 5.9 Hz, p-C(CH$_3$)$_3$)**, 124.5 (d, $^3J_{CP}$ = 4.4 Hz, ArCH), 124.3 (dd, , $^3J_{CP}$ = 7.4 Hz, $^4J_{CP}$ = 4.4 Hz, ArCH), 115.7 (dd, $^1J_{CP}$ = 34.1 Hz, $^2J_{CP}$ = 10.8 Hz, ArC_{ipso}), [39.2+38.6] (s, o-C(CH$_3$)$_3$), 35.7 (d, J = 1.7 Hz, p-C(CH$_3$)$_3$)**, 34.9 (d, $^{ts}J_{CP}$ = 11.9 Hz, o-C(CH$_3$)$_3$), 34.3 (s, o-C(CH$_3$)$_3$), 31.3 (d, J = 1.4 Hz, p-C(CH$_3$)$_3$)**, 12.1 (dd, $^1J_{CP}$ = 41.5 Hz, $^2J_{CP}$ = 4.2 Hz, CH$_3$ of PMe$_3$) ppm. * An expected doublet of doublets from $^3J_{CP}$ and $^4J_{CP}$ coupling could not be resolved. ** Unknown C-P coupling. **^{31}P{^{1}H} NMR** (CD_2Cl_2, 162 MHz, 298K): δ = 20.90 (d, $^1J_{PP}$ = 291.0 Hz, R-P(H)PMe$_3$), -87.23 (d, $^1J_{PP}$ = 291.0 Hz,

R-*P*(H)PMe_3) ppm. **^{31}P NMR** (CD_2Cl_2, 162 MHz, 298K): δ = 20.90 (*dm*, $^1J_{PP}$ = 290.4 Hz, R-P(H)*P*Me_3)***, -87.25 (dd, $^1J_{PP}$ = 291.0 Hz, $^1J_{PH}$ = 226.3 Hz, R-*P*(H)PMe_3) ppm. *** Expected doublet of decet of doublets could not be resolved. **IR** (ATR, cm^{-1}): 2952 (s), 2908 (m), 2865 (m), 2380 ν_{sym}(P-H) (vw), 1582 (m), 1519 (w), 1463 (m), 1402 (s), 1353 (m), 1310 (w), 1291 (m), 1235 (m), 1208 (m), 1126 (m), 949 (vs), 875 (s), 855 (m), 747 (s), 673 (s), 650 (m), 593 (w), 574 (w), 504 (w), 462 (w), 435 (m), 407 (w). **MS** (HR, ESI^+); calc. for $C_{21}H_{39}P_2$ $[M\text{-}GaCl_4]^+$ (found): 353.2532 (353.2526).

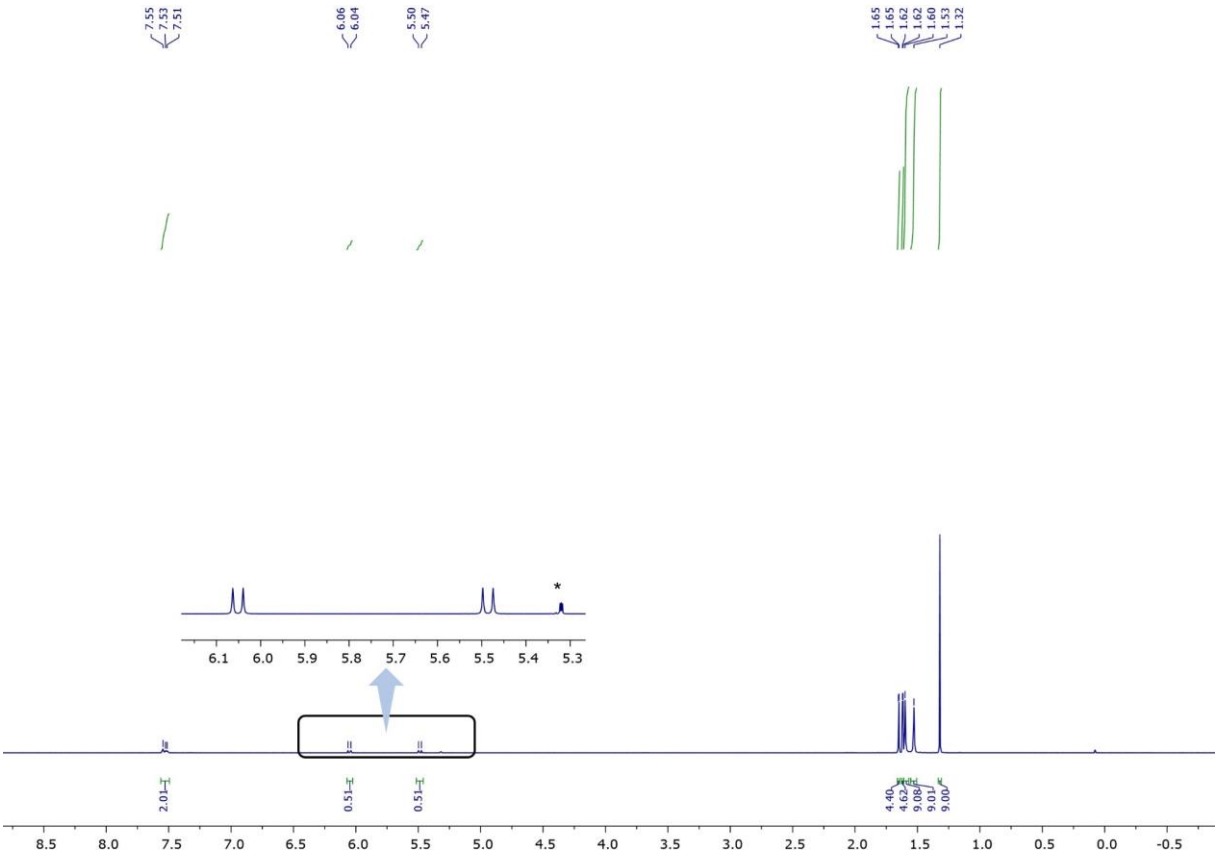

Figure S68: *^{1}H NMR of* ***12:Mes**** (given in ppm, CD_2Cl_2, 400 MHz, 298K). *Solvent signal.

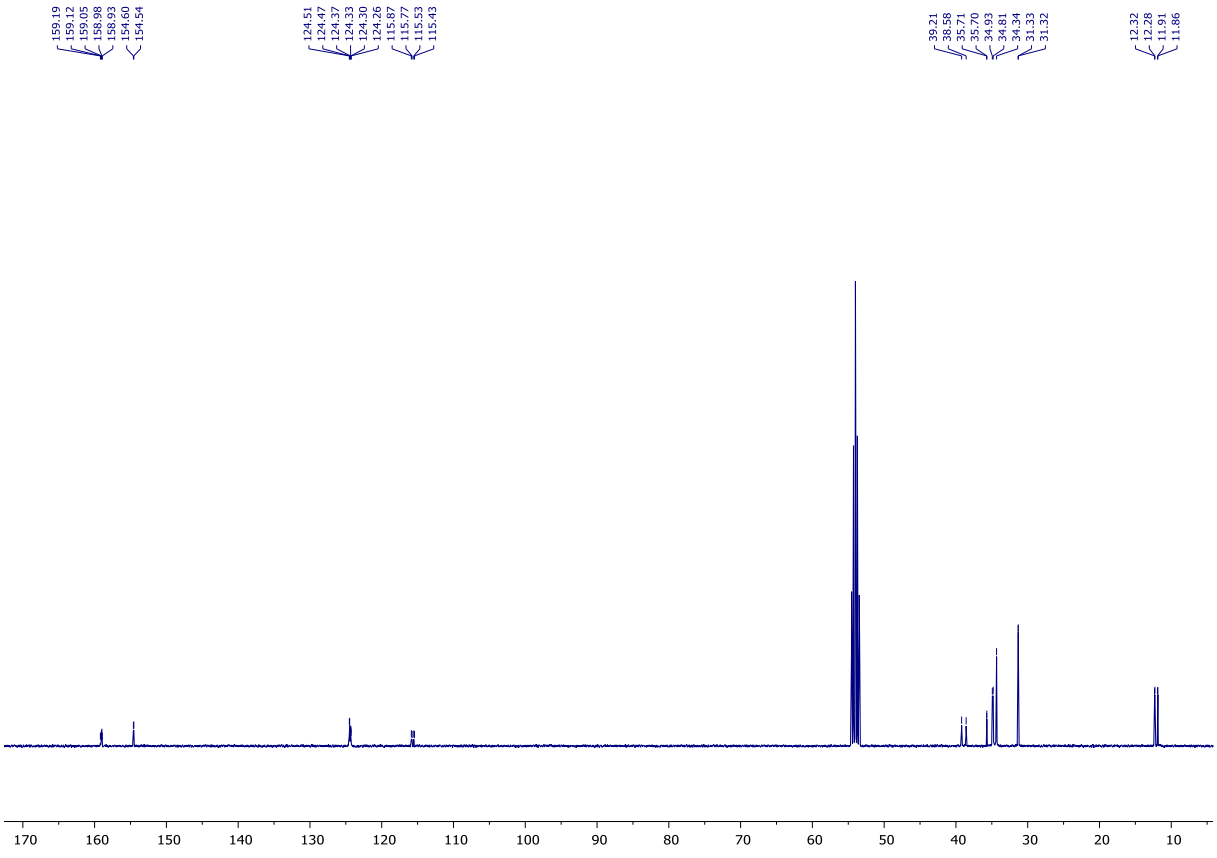

Figure S69: *$^{13}C\{^{1}H\}$ NMR of* ***12:Mes**** (given in ppm, CD_2Cl_2, 101MHz, 298K).

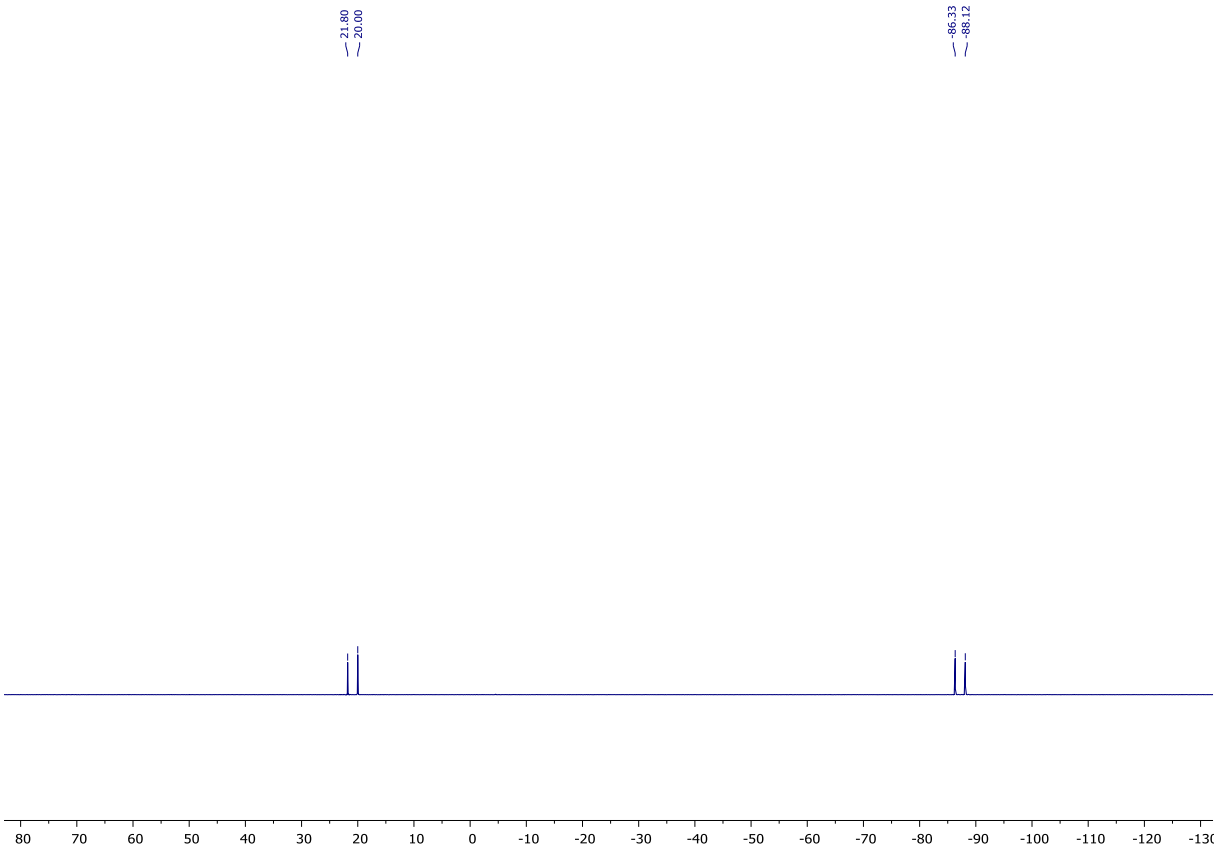

Figure S70: *$^{31}P\{^{1}H\}$ NMR of* ***12:Mes**** (given in ppm, CD_2Cl_2, 162 MHz, 298K).

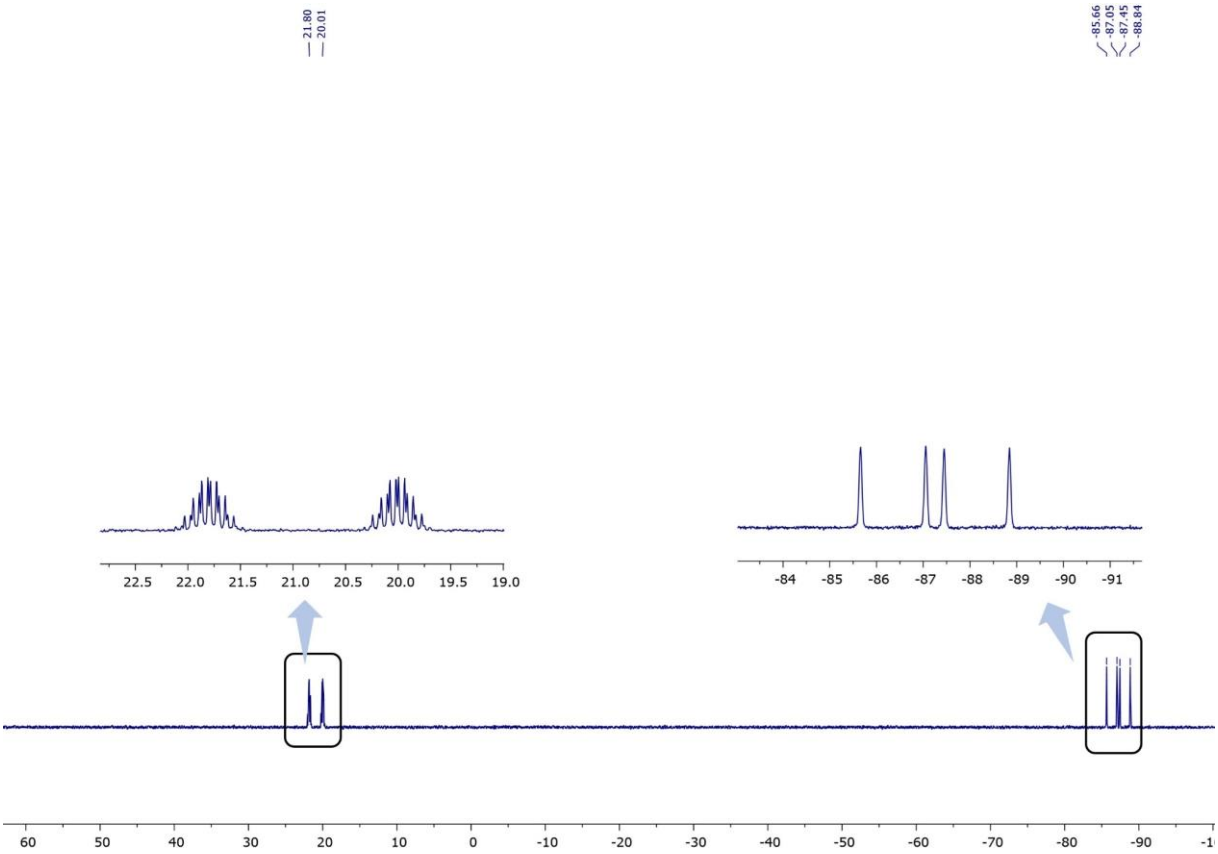

Figure S71: *^{31}P NMR of* ***12:Mes**** (given in ppm, CD_2Cl_2, 162 MHz, 298K).

3.18 [^{Mes}TerP(H)(PMe$_3$)]GaCl$_4$ (12:^{Mes}Ter)

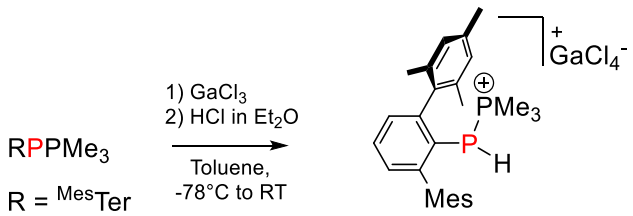

A 0.100 g portion of ^{Mes}TerPPMe$_3$ (0.238 mmol, 1.0 eq) together with 0.042 g of GaCl$_3$ (0.238 mmol, 1.0 eq) are placed in a Schlenk tube. At -78°C, 5 mL of toluene are added, and the resulting suspension is stirred for 30 min. at that temperature. The cooling bath is then removed and 0.14 mL of 2 M HCl in Et$_2$O (0.238 mmol, 1.0 eq) are immediately added to the solution. The mixture is stirred until a colorless, clear solution is obtained and the solvent is removed under reduced pressure. After thoroughly drying *in vacuo*, **12:^{Mes}Ter** is obtained as a pale-white microcrystalline powder in quantitative yield (>99%, 0.238 mmol).

^{1}H NMR (CD$_2$Cl$_2$, 300 MHz, 298K): δ = 7.73–7.67 (m, 1H, *p*-Ar*H*), 7.35–7.31 (m, 2H, *m*-Ar*H*), 7.11-7.08 (m, 4H, *m-H* of Mes), 4.33 (dd, $^1J_{PH}$ = 231.4 Hz, $^2J_{PH}$ = 9.6 Hz, 1H, R-P(*H*)PMe$_3$), 2.39 (s, 6H, C*H*$_3$ of Mes), 2.17 (s, 6H, C*H*$_3$ of Mes), 2.09 (s, 6H, C*H*$_3$ of Mes), 1.54 (dd, $^2J_{PH}$ = 13.6 Hz, $^3J_{PH}$ = 3.0 Hz, 9H, C*H*$_3$ of PMe$_3$) ppm. **^{13}C{^{1}H} NMR** (CD$_2$Cl$_2$, 75.5 MHz, 298K)*: δ = 147.5, 139.5, 137.4, 136.3, 135.2, 131.1, 130.3, 130.1, 129.6, 129.4, 122.8, [21.3, 21.3, 21.2, 21.2] (s, CH$_3$ of Mes), 12.3 (dd, $^1J_{CP}$ = 43.0 Hz, $^2J_{CP}$ = 6.3 Hz, CH$_3$ of PMe$_3$) ppm. *Due to chemical inequivalence of most of the C-atoms and poor signal to noise ratio, the ^{13}C{^{1}H} spectrum did not reveal all resonances. All aromatic C resonances which were found with a 1H/13C HMBC spectrum and that show reasonable correlations are listed. A clear assignment becomes questionable. **^{31}P{^{1}H} NMR** (CD$_2$Cl$_2$, 122 MHz, 298K): δ = 13.91 (d, $^1J_{PP}$ = 298.1 Hz, R-P(H)*P*Me$_3$), -93.99 (d, $^1J_{PP}$ = 298.1 Hz, R-*P*(H)PMe$_3$) ppm. **^{31}P NMR** (CD$_2$Cl$_2$, 122 MHz, 298K): δ =13.91 (dm, $^1J_{PP}$ =297.9 Hz, R-P(H)*P*Me$_3$)**, -93.99 (dd, $^1J_{PP}$ = 297.7 Hz, $^1J_{PH}$ = 230.9 Hz, R-*P*(H)PMe$_3$)** ppm. **Expected doublet of decet of doublets could not be resolved. **IR** (ATR, cm^{-1}): 2995 (m), 2949 (m), 2913 (s), 2855.96 (m), 2323 ν_{sym}(P-H) (w), 1610 (m),

1559 (w), 1448 (s), 1407 (s), 1377 (s), 1316 (vw), 1296 (w), 1182 (w), 1161 (w), 1136 (w), 1109 (w), 1084 (w), 1034 (m), 1014 (m), 957 (vs), 916 (s), 855 (s), 849 (s), 807 (s), 773 (w), 751 (m), 737 (m), 698 (m), 680 (w), 586 (m), 559 (w), 547 (w), 496 (w), 465 (w), 447 (w). **MS** (HR, ESI$^+$); calc. for $C_{27}H_{35}P_2$ $[M\text{-}GaCl_4]^+$ (found): 421.2219 (421.2220).

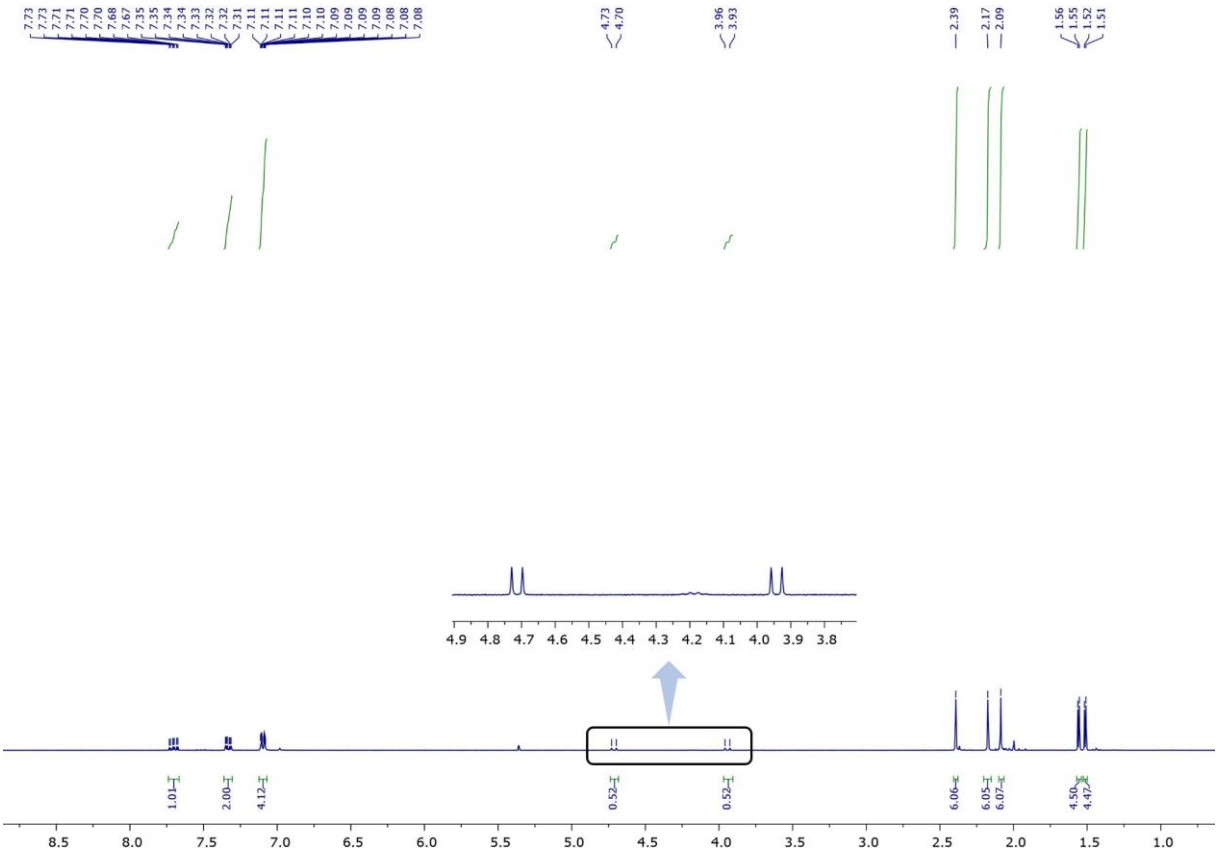

Figure S72: *^{1}H NMR of* ***12:^{Mes}Ter*** (given in ppm, CD_2Cl_2, 300 MHz, 298K).

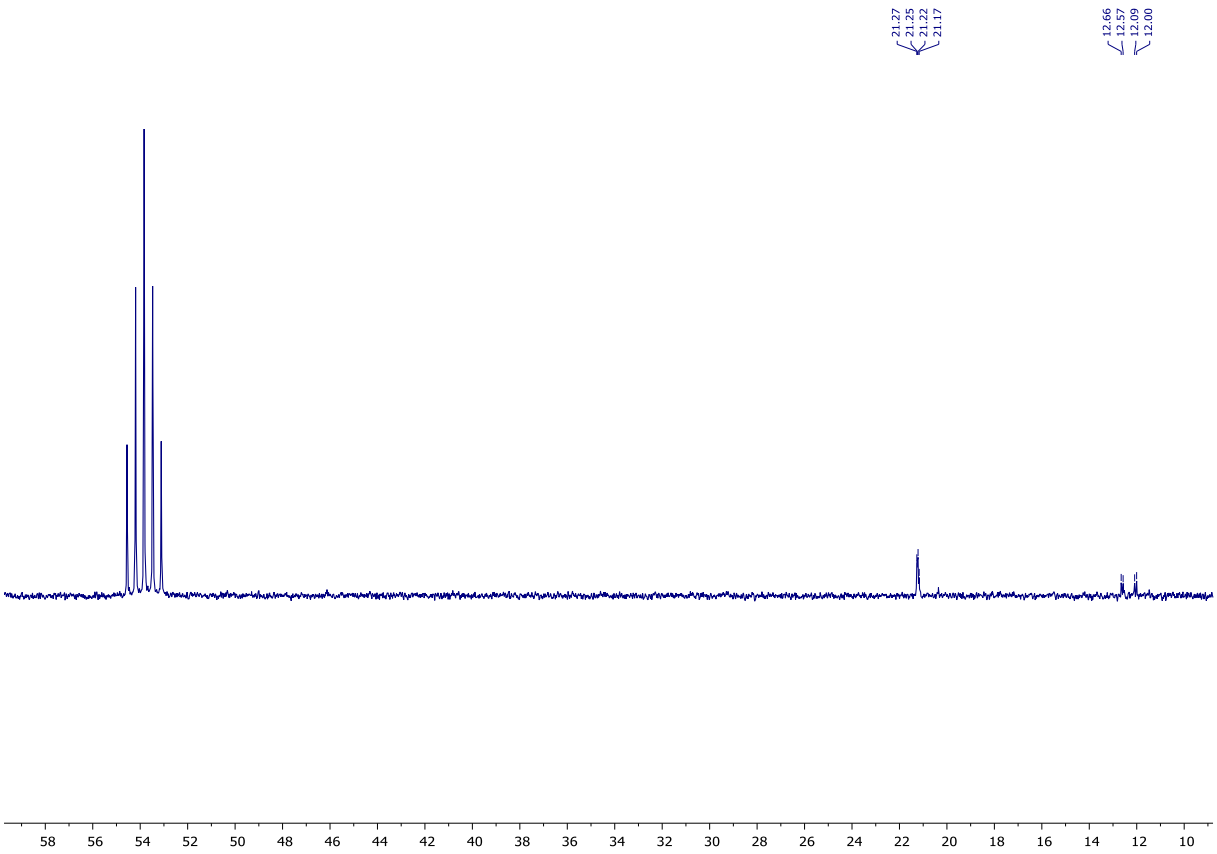

Figure S73: *^{13}C{^{1}H} NMR (high-field region only) of* ***12:^{Mes}Ter*** (given in ppm, CD_2Cl_2, 75.5 MHz, 298K).

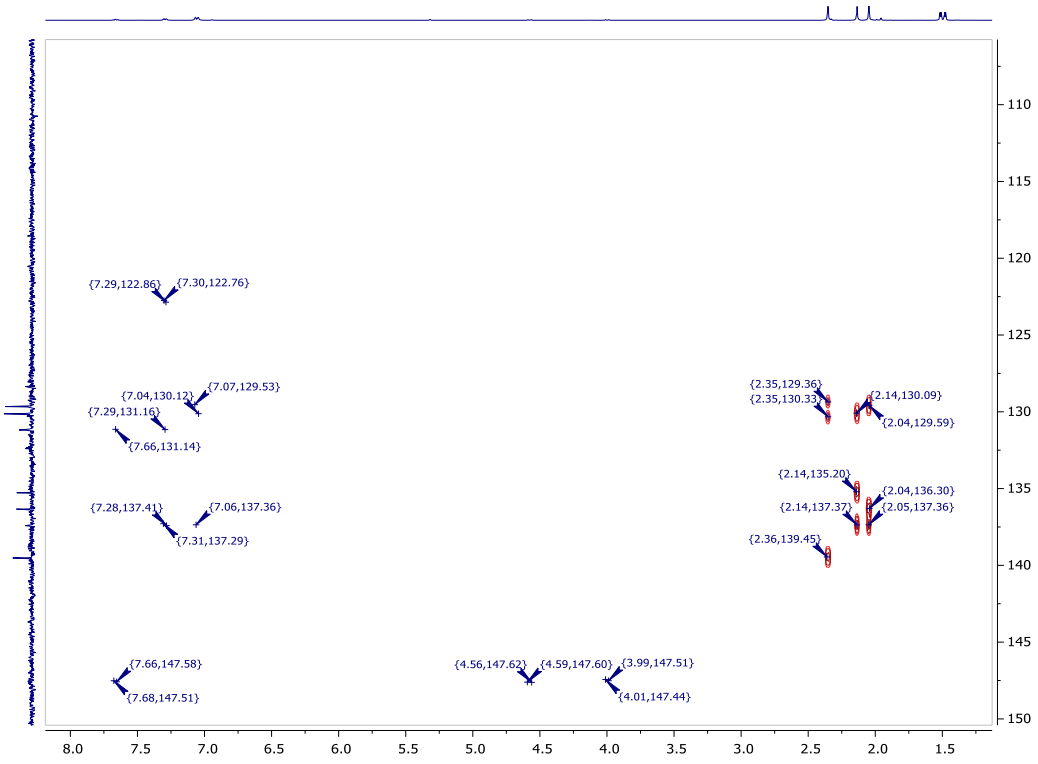

Figure S74: *$^{1}H/^{13}C$ HMBC NMR (low-field region only) of* ***12:^{Mes}Ter*** (given in ppm, CD_2Cl_2, 298K).

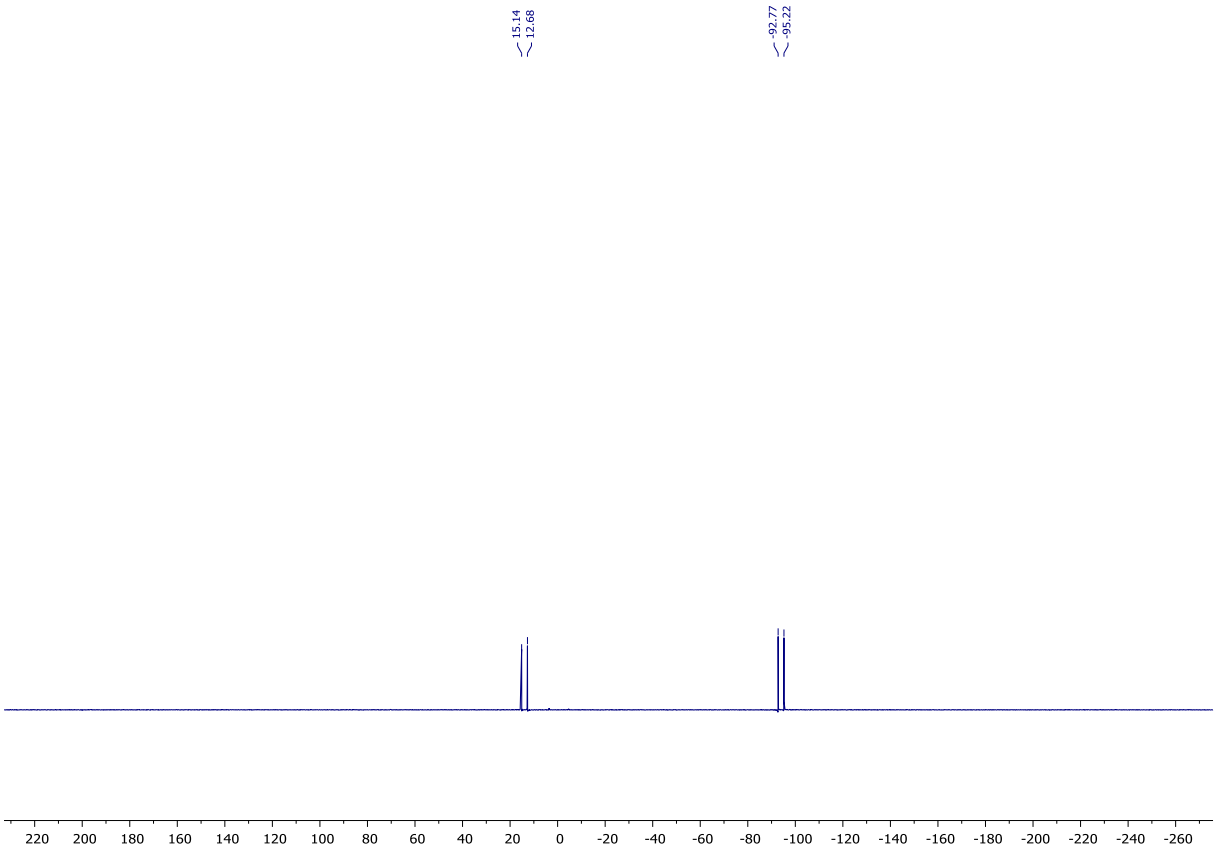

Figure S75: *$^{31}P\{^{1}H\}$ NMR of* ***12:^{Mes}Ter*** (given in ppm, CD_2Cl_2, 122 MHz, 298K).

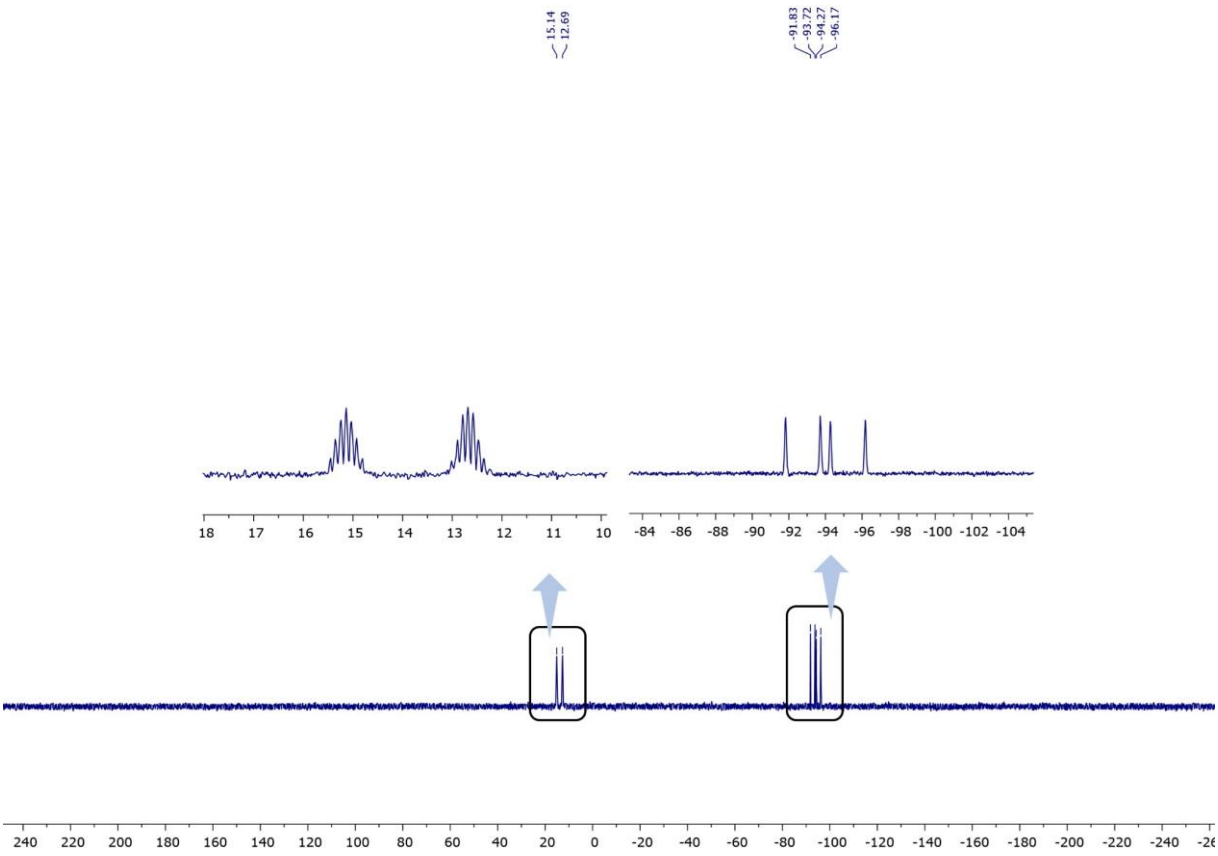

Figure S76: *^{31}P NMR of* ***12:^{Mes}Ter*** (given in ppm, CD_2Cl_2, 122 MHz, 298K).

3.19 [^{Dip}TerP(H)(PMe$_3$)]GaCl$_4$ (12:^{Dip}Ter)

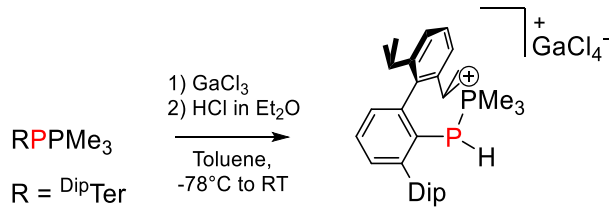

A 0.050 g portion of ^{Dip}TerPPMe$_3$ (0.100 mmol, 1.0 eq) together with 0.017 g of GaCl$_3$ (0.100 mmol, 1.0 eq) are placed in a Schlenk tube. At -78°C, 3 mL of toluene are added, and the resulting suspension is stirred for 30 min. at that temperature. The cooling bath is then removed and 0.05 mL of 2 M HCl in Et$_2$O (0.100 mmol, 1.0 eq) are immediately added to the solution. The mixture is stirred for another hour at ambient temperature followed by concentration to about 1.5 mL of toluene. After subsequent filtration, the solvent is removed under reduced pressure and the white precipitate is thoroughly dried *in vacuo*. **12:^{Dip}Ter** is obtained as a pale white microcrystalline powder (0.057 g, 0.079 mmol, 79%). Platelet-shaped crystals for SC-XRD are obtained from a saturated heptane/DCM mixture which is slowly evaporated in an Ar-flush at ambient temperature.

^{1}H NMR (C$_6$D$_6$, 400 MHz, 298K): δ = 7.67–7.63 (m, 1H, Ar*H*), 7.52–7.48 (m, 2H, Ar*H*), 7.43–7.40 (m, 2H, Ar*H*), 7.38–7.34 (m, 4H, Ar*H*), 4.22 (dd, $^1J_{PH}$ = 234.3 Hz, $^2J_{PH}$ = 9.3 Hz, P(*H*)PMe$_3$), 2.70 (hept, $^3J_{HH}$ = 6.9 Hz, C*H*(CH$_3$)$_2$, 2H), 2.44 (hept, $^3J_{HH}$ = 6.7 Hz, C*H*(CH$_3$)$_2$, 2H), 1.44 (dd, $^2J_{PH}$ = 13.6 Hz, $^3J_{PH}$ = 3.1 Hz, 9H, C*H*$_3$ of PMe$_3$), 1.35 (d, $^3J_{HH}$ = 6.8 Hz, CH(C*H*$_3$)$_2$, 6H), 1.29 (d, $^3J_{HH}$ = 6.9 Hz, CH(C*H*$_3$)$_2$, 6H), 1.15 (d, $^3J_{HH}$ = 6.6 Hz, CH(C*H*$_3$)$_2$, 6H), 1.03 (d, $^3J_{HH}$ = 6.7 Hz, CH(C*H*$_3$)$_2$, 6H) ppm. **^{13}C{^{1}H} NMR** (C$_6$D$_6$, 101 MHz, 298K): δ = 147.9 (s), 146.3 (s), 146.1 (dd, $^1J_{CP}$ = 11.9 Hz, $^2J_{CP}$ = 4.6 Hz, *ipso*–C$_{Aryl}$), 137.7 (d, *J* = 2.4 Hz), 132.1 (*ps*-t, *J* = 2.6 Hz)*, 131.1 (d, *J* = 3.4 Hz), 131.0 (s), 125.0 (d, *J* = 11.9 Hz), 32.01 (d, *J* = 4.9 Hz), [31.5, 26.8, 26.1] (s, CH(*C*H$_3$)$_2$)), 23.8 (d, *J* = 2.1 Hz), 23.14 (d, J = 2.6 Hz), 12.1 (dd, $^1J_{CP}$ = 43.2 Hz, $^2J_{CP}$ = 6.0 Hz, *C*H$_3$ of PMe$_3$) ppm. * Most likely an unresolved doublet of doublets. **^{31}P{^{1}H} NMR** (C$_6$D$_6$, 162 MHz, 298K): δ = 13.24 (d, $^1J_{PP}$ = 290.8 Hz, R-P(H)*P*Me$_3$), -92.45 (d, $^1J_{PP}$ = 288.8 Hz, R-*P*(H)PMe$_3$) ppm. **^{31}P NMR** (C$_6$D$_6$, 162 MHz,

298K): δ =13.24 (dm, $^{1}J_{PP}$ =287.0 Hz, R-P(H)*P*Me$_3$)**, -92.46 (dd, $^{1}J_{PP}$ = 290.0 Hz, $^{1}J_{PH}$ = 234.5 Hz, R-*P*(H)PMe$_3$) ppm. **Expected doublet of decet of doublets could not be resolved. **IR** (ATR, cm^{-1}): 3061 (w), 2960 (s), 2925 (m), 2911 (m), 2869 (w), 2318 ν_{sym}(P-H) (vw), 1591 (w), 1562 (w), 1458 (s), 1410 (m), 1386 (m), 1364 (m), 1323 (w), 1297 (s), 1250 (m), 1179 (w), 1161 (w), 1127 (w), 1109 (w), 1056 (w), 1041 (w), 957 (vs), 912 (m), 883 (vw), 857 (m), 821 (m), 808 (s), 794 (s), 760 (vs), 706 (w), 686 (w), 677 (w), 634 (w), 587 (w), 548 (w), 527 (w), 502 (w), 471 (w), 431 (w). **MS** (HR, ESI^{+}); calc. for $C_{33}H_{47}P_2$ [M-$GaCl_4$]$^{+}$ (found): 505.3158 (505.3152).

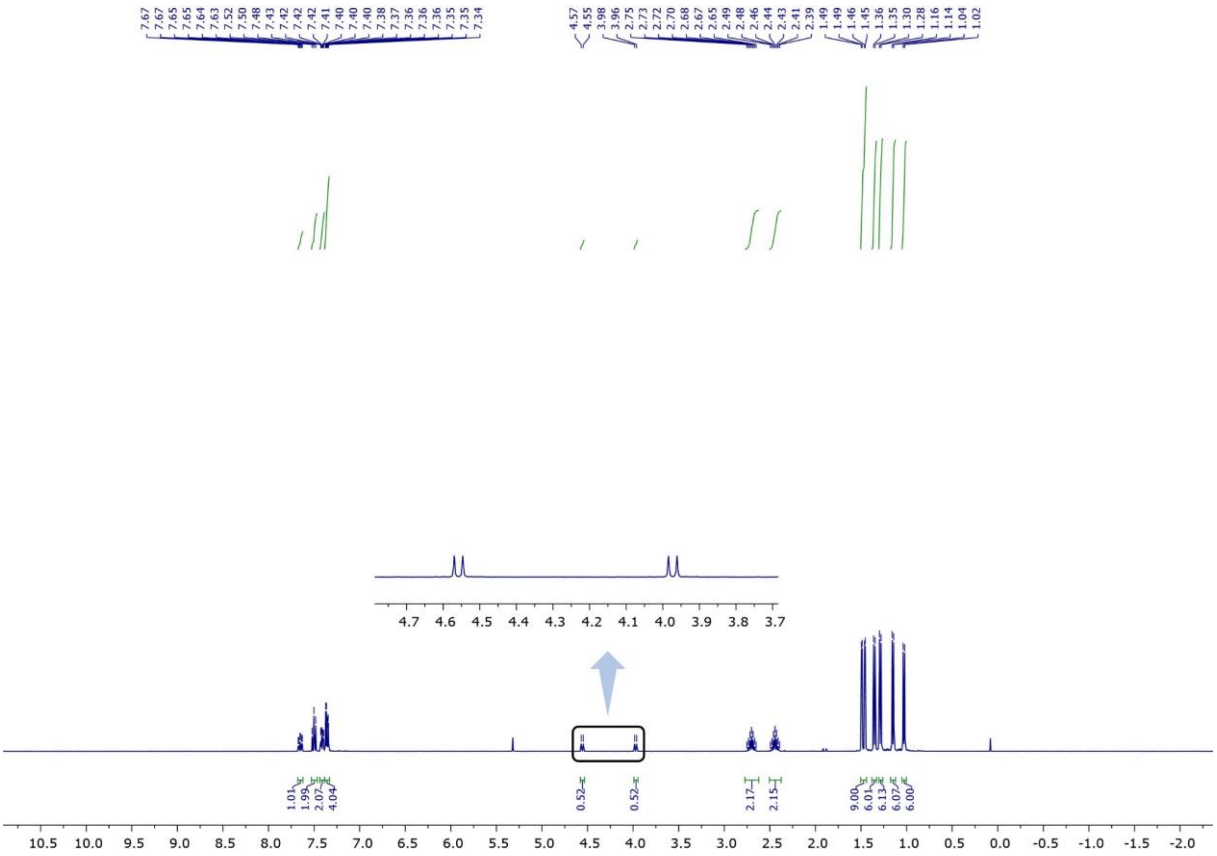

Figure S77: *^{1}H NMR of* ***12:^{Dip}Ter*** (given in ppm, CD_2Cl_2, 400 MHz, 298K).

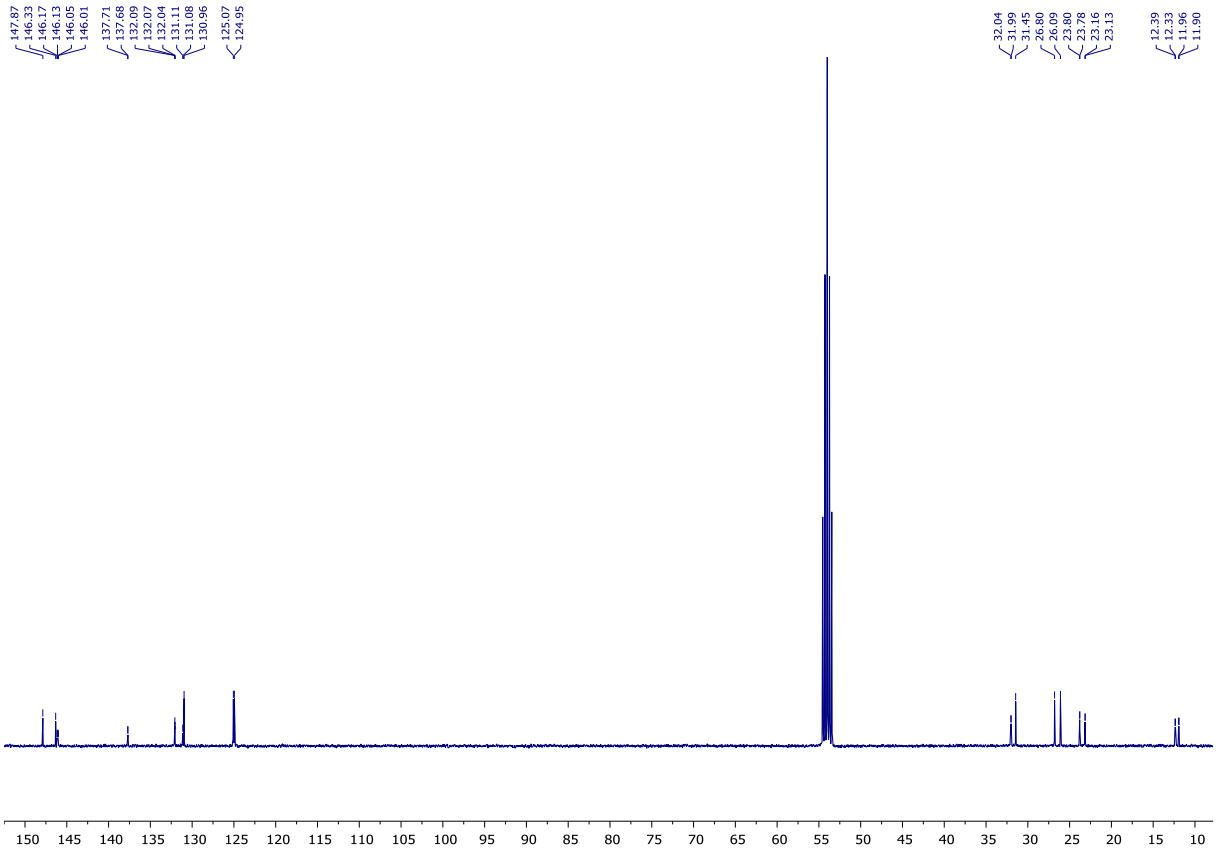

Figure S78: *$^{13}C\{^{1}H\}$ NMR of* ***12:^{Dip}Ter*** (given in ppm, CD_2Cl_2, 101MHz, 298K).

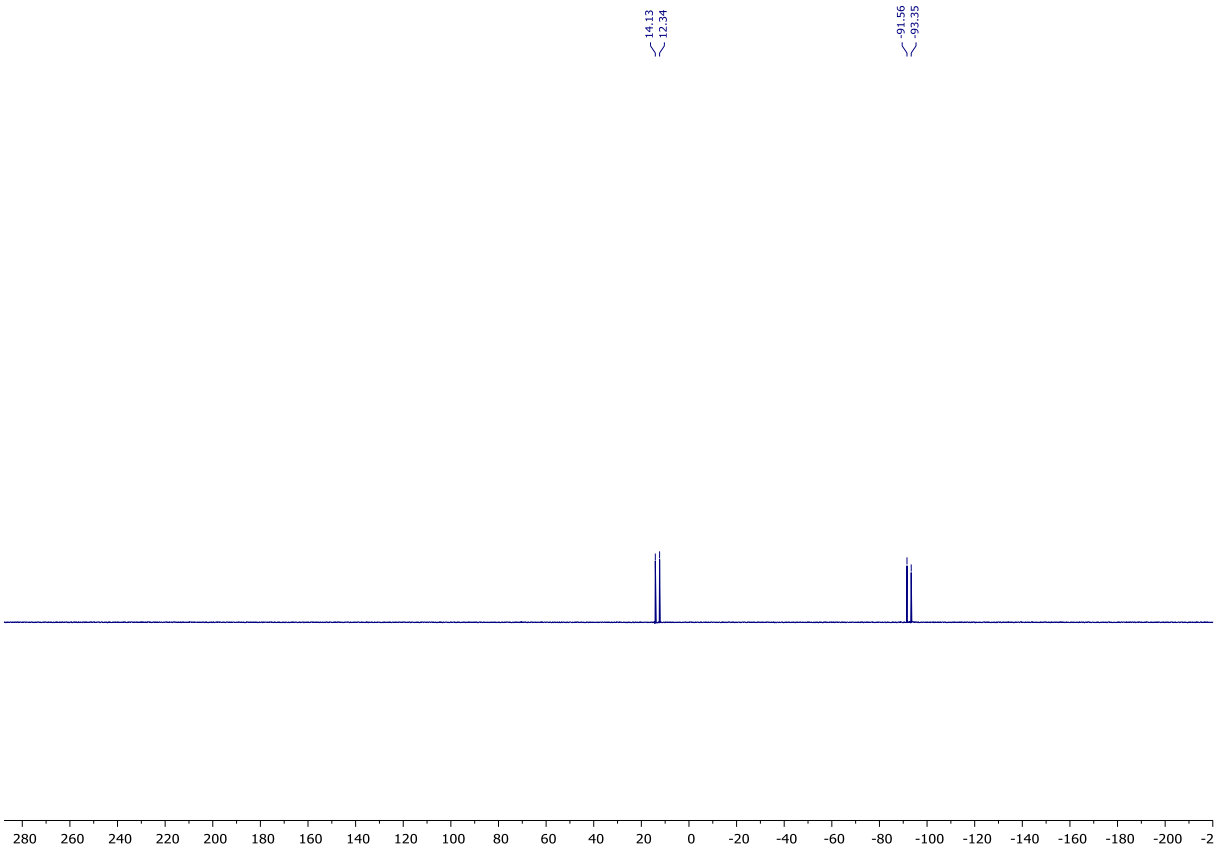

Figure S79: *$^{31}P\{^{1}H\}$ NMR of* ***12:^{Dip}Ter*** (given in ppm, CD_2Cl_2, 162 MHz, 298K).

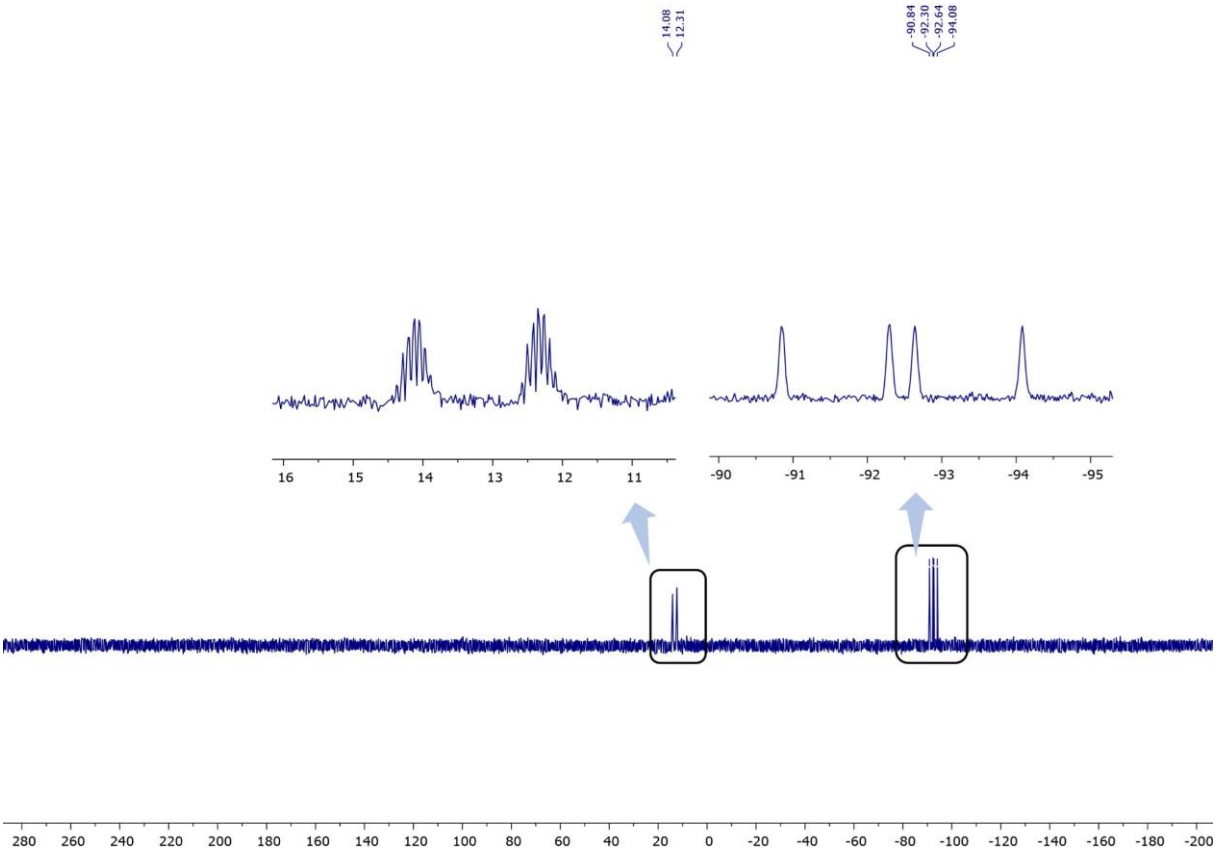

Figure S80: *^{31}P NMR of* ***12:^{Dip}Ter*** (given in ppm, CD_2Cl_2, 162 MHz, 298K).

4 Spectra to demonstrate reactivity

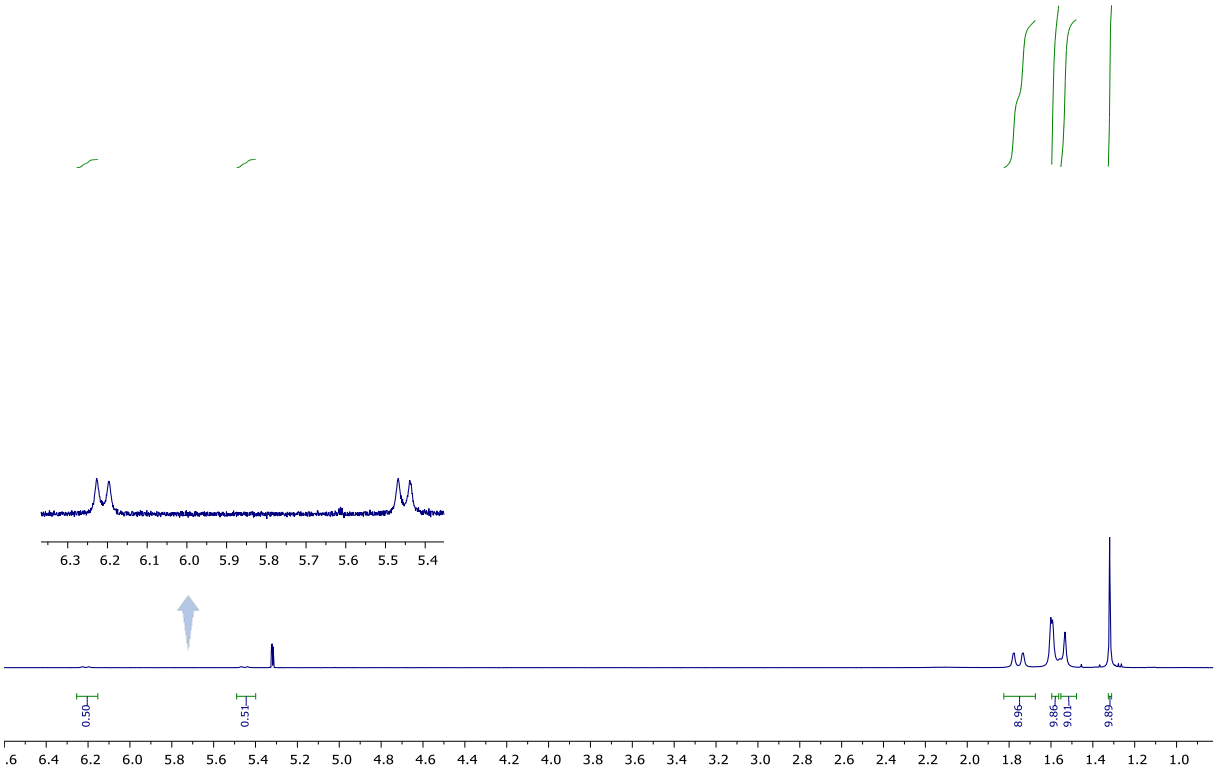

Figure S81: *^{1}H NMR of **7:Mes***+1 eq H_2O* (given in ppm, CD_2Cl_2, 300 MHz, 298K).

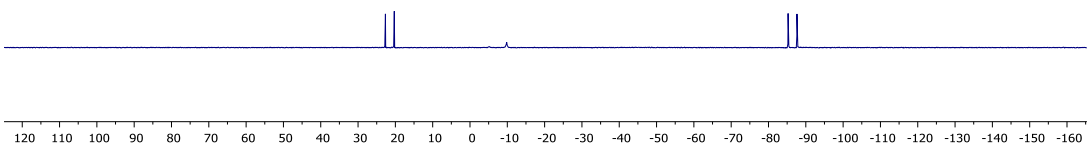

Figure S82: *$^{31}P\{^{1}H\}$ NMR of **7:Mes***+1 eq H_2O* (given in ppm, CD_2Cl_2, 162 MHz, 298K).

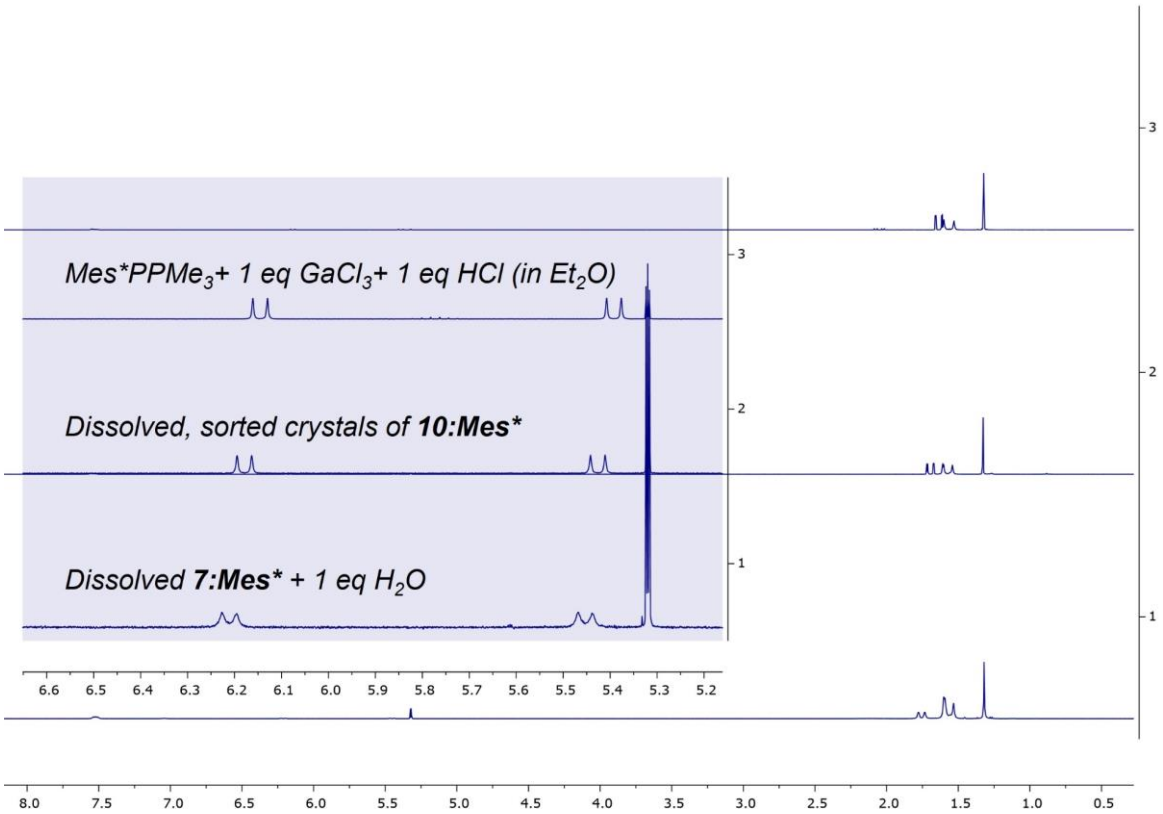

Figure S83: *Summary of ^{1}H NMRs of Mes*P(H)PMe$_3$[An] with regard to the characteristic doublet of doublets* (given in ppm, CD_2Cl_2, 300 MHz, 298K).

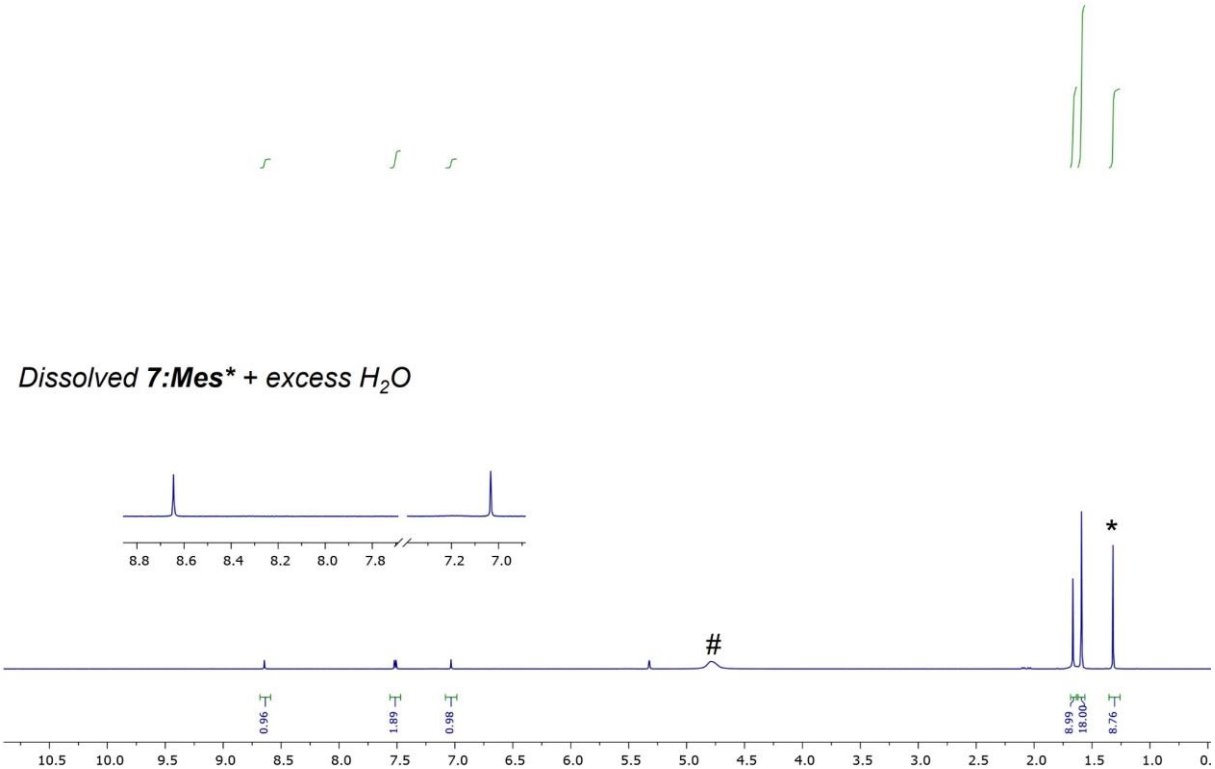

Figure S84: *^{1}H NMR showing **1:Mes*** if **7:Mes*** is converted with an excess of H_2O* (given in ppm, CD_2Cl_2, 300 MHz, 298K). *Unknown PMe_3 containing compound, #unknown OH-containing compound.

5 Computational details

Computations were carried out using Gaussian09[14] or ORCA 4.2.1[15] and the standalone version of NBO 6.0.[16–19]

Structure optimizations employed the hybrid DFT functional PBE0[20–22] in conjunction with Grimme's dispersion correction D3(BJ)[23,24] and the def2-SVP basis set[25] (notation PBE0-D3/def2-SVP). All structures were fully optimized and confirmed as minima by frequency analyses. Partial charges were determined by Natural Population analysis using the NBO program.

More accurate estimates of the electronic energy were obtained by single-point DLPNO-CCSD(T)/def2-TZVP[26] computations (notation DLPNO-CCSD(T)/def2-TZVP//PBE-D3/def2-SVP). The T_1 diagnostic was evaluated in each case to ensure reliable results. (Empirically, CCSD(T) results with T_1 values smaller than 0.02 are considered reliable.)[27]

Please note that all computations were carried out for single, isolated molecules in the gas phase (ideal gas approximation). There may well be significant differences between gas phase and condensed phase.

5.1 Summary of calculated data

Table S8. Summary of calculated data, including electronic energies and thermal corrections.

Compd.	NIMAG	ZPE [kcal·mol^{-1}]	E_{tot}[a]	ΔG[b]	$E_{CCSD(T)}$[c]	T_1
I:Mes*	0	341,8849	-1503,8422	0,4890	-1503,3024	0,0098
6:Mes*	0	345,2917	-4808,1626	0,4839	-4806,1730	0,0098
$GaCl_3$	0	2,4730	-3304,2426	-0,0263	-3302,8069	0,0106

[a] Total SCF energy in a.u.; [b] thermal correction to Gibbs energy in a.u. (298 K unless stated otherwise); [c] single-point DLPNO-CCSD(T)/def2-TZVP energy.

5.2 Thermochemistry

To evaluate the thermodynamic feasibility of the reactions described in the manuscript their respective $\Delta_R G°_{298}$ values were determined on the DLPNO-CCSD(T)/def2-TZVP // PBE0-D3/def2-SVP level of theory.

Mes*P(PMe_3) (**I:Mes***) + $GaCl_3$ → Mes*P($GaCl_3$)PMe_3 (**6:Mes***)

$\Delta_R G°_{298}$ = −111.35 KJ·mol^{-1}

5.3 Bonding and NBO Analysis

The electronic structure of **I:Mes*** and **6:Mes*** was investigated using the full model. First the Kohn-Sham orbitals (PBE0-D3/def2-SVP) were inspected and the LUMO+2 to HOMO-2 along with their respective energies are depicted below.

Figure S85. Relevant Kohn-Sham orbitals of **I:Mes*** (PBE0-D3/def2-SVP).

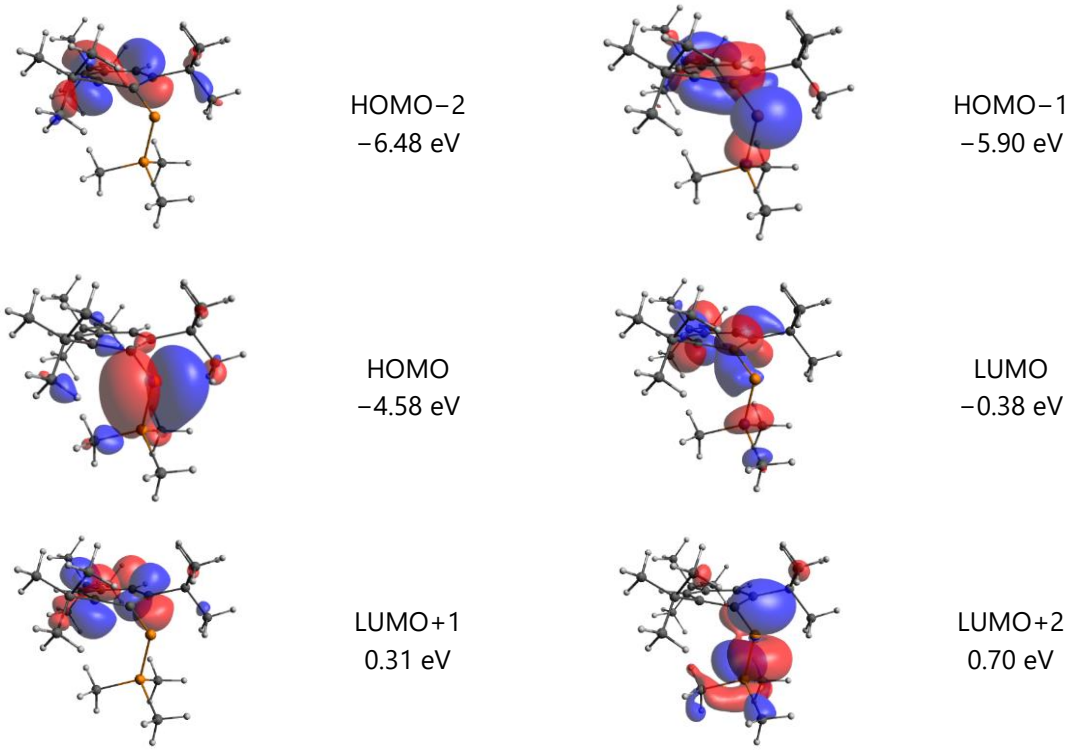

Figure S86. Relevant Kohn-Sham orbitals of **6:Mes*** (PBE0-D3/def2-SVP).

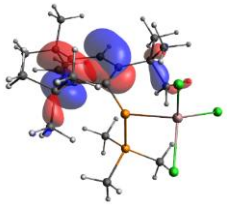

HOMO−2
−7.21 eV

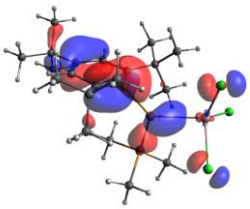

HOMO−1
−6.95 eV

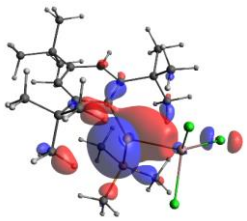

HOMO
−6.23 eV

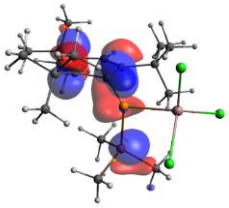

LUMO
−1.35 eV

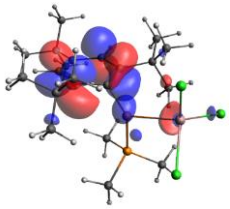

LUMO+1
−0.47 eV

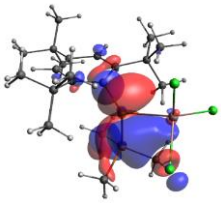

LUMO+2
−0.11 eV

Next NBO analyses were carried out on the PBE0-D3/ def2-SVP level of theory and additionally Wiberg-Bond-Indices (WBI) were determined and NLMOs (Natural localized molecular orbitals) were calculated. The results of these natural bond orbital analyses for **I:Mes*** and **6:Mes*** are summarized below.

Summary of NBO results for **I:Mes***:

NPA Charges

P 9 -0.19511

P 22 1.13056

WBIs

P9-P22 1.1750

Bonding

32. (1.93887) LP (1) P 9 s(71.65%)p 0.39(28.30%)d 0.00(0.04%)

33. (1.70278) LP (2) P 9 s(0.00%)p 1.00(99.79%)d 0.00(0.21%)

49. (1.95136) BD (1) P 9- P 22

(39.71%) 0.6301* P 9 s(12.14%)p 7.15(86.85%)d 0.08(1.00%)

(60.29%) 0.7765* P 22 s(30.93%)p 2.21(68.51%)d 0.02(0.55%)

2nd order perturbation [kcal/mol]

33. LP (2) P 9	121. BD*(1) C 11- P 22	11.42
33. LP (2) P 9	125. BD*(1) C 12- P 22	11.40

Figure S87. Selected NLMOs of **I:Mes*** (PBE0/def2-SVP).

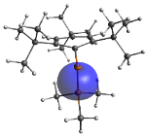

σ (P-P)
−15.6 eV
P1: 38.9%
P2: 58.9%

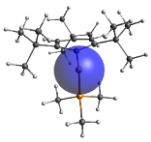

LP1(P1)
−13.2 eV
s: 71.3%
p: 28.7%

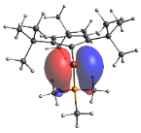

LP2(P1)
−5.1 eV
s: 0.0%
p: 99.8%

Summary of NBO results for **6:Mes***:

NPA charges

Ga 1 1.04199

P 2 -0.11740

P 3 1.19223

Cl 4 -0.47486

Cl 5 -0.50139

Cl 6 -0.46152

Wiberg Bond Indices

Ga1-P2 0.6324

P2-P3 0.9889

Bonding

61. (1.84909) LP (1) P 2 s(42.35%)p 1.36(57.55%)d 0.00(0.10%)

72. (1.91838) BD (1)Ga 1- P 2

(22.16%) 0.4708*Ga 1 s(31.06%)p 2.21(68.59%)d 0.01(0.35%)

(77.84%) 0.8823* P 2 s(22.26%)p 3.48(77.55%)d 0.01(0.19%)

75. (1.95668) BD (1) P 2- P 3

(42.90%) 0.6550* P 2 s(12.74%)p 6.77(86.30%)d 0.07(0.96%)

(57.10%) 0.7556* P 3 s(26.70%)p 2.72(72.64%)d 0.02(0.66%)

Figure S88. Selected NLMOs of Mes*P(H)CN (PBE0/def2-SVP).

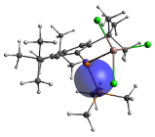

σ (P-P)
−16.3 eV
P1: 42.1%
P2: 56.0%

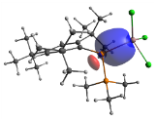

σ (P-Ga)
−13.1 eV
P: 74.8%
Ga: 22.5%

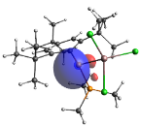

LP(P1)
−10.8 eV
s: 39.8%
p: 60.1%

5.4 Optimized structures (.xyz-files)

5.4.1 Mes*PPMe$_3$ (I:Mes*)

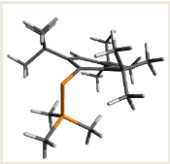

```
61
Mes*PPMe3 @ PBE0-D3/def2-SVP
C         0.2346584164      1.2410236160     -0.6144890782
C        -0.4676743255      0.0071056498     -0.7017813725
C         1.5299714218      1.2283335021     -0.0756576836
C         0.2813484369     -1.2053001063     -0.6264159387
C         2.1851641123      0.0520905517      0.2793246109
C         1.5707610096     -1.1469641347     -0.0901499635
H         2.0453003060      2.1750245373      0.0635832742
H         2.1287822599     -2.0736091805      0.0379205355
P        -2.3457968223     -0.0289709590     -0.7156822651
C        -4.2416149124     -0.0849671675      1.7988646127
C        -1.7373217796     -1.4419726653      2.3141292177
C        -1.7955103648      1.3724553063      2.3293027974
H        -4.7285267477      0.8027681963      1.3719470263
H        -4.6902193397     -0.9826609458      1.3512913560
H        -4.3884096860     -0.1007530830      2.8884237361
H        -0.6683543966     -1.5028601018      2.0619223442
H        -1.8517853551     -1.2854228009      3.3974588935
H        -2.2218823165     -2.3801792065      2.0185588756
H        -1.8977382466      1.1982014586      3.4111361717
H        -0.7314176669      1.4825434647      2.0728406565
H        -2.3213415591      2.2923549726      2.0467420334
P        -2.4691283389     -0.0441979074      1.3883558696
C        -0.1951079944     -2.5400233419     -1.2564472054
C        -1.2325577702     -3.3035515506     -0.4246378576
C        -0.7771708417     -2.2407742339     -2.6476693740
C         0.9883327570     -3.4951586007     -1.4714764696
H        -0.8221765112     -3.5800015984      0.5587790215
H        -2.1385521465     -2.6993301825     -0.2859558172
H        -1.5085183185     -4.2352389991     -0.9449636950
H        -0.0460575267     -1.7021285954     -3.2699196244
H        -1.0365919774     -3.1828538072     -3.1570494914
H        -1.6913547432     -1.6345872159     -2.5809649411
H         0.6389100242     -4.3736653114     -2.0348520778
H         1.7999449915     -3.0260015340     -2.0482051238
H         1.4065694294     -3.8680565341     -0.5240063061
C         3.5564372209      0.0330097880      0.9554642271
C         3.4533922894     -0.7659799608      2.2627716066
C         4.5799135889     -0.6343110404      0.0253300455
C         4.0528871208      1.4404299021      1.2885113596
H         2.7267819805     -0.3024026147      2.9482957186
H         3.1291565343     -1.8013970273      2.0806087662
H         4.4294145907     -0.8036717770      2.7728620068
H         4.6617457693     -0.0826824719     -0.9237293165
H         5.5754271536     -0.6563648180      0.4974422225
H         4.2995482277     -1.6707735599     -0.2134220191
H         5.0242705753      1.3827973128      1.8031921869
H         4.1950635691      2.0498104304      0.3830554439
H         3.3532116725      1.9718383649      1.9518539559
C        -0.2905543778      2.5662121632     -1.2257532393
C        -0.8670364772      2.2658609696     -2.6191836590
C        -1.3513782416      3.2823489863     -0.3811755529
```

```
C         0.8582529240      3.5648073756     -1.4328064164
H        -0.1199766151      1.7611445120     -3.2508780557
H        -1.7596290438      1.6277890509     -2.5584136416
H        -1.1602575636      3.2052944293     -3.1149841421
H        -0.9481191840      3.5614128890      0.6044556137
H        -1.6621944543      4.2098620415     -0.8891583917
H        -2.2347850697      2.6444075945     -0.2471010929
H         0.4761414259      4.4367318203     -1.9849925884
H         1.2667755116      3.9410585091     -0.4825223034
H         1.6835685832      3.1310846444     -2.0176832249
```

5.4.2 Mes*P(GaCl$_3$)PMe$_3$ (6:Mes*)

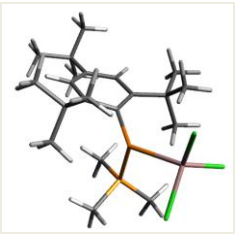

```
65
Mes*P(GaCl3)PMe3 @ PBE0-D3/def2-SVP
Ga        2.9893596371     -0.1756642114     -0.5351483910
P         0.8521701696      0.6940295826      0.0292446060
P         0.8262597114      0.5608208994      2.1975169129
Cl        3.6070631599     -2.2052771432     -0.0150374400
Cl        4.0750346475      1.2180262572      0.8226054676
Cl        3.1975954513      0.2883754636     -2.6516620584
C        -0.8717874090      0.1385738776     -0.3800652751
C        -1.3795153823     -1.1934352547     -0.3358961394
C        -1.3892788764      2.6375501934     -1.0697375422
C        -1.7829053795      1.2217408907     -0.5653446872
C        -0.5208147029     -2.4577744609     -0.5298875811
C        -3.1487604596      0.9685360260     -0.3746064942
H        -3.8444795887      1.7985530861     -0.4494817316
C        -3.6541726740     -0.2981901699     -0.1055842852
C        -0.7886608717      3.5351143163      0.0246388014
H        -1.4316764749      3.5430384011      0.9204437504
H        -0.7185691596      4.5711874038     -0.3428063254
H         0.2186349162      3.2071659386      0.3060268367
C         0.3617221484     -2.2787539330     -1.7737777024
H        -0.2656097780     -2.2398826761     -2.6773930990
H         1.0658540536     -3.1176541162     -1.8724481058
H         0.9520975700     -1.3557157855     -1.7620929193
C        -0.4263442059      2.5135652806     -2.2631762895
H         0.5281459562      2.0326305389     -2.0098167834
H        -0.1885535531      3.5153138758     -2.6535900943
H        -0.8913508681      1.9325431947     -3.0740830672
C        -2.7546565910     -1.3626795141     -0.1719817100
H        -3.1467206138     -2.3743352962     -0.0887221667
C        -0.8487353121      0.1834216942      2.7737931153
H        -1.5585353756      0.8796966133      2.3050164634
H        -0.8883777283      0.2786218746      3.8688867549
H        -1.1216641089     -0.8358657964      2.4713786967
C         1.9735347218     -0.5689201259      3.0371983045
H         1.8180953781     -1.6064300988      2.7198055304
H         1.8234966687     -0.4776405103      4.1236274030
H         2.9960516597     -0.2633892849      2.7712218697
C         0.3081317078     -2.7562963418      0.7199722360
H         1.0235048218     -1.9550285958      0.9193348331
H         0.8975207622     -3.6749209345      0.5842053513
H        -0.3481397845     -2.8946242007      1.5950482591
C        -2.6230692062      3.3846973406     -1.6049618437
H        -3.1695189544      2.7972534089     -2.3578519977
H        -2.2873055478      4.3148803224     -2.0864093369
```

```
H       -3.3257796181      3.6731974678     -0.8086103867
C       -1.3796283775     -3.7026726172     -0.7923635193
H       -1.9670087921     -4.0078424561      0.0871388404
H       -0.7116440080     -4.5411020179     -1.0394899900
H       -2.0660700246     -3.5619282335     -1.6407453145
C        1.2536084290      2.1912355371      2.8632519829
H        2.2402747224      2.4597063969      2.4577026992
H        1.2925642537      2.1574828155      3.9622235019
H        0.5116074545      2.9292689457      2.5324968545
C       -5.1313500596     -0.5621544947      0.1819104344
C       -5.9524102451      0.7273837438      0.2079625100
H       -5.5859819635      1.4295864102      0.9725072681
H       -7.0018079670      0.4956803863      0.4447219541
H       -5.9396928997      1.2414300135     -0.7651066755
C       -5.2509859931     -1.2433460901      1.5533261870
H       -4.7052638054     -2.1981112741      1.5826202836
H       -6.3065213980     -1.4525368045      1.7888313864
H       -4.8451879855     -0.5986232712      2.3485328854
C       -5.7065753108     -1.4842338843     -0.9030929082
H       -5.6180764553     -1.0216968403     -1.8978955869
H       -6.7727848868     -1.6832285604     -0.7108928198
H       -5.1869847826     -2.4531369688     -0.9360247436
```

5.4.3 $GaCl_3$

```
4
GaCl3
Ga      -0.4681829441      1.06244578       -0.0122598
Cl      -1.5283218854      2.8986602907     -0.0122598
Cl       1.6520949395      1.0624457793     -0.0122598
Cl      -1.5283218866     -0.77376873       -0.0122598
```

6 References

[1] P. Gupta, J-E. Siewert, T. Wellnitz, M. Fischer, W. Baumann, T. Beweries, C. Hering-Junghans, *Dalton Trans.*, **2021**, *50*, 1838-1844.

[2] K. Bläsing, J. Bresien, R. Labbow, D. Michalik, A. Schulz, M. Thomas, A. Villinger, *Angew. Chem. Int. Ed.* **2019**, *58*, 6540–6544.

[3] G. M. Sheldrick, *Acta Crystallogr. Sect. A* **2015**, *71*, 3–8.

[4] G. M. Sheldrick, *Acta Crystallogr. Sect. C* **2015**, *71*, 3–8.

[5] O. V. Dolomanov, L. J. Bourhis, R. J. Gildea, J. A. K. Howard, H. Puschmann, *J. Appl. Crystallogr.* **2009**, *42*, 339–341.

[6] X-AREA and LANA; Stoe & Cie: Darmstadt, Germany, **2020**.

[7] SADABS within APEX2; Bruker AXS Inc.: Madison, WI, **2010**.

[8] K. Brandenburg, DIAMOND V. 4.6.5, **2021**.

[9] Mestrelab Research S.L., MestReNova V. 9.0.1-13254, **2014**.

[10] OPUS; Version 7.2; Bruker Opt. GmbH: Ettlingen, Germany, **2012**.

[11] OMNIC; Version 9.11.697, **2017**.

[12] W. Kandioller, J. Theiner, B. K. Keppler, C. R. Kowol, *Inorg. Chem. Front*, **2022**, *9*, 412-416.

[13] J. Bresien, K. Faust, A. Schulz, A. Villinger, *Angew. Chem. Int. Ed*. **2015**, 54, 6926–6930.

[14] *Gaussian 16, Revision C.01*, M. J. Frisch, G. W. Trucks, H. B. Schlegel, G. E. Scuseria, M. A. Robb, J. R. Cheeseman, G. Scalmani, V. Barone, G. A. Petersson, H. Nakatsuji, X. Li, M. Caricato, A. V. Marenich, J. Bloino, B. G. Janesko, R. Gomperts, B. Mennucci, H. P. Hratchian, J. V. Ortiz, A. F. Izmaylov, J. L. Sonnenberg, D. Williams-Young, F. Ding, F. Lipparini, F. Egidi, J. Goings, B. Peng, A. Petrone, T. Henderson, D. Ranasinghe, V. G. Zakrzewski, J. Gao, N. Rega, G. Zheng, W. Liang, M. Hada, M. Ehara, K. Toyota, R. Fukuda, J. Hasegawa, M. Ishida, T. Nakajima, Y. Honda, O. Kitao, H. Nakai, T. Vreven, K. Throssell, J. A. Montgomery, Jr., J. E. Peralta, F. Ogliaro, M. J. Bearpark, J. J. Heyd, E. N. Brothers, K. N. Kudin, V. N. Staroverov, T. A. Keith, R. Kobayashi, J. Normand, K. Raghavachari, A. P. Rendell, J. C. Burant, S. S. Iyengar, J. Tomasi, M. Cossi, J. M. Millam, M. Klene, C. Adamo, R. Cammi, J. W. Ochterski, R. L. Martin, K. Morokuma, O. Farkas, J. B. Foresman, and D. J. Fox, Gaussian, Inc., Wallingford CT, **2016**.

[15] F. Neese, *WIREs Comput. Mol. Sci.* **2018**, *8*, e1327.

[16] E. D. Glendening, J. K. Badenhoop, A. E. Reed, J. E. Carpenter, J. A. Bohmann, C. M. Morales, C. R. Landis, F. Weinhold, *NBO 6.0*, Theoretical Chemistry Institute, University of Wisconsin, Madison, **2013**.

[17] J. E. Carpenter, F. Weinhold, *J. Mol. Struct.: THEOCHEM* **1988**, *169*, 41–62.

[18] F. Weinhold, J. E. Carpenter, *The Structure of Small Molecules and Ions*, Plenum Press, **1988**.

[19] F. Weinhold, C. R. Landis, *Valency and Bonding. A Natural Bond Orbital Donor-Acceptor Perspective*, Cambridge University Press, **2005**.

[20] J. P. Perdew, K. Burke, M. Ernzerhof, *Phys. Rev. Lett.* **1996**, *77*, 3865–3868.

[21] J. P. Perdew, K. Burke, M. Ernzerhof, *Phys. Rev. Lett.* **1997**, *78*, 1396–1396.

[22] C. Adamo, V. Barone, *J. Chem. Phys.* **1999**, *110*, 6158–6170.

[23] S. Grimme, J. Antony, S. Ehrlich, H. Krieg, *J. Chem. Phys.* **2010**, *132*, 154104.

[24] S. Grimme, S. Ehrlich, L. Goerigk, *J. Comput. Chem.* **2011**, *32*, 1456–1465.

[25] F. Weigend, R. Ahlrichs, *Phys. Chem. Chem. Phys.* **2005**, *7*, 3297–305.

[26] a) C. Riplinger, F. Neese, *J. Chem. Phys.* **2013**, *138*, 034106; b) D. G. Liakos, M. Sparta, M. K. Kesharwani, J. M. L. Martin, F. Neese, *J. Chem. Theory Comput.* **2015**, *11*, 1525–1539; c) C. Riplinger, P. Pinski, U. Becker, E. F. Valeev, F. Neese, *J. Chem. Phys.* **2016**, *144*, 024109

[27] C. J. Cramer, *Essentials of Computational Chemistry: Theories and Models*, John Wiley & Sons, Ltd, Chichester, UK, **2004**.